The Cell Switch-off Approach for Energy-Efficient Cellular Networks

by

Tamer Beitelmal, **B.Sc., M.Sc.**

A dissertation submitted to the
Faculty of Graduate and Postdoctoral Affairs
in partial fulfillment of the requirements for the degree of

Doctor of Philosophy in Electrical and Computer Engineering

Ottawa-Carleton Institute for Electrical and Computer Engineering
Department of Systems and Computer Engineering
Carleton University
Ottawa, Ontario
December, 2016

Abstract

Network densification is a key enabler for providing high data rates and ubiquitous coverage. Although it enables the ambitious target of 1,000-fold gains in capacity, installing more base stations (BSs) challenges the energy efficiency targets of future networks. Cell switch-off (CSO) approaches are proposed to reduce energy consumption in off-peak periods by switching off some BSs. In this thesis, we define an energy-efficient cellular network as one in which as few BSs as possible are switched on while still satisfying all the users demand and quality of service. This thesis contributes to the current state of knowledge by directing the CSO research towards a more realistic, feasible, and practical implementation. We do this by arguing for employing offline (static) CSO and for considering spatially irregular BS deployments. First, we propose a dynamic CSO algorithm based on the well-known set cover problem. Our algorithm outperforms a benchmark algorithm in terms of the total number of switched-off BSs. While dynamic CSO algorithms are designed to adapt to fast changes in demand distribution, proper interference modelling is very challenging. To overcome this challenge, we next study regular static CSO patterns and describe them systematically. We propose sector-based patterns, where not only entire BSs could be switched off (site-based), but their individual sectors too. We compare the performance of different CSO patterns in terms of their energy efficiency and the number of supported users. CSO patterns are advantageous for modelling interference properly, reducing coverage holes, and making the uplink transmissions more energy-efficient for users. Nevertheless, the underlying assumption is that the BSs are deployed according to a regular grid. Finally, we consider spatially irregular BS deployments as a more realistic network model; therefore, we study applying CSO to irregular network layouts with the objective of making the active BS locations as regular as possible. We test the suitability of several algorithms from the p-dispersion problem literature for networks with BSs deployed with variable amounts of regularity. We also demonstrate some of these algorithms on real BS locations.

In the name of Allah (God), the most Gracious, the most Merciful

"Read! In the name of your Lord Who has created (all that exists) - created man from a clot. Read! And your Lord is the Most Generous - He Who has taught (the use of) the pen. He has taught man that which he did not know."

The Holy Qur'an, Chapter 96, Verses 1-5

Dedicated to:

The soul of my father (Ahmed Beitelmal) - may Allah have mercy on him-
who left this world 4 weeks before this great accomplishment.
To whom it would have mattered the most to him.

Acknowledgments

First and foremost, I am most grateful to Allah (God), the Creator and Sustainer of the universe, for His uncountable bounties on me including the ability to perform this research and to write this thesis.

It is a pleasure to express my gratitude to many people who directly and indirectly helped and made this thesis possible. My sincerest gratitude and respect go to my supervisor, Professor Halim Yanikomeroglu for his abundant support, patience, and knowledge. You kept believing in me and my ability to finish this thesis. I am greatly indebted to my colleague, co-supervisor, and friend Dr. Sebastian S. Szyszkowicz. You saved my Ph.D. by giving me the motivation to continue this journey; through countless late-night discussions, intelligent advice, and elegant research directions. Many thanks to the thesis committee: Prof. Wessam Ajib, Prof. Saban Alaca, Prof. Burak Kantarci, and Prof. Roshdy Hafez for spending the time reading and evaluating my thesis, as well as for a pleasant defence experience. I am thankful to my colleagues and friends, far and near, your support and encouragement meant a lot to me. Special thanks to the people at the office MC4038. I enjoyed being and chatting with you.

I am deeply grateful to my parents who raised me and instilled in me the love and appreciate of knowledge, and to my sisters and my brother who believed in me and cheered me up. I also offer deep thanks to my parents-in-law. To my children: Zainab, Ahmad, and Yamen, your smiles and laughter gave me the hope and motivation; thanks for being patient and for your limitless unconditional love. Last but not least, I am extremely thankful to my wife, Asma, for her constant support and endless patience, for her understanding and encouraging throughout this period.

My Ph.D. study was mostly sponsored by the Libyan Government through the Ministry of Higher Education and Scientific Research (MOHESR). This work was also supported in part by the Ontario Graduate Scholarships (OGS) and in part by TELUS Corporation; I thankfully acknowledge this support.

Contents

List of Tables

List of Figures

Nomenclature

Acronyms

Acronym	Meaning
3GPP	3rd generation partnership project
5G	fifth generation
AMC	adaptive modulation and coding
BS	base station
CDF	cumulative distribution function
CN	core network
CSO	cell switch-off
ESE	equivalent spectral efficiency
FLP	facility location problem
$G_{\mathrm{SIR}}(X)$	downlink SIR gain for X% of users
HLP	hub location problem
ICIC	inter-cell interference coordination
IMT	international mobile telecommunications
InP	infrastructure provider
ITU	international telecommunication union
LTE	long term evolution
MCLP	maximal covering location problem
MNO	mobile network operator
MVNO	mobile virtual network operator
NFV	network function virtualization
NSO	network switch-off
PCP	p-center problem
PDP	p-dispersion problem
PMP	p-median problem
PPP	Poisson point process
PTL	perturbed triangular lattice

RAN	radio access network
RNC	radio network controller
RPP	repulsive point processes
SCP	set cover problem
SDN	software defined networking
SE	spectral efficiency
SINR	signal-to-interference-plus-noise ratio
SIR	signal-to-interference ratio
SNR	signal-to-noise ratio
SP	service provider
TL	triangular lattice
UE	user equipment
U-FCLP	un-capacitated fixed charge location problem
UIL	user-in-the-loop
UT	user terminal
WSN	wireless sensor network

Mathematical Symbols

Notation	Meaning
b_i	bandwidth required by user i
b_{ij}	required bandwidth for user i if served by cell j
$\mathbf{B}$	$= [b_{ij}]$: required bandwidth matrix
c_{ij}	cost of connecting customer i to facility j
C	cost per unit demand per unit distance
$\mathcal{C}$	set of the cost associated to each facility (BS)
C_{D}	coefficient of variation of the Delaunay triangulation edge lengths
$\mathbb{C}\mathrm{oV}\{X\}$	coefficient of variation of a random variable X
d_{ij}	distance between user (customer) i and BS (facility) j
D	minimum separation distance between active BSs (open facilities)
D_{c}	cover distance (maximum distance a facility can serve a customer)
D_{ij}	distance between BS i and BS j
D_M	a large constant ($\geq \max\{D_{ij}\}$)
f_j	fixed cost of opening a facility at site j
$G_{\mathrm{SIR}}(X)$	downlink SIR gain for fraction X of users
$\mathcal{G}_i$	set of facilities that can cover customer i
h_{ij}	number of units of flow between nodes i and j
k_{D}	normalization factor for C_{D}
K	maximum distance between any customer and its serving facility
$\mathcal{L}$	set of active cells
M	number of BSs in the network
$\mathcal{M}_j$	set of users currently served by cell j

N	number of users that can be served per active sector
$\bar{N}(w)$	renewal process
$\mathcal{N}_j$	set of users covered by cell j
p	required number of facilities to be open
P_{C}	common power consumed at a site
P_o	probability of signal outage
P_{pattern}	power consumed per system site for the selected pattern
P_{site}	total power consumed at a fully active site
P_{S}	power consumed per sector
$\mathsf{P}_{\mathrm{X}}(n/m, k/3)$	CSO pattern where n out of m BSs are active and
	k out of 3 sectors are active.
	X is to distinguish between different rotations
r	hard-core distance
R_i	rate (demand) required by user (customer) i
$\mathcal{S}$	set of candidate facility (BSs) locations
$\mathcal{S}_j$	set of users who can be served by cell j
$\mathcal{U}$	set of users (customers)
$\mathcal{V}$	set of connected/served users
W	total system bandwidth
W_j	bandwidth (capacity) of cell (facility) j
x_{ij}	binary variable, = 1 if user i is connected to cell j
$\mathbf{X}$	$= [x_{ij}]$: user-to-cell assignment matrix
y_j	binary variable, = 1 if cell (facility) j is active (open)
z_i	binary variable, = 1 if user (customer) i is covered

α	$= P_{\mathrm{c}}/P_{\mathrm{s}}$
β_{ij}	SNR of user i when connected to cell j
γ_i	SINR between user i and its serving sector
$\gamma_{\max}$	maximum SINR that can be supported
$\gamma_{\min}$	minimum SINR at which a user can receive information
Γ	disc radius for uniform PTL
$\tilde{\Gamma}$	normalized perturbation radius $= \Gamma/\Delta$
δ	ratio of ESEs of two patterns
Δ	inter-site distance between BSs
η_{eq}	equivalent spectral efficiency (ESE)
η_i	spectral efficiency of user i
η_{ij}	spectral efficiency between user i and cell j
η_{th}	spectral efficiency of a central user
λ	BS density
λ_{P}	BS density of a PPP
μ_{D}	mean of the Delaunay edge lengths
ρ	fraction of active sectors or BSs in the network
σ_{D}	standard deviation of the Delaunay edge lengths

Chapter 1

Introduction

Energy efficiency has become an essential performance metric in the design of cellular networks. Cellular operators are looking for ways to improve energy efficiency and reduce their negative environmental impact. Cell switch-off (CSO) approaches are proposed to reduce energy consumption in off-peak periods by switching off some base stations (BSs).

In this thesis, we define an energy-efficient cellular network as one in which as few BSs as possible are switched on while still satisfying all the users demand and quality of service. Throughout this thesis, we use the terms energy efficiency and energy saving interchangeably.

1.1 Motivation

Cellular networks have become the preferred means to access the Internet. The demand for ubiquitous high data rates is increasing exponentially and the paradigm of the cellular network is shifting from principally voice-centric to more data-centric [1]. Fifth generation (5G) wireless networks are expected to support up to 1,000-fold gains in capacity. Several sophisticated techniques are to be employed to achieve this ambitious target. A key enabler to provide high data rates and ubiquitous coverage requirements is by installing small cells more densely (network densification) which can be seen as bringing the network closer to the users in order to improve their received power [2]. However, this introduces a challenge for energy efficiency targets, as the growth of the number of BSs increases the overall energy consumption.

BSs can be seen as the wireless supply and the mobile users as the wireless demand. Outside the peak hours, the wireless demand dramatically drops; yet the wireless

Issues and Challenges

»²¬ Ó»³¾»® xÛÛÛî Hamidreza Boostanimehr, Í¬«¼»²¬ Ó»³¾»® xÛÛÛî
and Vijay K. Bhargava, Ú»´´±© xÛÛÛ

lular networks is a growing
t only maintain profitability,
nment effects. This emerging
cy in cellular networks is
rities and network operators
nologies in order to bring
nfrastructure. In this article,
hods to improve the power
re some research issues and
iques to enable an energy
Since base stations consume
gy used in a cellular system,
ve survey on techniques to
ions. Next, we discuss how
based on micro, pico and
this goal. Since cognitive
disputed future technologies
arch vision to make these
. Lastly, we explore some
a "green" cellular network

tion, energy efficient net-
s, picocells, femtocells, cog-

CTION

been tremendous growth in
mber of subscribers and the
alated astronomically. With
hone devices, use of Ebook
and the success of social
k, the demand for cellular
ntly in recent years. Hence,
e new demands in wireless
hey have to keep their costs

ellular industry has pushed
n wireless networks. There
base stations (BSs) serving
verage of 25MWh per year.
g regions are expected to
in Fig. 1. Information and
already represents around
f which mobile networks
expected to increase every
ental aspects, energy costs

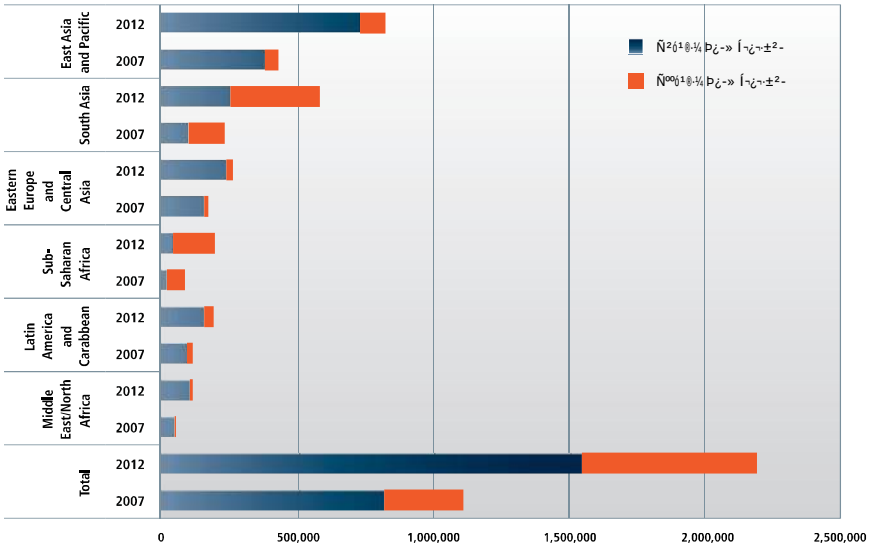

Figure 1.1: Growth in base stations in developing regions (2007-2012) (GSMA Research) [1]

supply, which was designed to match the peak demand, is still consuming close to the peak power. CSO is a promising approach that aims at improving energy efficiency of cellular networks by switching off some BSs during off-peak hours. In other words, CSO attempts to solve the demand-supply matching problem by adjusting the number of active BSs according to the expected demand.

1.2 Energy Consumption in Cellular Networks

The number of BSs in different regions has almost doubled in the period from 2007-2012, as illustrated in Fig. 1.1. On top of network densification, aggressive frequency reuse is adopted to efficiently utilize the scarce spectrum. Although it promises to achieve higher rates, installing more cells results in higher energy consumption and increase in carbon dioxide emissions [3]. This is because BSs consume 50-80% of the total energy in a cellular network [3, 4], as shown in Fig. 1.2.

Energy efficiency has become a major concern in the design of 5G cellular networks [2], therefore, different solutions were proposed to reduce BSs energy consumption, including implementing energy-efficient hardware, utilizing solar energy sources, and

operate, the off-grid BSs in remote areas generally run on diesel power generators and may cost ten times more.

The rising energy costs and carbon footprint of operating cellular networks have led to an emerging trend of addressing energy-efficiency amongst the network operators and regulatory bodies such as 3GPP and ITU [4], [5]. This trend has stimulated the interest of researchers in an innovative research area called "green cellular networks". In this regard, the European Commission has recently started new projects within its seventh Framework Programme to address the energy efficiency of mobile communication systems, viz. "Energy Aware Radio and NeTwork TecHnologies (EARTH)", "Towards Real Energy-efficient Network Design (TREND)" and "Cognitive Radio and Cooperative strategies for Power saving in multi-standard wireless devices (C2POWER)" [6], [7], [8]. "Green radio" is a vast research discipline that needs to cover all the layers of the protocol stack and various system architectures, and it is important to identify the fundamental trade-offs linked with energy efficiency and the overall performance [9]. Figures 2(a) and 2(b) show a breakdown of power consumption in a typical cellular network and gives us an insight into the possible research avenues for reducing energy consumption in wireless communications. In [9], the authors have identified four key trade-offs of energy efficiency with network performance; deployment efficiency (balancing deployment cost, throughput), spectrum efficiency (balancing achievable rate), bandwidth (balancing the bandwidth utilized)

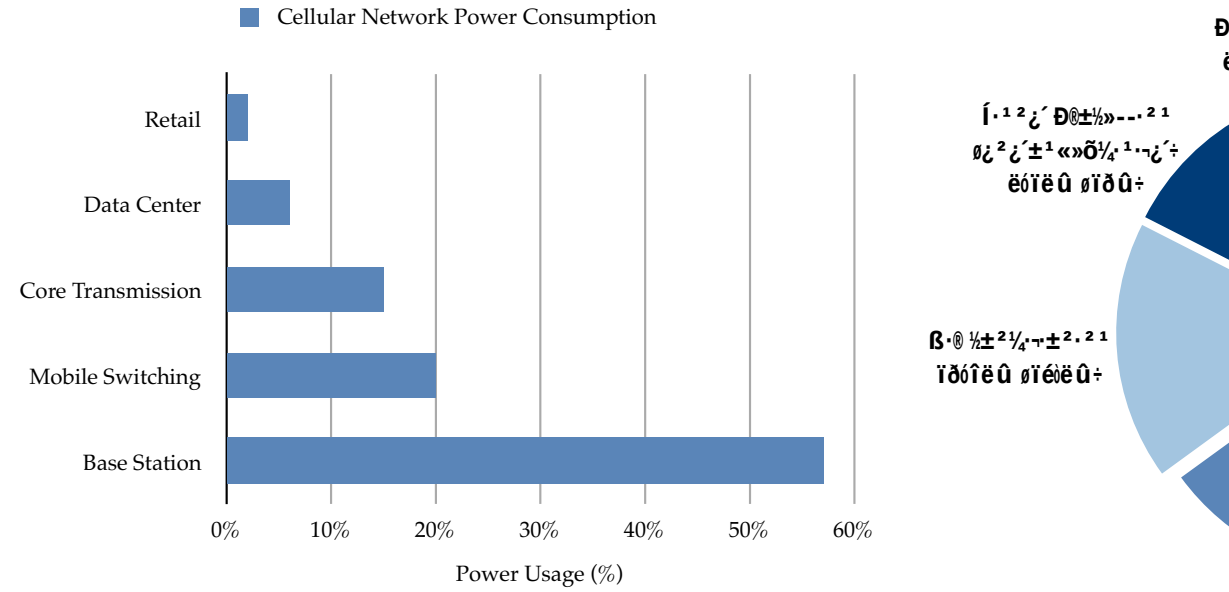

(a) Power consumption of a typical wireless cellular network [2](ref. therein) (b) Power consumption d

Figure 1.2: Power consumption distribution in a cellular network. Source: [3].

Fig. 2. Breakdown of power consumption in a typical cellular network and corresponding base stations

reducing the number of active BSs [3]. Energy consumption of a cell is not proportional to its load level, i.e., a lightly loaded cell consumes approximately the same energy as a fully loaded one [5, 6].

wireless networks and thereby to maintain profitability, it is crucial to consider various paradigm-shifting technologies, such as energy efficient wireless architectures and protocols, efficient BS redesign, smart grids, opportunistic network access or cognitive cooperative relaying, and heterogeneous network deployment based on smaller cells.

1.3 Cell Switch-Off: An Energy Saving Approach for Cellular Networks

Among all the promising energy saving techniques, cognitive radio and cooperative relaying, although already getting matured in many aspects, but still are in their infancy when it comes to the deployment issues in cellular networks. Therefore, it is crucial to promote the potentials of these techniques in cellular wireless networks. Moreover, it is necessary to be aware that still many energy concerns in cognitive and cooperative networks have remained as unanswered challenges, which raises the importance of further exploring these concerns.

Strategically switching off cells in off-peak times is an important way of improving the energy efficiency of cellular networks. Choosing which cells to switch off when is a research topic known as CSO. During the planning phase, cells are deployed in large numbers to cope with the peak traffic times. Therefore, some cells become underutilized or even redundant outside the peak traffic. Despite being underutilized, these cells still consume a major portion of their peak energy [5, 6].

This excessive energy consumption conflicts with the energy efficiency targets of 5G networks[2]. Therefore, the CSO approach was proposed [7] to save energy by entirely switching off some cells and handover their users to neighbouring cells without violating the quality of service (QoS) in the network.

In this paper, we provide a brief survey on some of the work that has already been done to achieve power efficiency in cellular networks, discuss some research issues and challenges and suggest some techniques to enable an energy efficient or "green" cellular network. We also put a special emphasis on cognitive and cooperative techniques, in order to bring attention to the benefits cellular systems can gain through employing such techniques, and also highlight the research

Implementing CSO approaches is not expected to be a challenging task. In particular,

management, using
some simple archite
energy efficiency fr
we discuss how diff
smaller cells can
of a wireless syste
explain the use of
as cognitive radio
communication in c
this idea further in
where we discuss h
both cognitive and
energy efficient at
energy spectrum se
and routing, efficien
and addressing unce
context. Some broad
and conclusions are

II. Measu

Before starting a
first question natura
is "green"? How d
"greenness" in telec

switching off at inappropriate times and locations may deteriorate the overall system performance. Although relatively new, several CSO approaches have been proposed to tackle CSO issues from different angles (see survey papers [8, 9] for details).

Alternative terms for CSO: Other terms are sometimes used the literature when referring to CSO and similar concepts; some of these terms are cell shaping, topology adaptation, network restructuring, load concentration, network adaptation, BS management, BS switching, cell zooming, and BS sleep mode.

1.3.1 CSO Classifications

There are two main CSO categories: online and offline.

Whereas *online* CSO, based on immediate user demands and channel states, is problematic to implement and difficult to model, *offline* CSO [10–17] is more practical and tractable. Furthermore, it is known that regular cell layouts generally provide the best coverage and spectral efficiency [2], which leads us to preferring regular static (offline) CSO.

1.3.1.1 Online CSO

In online CSO, an algorithm is executed in real time to determine the set of cells to be switched off. This requires global knowledge of channel state information between each user and each cell, as well as the load levels of all cells in the network. It is difficult for this vast amount of information to be exchanged by the network in a timely manner [8]. The computational time for the optimization might also be prohibitive for large networks. Finally, another challenge in online CSO is interference modeling, due to the fact that the set of active cells is not known a priori.

Several algorithms were proposed to implement the dynamic CSO, and most of them rely on heuristic methods [7, 18, 19]. Using heuristics is reasonable in such complicated scenarios as they provide good solutions in a timely manner. A simple greedy-drop algorithm was proposed in [7] and was dubbed *cell-zooming*. In this algorithm, cells are sequentially switched off, based on their loads starting with the least loaded one. The algorithm terminates when it encounters the first cell that cannot be switched off because one or more of its users cannot be served by any of the neighboring cells. An improved version of this algorithm, *improved cell-zooming*, was proposed in [18]; performance enhancement was obtained by slightly adjusting

the termination criterion such that the algorithm does not terminate prematurely, but rather checks all the cells in the network for possible switch-off. Applying this new termination criterion resulted in more energy saving, by switching off more cells. A greedy-add algorithm was proposed in [19] to switch on as few cells as possible to accommodate all the demand. Cells are switched on based on their load and the algorithm terminates when every user is assigned to an active cell. Other different algorithms inspired from other fields of research were considered to tackle the CSO approach, e.g., a utility-based algorithm [20] and a genetic algorithm [18]. The common practice is to switch off cells based on their current load [7, 18, 19].

Online CSO is also known as *dynamic* CSO [9] and can be further classified as *fast-reaction* or *slow-reaction*.

Fast Reaction Online CSO In fast reaction online CSO, the algorithms are supposed to adapt quickly to changes in the current user demand and attempt to find the combination of active cells that results in the best energy saving [21]. This category allows for a fast change in the network configuration (within a few seconds at most).

Slow Reaction Online CSO In slow reaction online CSO, the change in the network configuration requires a relatively longer time and only allows for long term changes (within tens of seconds to minutes). These algorithms operate based on the average traffic measures or available user demand statistics, usually relying on predicting user density at certain times.

Another important obstacle to the practical implementation of online CSO is the time required for the on-off/off-on switching of BSs and for completing the handover procedures [22].

1.3.1.2 Offline CSO

One important issue in CSO is interference modelling, which is challenging because it is hard to know the set of active cells a priori. Typically, users are assigned to the best sector in terms of downlink signal-to-interference-plus-noise ratio (SINR). However, when switching off a cell, its users need to be reassigned to another, perhaps less advantageous, cell. Without a proper interference characterization, these users might encounter a large amount of interference because the set of active cells that contribute to the interference is only known at the final stage. The predicted performance is

hence inaccurate. Indeed, some CSO approaches assume zero interference, i.e., there is a perfect inter-cell interference coordination (ICIC) [5, 7]. This assumption is too optimistic and produces an unachievable upper bound on the number of switched-off cells. Other approaches model interference by assuming that all cells fully contribute to the interference, as if they were active all the time [18]. This assumption yields a poor lower bound on the number of switched-off cells.

One accurate way to model interference, thus alleviating the aforementioned problem, is by predetermining the set of active cells, i.e., the cells that actually generate the interference in the system. This is sometimes referred to as offline or static CSO [8,9]. It is possible to predetermine several configurations of active cells for different traffic densities and then select an appropriate configuration to accommodate the specific demand distribution.

It is possible to predetermine several sets of active cells for different traffic densities and then select an appropriate set to accommodate the current traffic density.

In offline CSO, different sets of active cells are predetermined offline, and the operator choses the appropriate set to accommodate the current traffic density [10]. Only information related to the predetermined set of active cells is needed. Offline CSO is usually applicable for longer time scales (hours) and is often based on historical load distribution.

Offline CSO is also known as static CSO [9] and can be further classified as *static* or *regular static* CSO.

Static CSO Static CSO is different from online CSO because the network configuration remains static for a long period of time. Therefore, the interference could be modelled appropriately (in statistical terms) by considering only the predetermined set of active cells [6].

Static CSO can be seen as a cell planning problem, but with a constrained set of BS locations. While in cell planning the cell placement is based on a wider set of possible locations, here the candidate locations are restricted to actual sites of BSs, from which a subset is chosen to be active.

Regular CSO Regular CSO [10–17] is a special case of static CSO, also known as *CSO patterns*. Besides being predetermined offline, the set of active cells is selected according to a periodic spatial pattern [9]. Regular CSO patterns resemble the intuitive well-known frequency reuse patterns [11].

By applying regular CSO, the choice of active cells minimizes coverage holes. This aspect is usually overlooked in the literature [23]. Also, regular CSO is more energy-efficient for users in the uplink, as there is always a nearby active cell [24,25]. Regular CSO patterns reduce the signal interference between cells due to the careful selection of active BSs so that their are located as far away from each other as possible. The patterns are conceptually simple and can be described in a systematic way. Regular Static CSO is useful when the user distribution is approximately uniform in space.

The effect of different CSO patterns on the outage probability is investigated in [10, 11], while the effect on the blocking probability is studied in [12, 14]. Authors in [16] introduce a set of CSO patterns and propose a scheduler to jointly ensure full coverage for both downlink and uplink.

In the context of regular static CSO, sector-based CSO may offer additional opportunities for energy saving that have not been explored, therefore we examined them in Chapter 5.

1.3.1.3 Hybrid CSO

For best system performance, it might be necessary to have a hybrid CSO approach, where an online CSO algorithm is executed on top of the offline one. Hybrid approaches have a static set of active cells to provide coverage and collect network information. The remaining cells participate in an online CSO algorithm to accommodate the fast variability in the demand distribution [10]. Hybrid CSO is particularly useful when users are non-uniformly distributed in space.

1.3.2 Switching Off Sectors

Most of the research in online CSO is executed in a sector-based manner, i.e., each sector can be turned off individually [6, 18]. To the best of our knowledge, this is not the case for regular CSO patterns, where only the entire BS is turned off; i.e., individual sector switch-off is not considered in literature. Regular CSO patterns with individual sector switch-off can be efficient in several interesting cases. In our simulation, each BS site has three 120°-sectors and the azimuth orientation of the sectors is the same for all sites. We are the first to investigate sector-based regular CSO patterns, as detailed in Chapter 5.

1.4 Thesis Contribution

This thesis contributes to the current state of knowledge by directing the CSO research towards a more realistic, feasible, and practical implementation. We do this by arguing for employing offline (static) CSO and for considering spatially irregular BS deployments.

This thesis started by investigating the dynamic CSO, the most commonly used category. We identified some practical difficulties with dynamic CSO, therefore, we moved on to study regular static CSO patterns. Still the underlying assumption was that the BSs are regularly placed in a hexagonal layout. Hence, we then focused on testing static CSO algorithms for networks with spatial irregularly deployed BSs.

At each phase of the thesis, the advantages and disadvantages are highlighted with some possible extensions.

1.4.1 Contributions in Detail

In this thesis, we study CSO as a promising approach for energy-efficient cellular networks. The concept is simple: During low traffic periods, some BSs are switched-off to save energy. Throughout the course of this thesis, we start the study with designing a dynamic CSO algorithm that is based on a well-known mathematical tool from the field of operation research. The interference modelling is very challenging as the active cells which contribute to the interference are not known a priori. Therefore, we relied on a simplified assumption of perfect interference coordination.

Motivated to overcome this challenge of interference modelling, we study CSO patterns which predetermine the set of active cell offline and hence the interference can be properly modelled. These offline approaches do not require the extra-fast time needed for online algorithms that adapt to fast changes in demand distributions. Besides being predetermined, the active cells are selected so that their locations form a regular grid. Based on the traffic density levels, it is possible to predetermine several configurations, and operators can then select the appropriate configuration to accommodate the current demand density.

In current cellular networks, the locations of BSs are not regular; however, the underlying assumption of the CSO patterns is that the original network layout is regular. This regularity facilitates the achieving of regular layout after CSO. This encourages us to investigate the possibility of applying the CSO approach to networks

with spatially irregular BS deployments. Therefore, we evaluate the suitability of several heuristic algorithms to be adopted for CSO for networks with irregular BS deployments with the extra objective of making the locations of active cells as close to regular as possible. We conclude the study by demonstrating the effect of some of these algorithms when applied to simulated BS locations, as well as real BS locations obtained from two major cellular operators in Canada.

In this section, we highlight the contributions of the main chapters of the thesis as follows:

1. The major contributions of Chapter 3 are:

    - Introducing the facility location problem (FLP) as an efficient tool in the context of CSO. We used two basic models of the FLP to formulate the problems in both Chapter 4 and Chapter 6.
    - Summarizing several FLP models and highlighting some possible applications in cellular networks.

2. The major contributions of Chapter 4 are:

    - Implementing the CSO approach as a set cover problem (SCP), which is a basic model of the FLP, and proposing a greedy-add algorithm that provides a good solution.
    - Investigating different cell sorting criteria (the order in which cells are switched on) and comparing their impact on energy saving.
    - Providing an overview of the applications of the set cover problem in wireless networks.

3. The major contributions of Chapter 5 are:

    - Investigating sector-based regular CSO patterns, where not only entire BSs could be switched off, but their individual sectors too. Note that switching off sectors individually is a common practice in online CSO literature.
    - Analytically comparing site-based versus sector-based CSO patterns in terms of energy efficiency. Because switching off one sector in three per BS does not necessarily result in one-third of energy saving, we take into account the power consumption of the common hardware shared between sectors of the same site.

- Comparing the performance of different CSO patterns in terms of the number of supported users. We introduce a novel metric, the *equivalent spectral efficiency* (ESE): the mean performance of a given pattern can be captured using only this one metric, abstracting from the bandwidth and the rate; the ESE is proportional to the mean number of supported users. We used a realistic and complex channel model [26], which makes the ESE analytically intractable. As such, we obtain the ESE values using simulation. From the simulated values, we analytically obtain the distribution of the number of users using renewal process theory, which is a novel tool in this context. We illustrate this in detail with a case study.
- Organizing the existing and newly introduced patterns using a systematic nomenclature.

4. The major contributions of Chapter 6 are:

   - Testing the suitability of several algorithms for applying CSO to irregular network layouts with the objective of making the active BS locations as spatially regular as possible. The problem is formulated as a p-dispersion problem (PDP), which is a basic model of the FLP.
   - Finding the optimal algorithms for different amounts of regularity and percentages of switched-off cells.
   - Observing the qualitative behaviour of these algorithms when applied to both simulated and real BS locations.

1.5 Publications from this Thesis

WCL2'16 Quoc-Nam Le-The, Tamer Beitelmal, Faraj Lagum, Sebastian Szyszkowicz, and Halim Yanikomeroglu, "Cell switch-off algorithms for spatially irregular base station deployments", under review in *IEEE Wireless Communications Letters* (submission: 31 October 2016, 1st results: 16 December 2016).

WCL1'16 Faraj Lagum, Quoc-Nam Le-The, Tamer Beitelmal, Sebastian Szyszkowicz, and Halim Yanikomeroglu, "Cell switch-off for networks deployed with variable spatial regularity", under review in *IEEE Wireless Communications Letters* (submission: 03 October 2016, 1st results: 01 November 2016, 1st revision: 07 January 2017).

TWC'16 Tamer Beitelmal, Sebastian Szyszkowicz, David Gonzalez G, and Halim Yanikomeroglu, "Sector and site switch-off regular patterns for energy saving in cellular networks", under review in *IEEE Transaction on Wireless Communications* (submission: 11 October 2016).

VTC'16 Tamer Beitelmal, Sebastian Szyszkowicz, and Halim Yanikomeroglu, "Regular and static sector-based cell switch-off patterns", *IEEE Vehicular Technology Conference (VTC2016-Fall)*, September 2016, Montreal, QC, Canada.

CORS'14 Tamer Beitalmal and Halim Yanikomeroglu, "Energy saving in cellular networks by modeling the cell switch-off approach as a set cover problem", *Canadian Operational Research Society (CORS) International Conference (Network Planning Session)*, May 2014, Ottawa, Canada.

ICC'14 Tamer Beitalmal and Halim Yanikomeroglu, "A set cover based algorithm for cell switch-off with different cell sorting criteria", *IEEE International Conference on Communications Workshop (ICC Workshop on Small Cell and 5G Networks)*, June 2014, Sydney, Australia.

VTC'12 Rainer Schoenen, Gurhan Bulu, Amir Mirtaheri, Tamer Beitelmal, and Halim Yanikomeroglu, "First survey results of quantified user behavior in user-in-the-loop scenarios for sustainable wireless networks", *IEEE Vehicular Technology Conference (VTC-Fall)*, September 2012, Quebec City, Quebec, Canada.

ICC'12 Tamer Beitelmal, Rainer Schoenen, and Halim Yanikomeroglu, "On the impact of correlated shadowing on the performance of user-in-the-loop for mobility", *IEEE Workshop on User-Centric Networking (ICC U-NET workshop)*, June 2012, Ottawa, Canada.

EW'12 Rainer Schoenen, Gurhan Bulu, Amir Mirtaheri, Tamer Beitelmal, and Halim Yanikomeroglu, "Quantified user behavior in user-in-the-loop spatially and demand controlled cellular systems", *European Wireless Conference (EW)*, April 2012, Poznan, Poland.

1.6 Thesis Summary

This thesis is organized as follows: the channel model and simulation setup model are described in Chapter 2. Chapter 3 introduces the FLP which is a useful mathematical tool for locating facilities (BSs in this context). Two versions of the FLP are found very similar to the problems introduced in Chapters 4 and 6. Chapter 4 is about dynamic CSO, where we use the SCP to model dynamic CSO. Chapter 5 investigates the sector-based regular static CSO patterns. Chapter 6 evaluates some heuristic algorithms to apply CSO for irregular BS deployments. The thesis ends with the conclusion and future work in Chapter 7.

1.6.1 Chapter 2

In order to study, compare, and evaluate different CSO algorithms, we first design a system-level simulation platform according to the long term evolution (LTE) standards. We calibrate our simulated SINR curves were calibrated against the SINR CDFs obtained from WINNER+ partners.

1.6.2 Chapter 3

In order to formulate the CSO problem, we found a well-studied optimization problem that has a similar objective to CSO, which is managing facility locations. This problem is called the FLP and is well-known in the fields of operation research and decision making [27]. We introduce the FLP in this Chapter and highlight its different models with possible application in cellular networks. Among the different FLP models, we used the the SCP formulation to model and solve a dynamic CSO approach in Chapter 4; also we used the PDP to formulate the CSO approach for irregular BS deployment in Chapter 6.

1.6.3 Chapter 4

In dynamic CSO, an algorithm is executed in real time to determine the set of cells to be switched off. This requires global knowledge of the channels between each user and each BS, in order to execute the CSO algorithm. Dynamic CSO allows for a fast change in the set of active BSs to adapt to the rapid changes in immediate user demand. We found that, this problem formulation is similar to the well-known SCP

mathematical tool. We devised a heuristic algorithm that is designed for the SCP to jointly solve the dynamic CSO and user-to-BS assignment problems. Our algorithm outperforms a benchmark algorithm. Another important aspect we investigate here is the cell sorting criterion, which is the order in which BSs are selected to be switched on. The common criterion is to switch off cells based on their current load, which, as our results show, might not always be the best criterion. We faced two major challenges while working with dynamic CSO; the first one is interference modelling, since the set of active BSs is not known a priori. The second challenge is adapting to the fast changes in the users' arrivals and departures, and the computational cost of executing the algorithm online.

1.6.4 Chapter 5

One accurate way to model interference properly is by predetermining the set of active cells (configurations), which are the cells that actually generate the interference in the system. Based on the traffic density levels, it is possible to predetermine several configurations, and operators can then select the appropriate configuration to accommodate the current traffic density. Static CSO is usually designed for longer time scales (hours) and often based on historical load distributions. Regular static CSO is a special case of static CSO, also known as CSO patterns. Regular CSO patterns are advantageous in terms of modeling interference properly, reducing coverage holes, and making the uplink transmissions more energy-efficient for users in the uplink as there is a guaranteed maximum distance to an active (nearby) BS. We introduce sector-based regular CSO patterns for the first time. We organize the existing and newly introduced patterns using a systematic nomenclature; studying 26 patterns in total. We compare these patterns in terms of energy efficiency and the average number of users supported, via a combination of analysis and simulation. We also compare the performance of CSO with two benchmark algorithms. We show that the average number of users can be captured by one parameter. Moreover, we find that the distribution of the number of users is close to Gaussian, with a tractable variance. Our results demonstrate that several patterns that activate only one out of three sectors per BS are particularly beneficial. For instance, the network can support half the users with only one third of the sectors on; such CSO patterns have not been studied before.

1.6.5 Chapter 6

In most of the CSO literature, the BS deployment is usually assumed to follow a regular grid or sometimes a fully random (Poisson point process) placement. Given that the best network performance can be achieved when BSs are located on a regular grid, we evaluate different algorithms for applying CSO to irregular network layouts with the objective of making the active BS locations as regular as possible. This problem has been introduced only recently. We test the suitability of several CSO algorithms from the literature of facility location management for this new problem. We also evaluate a recent algorithm which performs very well when the number of BSs to switch off is high. We vary the amount of spatial regularity of the BS locations from perfectly regular to totally random. Moreover, we also demonstrate some algorithms on real BS locations obtained from two major cellular operators in Canada.

1.6.6 Appendix A

In Appendix A, we touched on improving the efficiency at the demand side by including the users as active participants of the system, not just as consumers. The user-in-the-loop (UIL) concept was proposed to incentivize users to assist the cellular network when needed. If some users are willing to assist the network, by changing physical location or postponing their data request, then some radio resources could be saved. These saved resources might be used to provide higher data rates or to serve more users. We analyze the UIL concept in a more realistic environment by integrating the effect of spatially-correlated shadowing. We also evaluate the impact of the shadowing model on the resulting average moving distance for users, considering both cases of uncorrelated and spatially-correlated shadowing.

1.7 Thesis at a Glance

The organization of the thesis is illustrated in Fig. 1.3, which shows the chapters of the thesis and how they are related, providing the related publications.

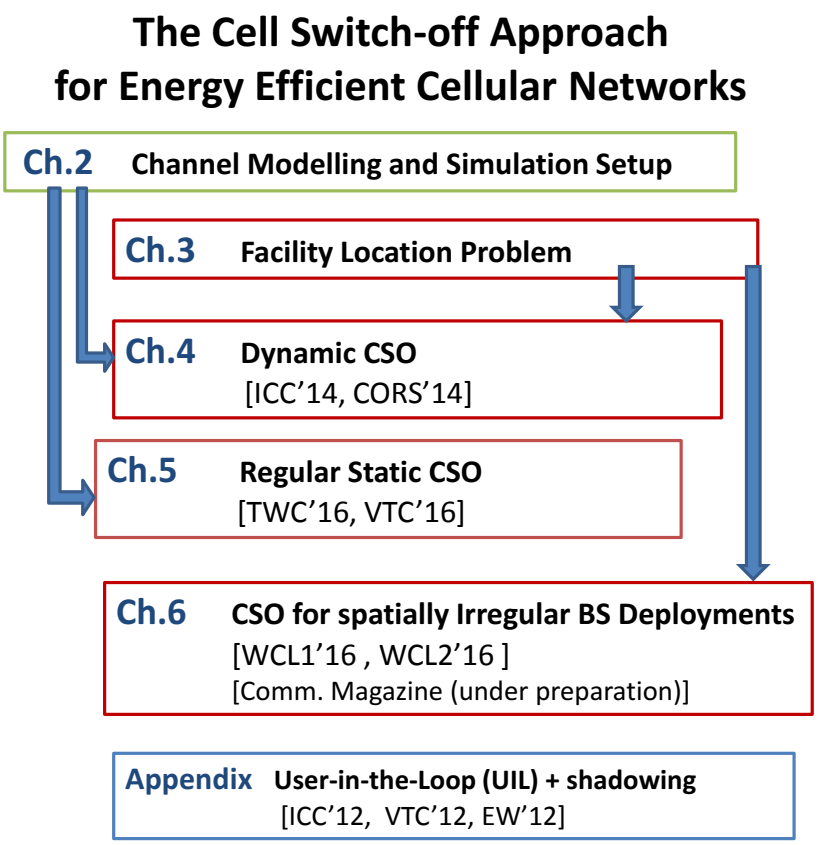

Figure 1.3: Thesis at a glance.

Chapter 2

Simulation Setup

2.1 Introduction

A realistic and validated simulation platform is necessary to ensure accurate results when applying, testing, and comparing different algorithms. In Chapters 4 and 5, we consider a cellular network based on the guidelines of the International Mobile Telecommunications-Advanced (IMT-Advanced) [26]. These guidelines provide details on how to realistically model the wireless channel between the transmitter and the receiver. We design a system-level simulator to evaluate the downlink system performance of a cellular network.

The problems we consider throughout this thesis operate on a slow time scale; therefore, it is not necessary to take into account small scale variation when evaluating our algorithms.

Our results are based on a snapshot analysis, where users are randomly uniformly distributed over the network area and assumed to be fixed with all channel conditions unchanged for the snapshot duration. Then we obtain all channel measurements between users and BSs including distance, antenna gain, pathloss, large scale shadowing and received power.

The simulation parameters described in this chapter are generally used, unless specified inside the chapter. However, the network layout varies in each chapter, depending on the nature of the problem, and is explained in each chapter. Also, the spatially-correlated shadowing model is not always the same; in particular, in the appendix, a different shadowing model is implemented, and is explained in detail therein.

2.2 Channel Model

We now describe the two test environments used in the thesis, namely: *urban micro-cell* (UMi) and *urban macro-cell* (UMa).

The UMi scenario describes a dense small cell implementation, with high user density and low-to-no mobility. This is a typical representative of city centres in a dense urban region. The distinct characteristic of this environment is high traffic load. This scenario is interference-limited. Micro cells are installed outside and below rooftops, where the line-of-sight (LOS) condition is not common due to obstacles.

The UMa scenario describes large cell implementation for continuous coverage, where BSs are located above rooftops, non-LOS (NLOS), or obstructed LOS, condition is common. This scenario is interference-limited as well.

The general simulation parameters for the channel models of IMT-Advanced are listed in Table 2.1. The system is reuse-one, i.e., the whole spectrum is used in each cell.

2.2.1 Pathloss and Shadowing Model

Our essential performance metric is the downlink signal-to-noise-plus-interference ratio (SINR), which is the ratio of the average power received from the serving cell to the sum of the average powers received from all other cells, plus the noise power at the receiver. The average received power P_r by a user is calculated in a simple way, and without loss of generality, from the following equation:

$$P_r \text{ [dB]} = P_t + G_t + G_r - PL + X_i, \tag{2.1}$$

where: P_t is the transmitted power in dB, G_t is the transmitter antenna gain, G_r is the receiver antenna gain, and PL and X_i are the distance-dependent pathloss and the shadowing effect; their expressions are provided later. The antenna patterns used in our simulation are the same as described in in [26, Sec. 8.5.1].

The propagation conditions are based on the LOS and the NLOS cases. To find the pathloss, we first determine the LOS probability.

Table 2.1: Simulation Parameters for UMi and UMa Scenarios

Parameter	Setting	
ITU scenario	UMi	UMa
Cell transmitted power	41 dBm	46 dBm
Inter-site distance	200 m	500 m
BS antenna height	10 m	25 m
Maximum forward-to-backward	20 dB [26, Sec. 8.5]	
user antenna height	1.5 m	
Carrier frequency	2.5 GHz	2 GHz
User distribution	independent and uniform	
Probability of indoor user	0.5	0
User noise figure	5 dB	
BS noise figure	7 dB	
Thermal noise	-174 dBm/Hz	
LOS shadowing spread	3 dB	4 dB
NLOS shadowing spread	4 dB	6 dB
LOS correlation distance	10 m	37 m
NLOS correlation distance	13 m	50 m
SINR range	[-7, 18] dB	
Traffic type	full queue	
LOS pathloss model	(2.3), (2.4)	
NLOS pathloss model	(2.5)	(2.6)
Antenna gain (boresight)	17 dB_i	
Antenna tilt	-12° [28]	
Antenna aperture, horizontal	70°	
Antenna aperture, vertical	15°	
Loss through wall	20 dB	N/A

2.2.1.1 Probability of Line-of-Sight

After placing each user, we find the distance d between that user and the BS. Based on this distance, the probability of LOS is then calculated according to

$$P_{\text{LOS}}(d) = \min(18\,\text{m}/d, 1)(1 - e^{-d/d_0}) + e^{-d/d_0}, \tag{2.2}$$

where $d_0 = 36\,\text{m}$ for the UMi scenario, and 63 m for the UMa scenario. Based on this probability, we decide if a user has a LOS signal to the transmitting BS or not, and calculate the pathloss accordingly.

2.2.1.2 Pathloss

The pathloss calculation depends on the LOS probability, the pathloss exponent, and the distance to the transmitter. The pathloss is measured in dB in the following equations. For the LOS case, both the UMi and UMa have the same expressions, which depend on the breakpoint distance $d'_{BP} = 4h'_{BS}h'_{user}f_c/c$, where f_c is the carrier frequency, $c = 2.998 \times 10^8$ m/s is the propagation velocity in free space, and h'_{BS} and h'_{user} are the effective heights of the BS and user antennas, respectively, and calculated by subtracting 1 meter from the actual antenna height [26]. If a user is receiving a LOS signal from the transmitter, then its pathloss is calculated as

$$\text{PL}_{\text{LOS}}(d) = 28.0 + 22.0\log_{10}(d) + 20\log_{10}(f_c), \qquad \text{for } d < d'_{BP}, \tag{2.3}$$

and,

$$\begin{aligned}\text{PL}_{\text{LOS}}(d) = {} & 7.8 + 40\log_{10}(d) - 18\log_{10}(h'_{\text{BS}}) \\ & - \ 18\log_{10}(h'_{\text{user}}) + 2\log_{10}(f_c), \qquad \text{for } d > d'_{BP}.\end{aligned} \tag{2.4}$$

If a user is receiving a NLOS signal, there are different expressions to calculate the pathloss in UMi and UMa. For UMi, the pathloss is given by

$$\text{PL}_{\text{NLOS}}(d) = 22.7 + 36.7\log_{10}(d) + 26\log_{10}(f_c), \tag{2.5}$$

while for the UMa, the NLOS pathloss is given by

$$\begin{aligned} \mathrm{PL}_{\mathrm{NLOS}}(d) = \; & 161.04 - 7.1\log_{10}(w) + 7.5\log_{10}(h) \\ - \; & (24.37 - 3.7(h/h_{\mathrm{BS}})^2)\log_{10}(h_{\mathrm{BS}}))(\log_{10}(d) - 3) \\ + \; & 20\log_{10}(f_c) - (3.2(\log_{10}(h_{\mathrm{user}}))^2 - 4.97), \end{aligned} \tag{2.6}$$

where h_{BS} and h_{user} are the antenna heights of BS and user, respectively; $h = 20$ m is the average building height, and $w = 20$ m is the street width.

2.2.1.3 Shadowing Model

The shadow fading X_i is measured in dB, and assumed to be log-normal, with zero-mean and with standard deviation given in Table 2.1 depending on the propagation case. The shadowing is used to consider the effect of obstacles between transmitter and receiver. The fading values of adjacent receivers are correlated. The correlated shadowing is calculated as a function of the distance Δx between two receivers and is described by

$$R(\Delta x) = e^{-|\Delta x|/d_{cor}}, \tag{2.7}$$

where d_{cor} is the correlation distance tabulated in Table 2.1. Besides the correlation between one BS and many receivers, there is the correlation among BSs, which is assumed to be 50%.

2.3 User Distribution and SINR Ranges

Users are independently and uniformly distributed in the region of interest. the users' traffic profile is assumed to be full buffer with infinite queue, i.e., there is always a packet to be sent and there is no packet loss.

User-to-cell assignment is based on the strength of the received power, i.e., users are connected to the cell that provides them with the strongest received power. Each user is assumed to have a minimum rate requirement that is needed in order to guarantee its quality of service (QoS).

The relationship between the SINR values and the corresponding spectral efficiencies γ is summarized in Table 2.2, and is based on the adaptive modulation and coding (AMC) scheme. The highest γ of 5 bps/Hz is achieved when using 64QAM with a coding rate of 5/6. On the other extreme, a γ as low as 2/3 bps/Hz is obtained

from QPSK with a 1/3 coding rate.

Table 2.2: AMC scheme based on SINR intervals in LTE.

Index m	1	2	3	4	5	6	7	8
SINR[dB]	0.9	2.1	3.8	7.7	9.8	12.6	15.0	18.2
Modulation	QPSK			16QAM			64QAM	
Coding Rate	1/3	1/2	2/3	1/2	2/3	5/6	2/3	5/6
$\gamma[b/s/Hz]$	2/3	1	4/3	2	8/3	10/3	4	5

Among the users that select to be connected to a sector j, some of them might have a very weak SINR ($< \gamma_{\min}$); below this value, a user cannot receive any useful communication and is considered in outage. Other users might have very high SINR values ($> \gamma_{\max}$), which is higher than what the current constellations can use; therefore, these values are truncated to $\gamma_{\max}$. For LTE networks, typical values for $\gamma_{\min}$ and γ_{max} are -7 dB and 18 dB, respectively [28, 29].

2.4 Calibration

In this section, we validate our results for the UMi scenario for a network layout consists of 19 BS sites with three 120° sectors at each BS, with the whole spectrum reused at each sector (reuse-one), as shown in Fig. 2.1. In reality, this network represents just a sample of the network, and this network will be extended in all directions to cover a whole city.

Our simulation is wrapped-around to avoid edge effects. The wrap-around is necessary in particular so that each cell will experience the same level of interference. For example, if we look at cell 57 in Fig. 2.1, without a wrap-around, it will only have three neighbouring interferers whereas cell 1 will have 7 neighbouring interferers. With wrap-around, each cell will have the same number of interferers so that the cells are equivalent.

We place many users uniformly in the network area, and then each user determines its best sector based on the received power values. At each sector j, we randomly select 10 users from the those who chose sector j as the best serving sector. This is done mainly to avoid bias towards users with high received power.

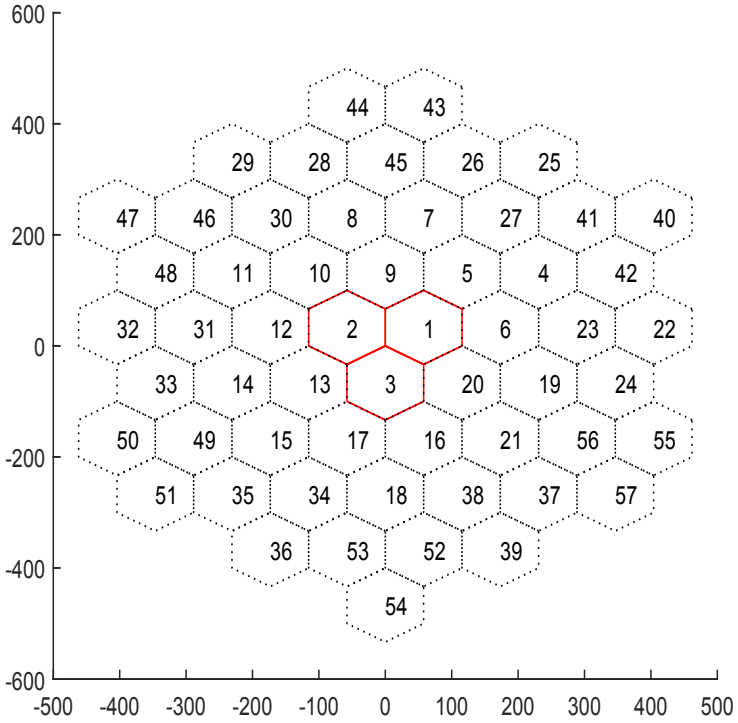

Figure 2.1: A network layout consisting of 19 BSs (57 hexagonal sectors).

The implementation of the wrap-around is checked by comparing the SINRs of different ring of sectors (sectors 1, 2, and 3 represents the first ring). Fig. 2.2 illustrates that the cumulative distribution function (CDF) of the SINR from different rings are matched, meaning that our wrap-around is working, and there is no edge effect in the obtained results.

To calibrate our simulation platform, we compare our results with the simulated SINR CDF obtained from the WINNER+ project partners using multiple simulation tools [28]. As shown in Fig. 2.3 the SINRs obtained by our simulator closely matches the WINNER+ results.

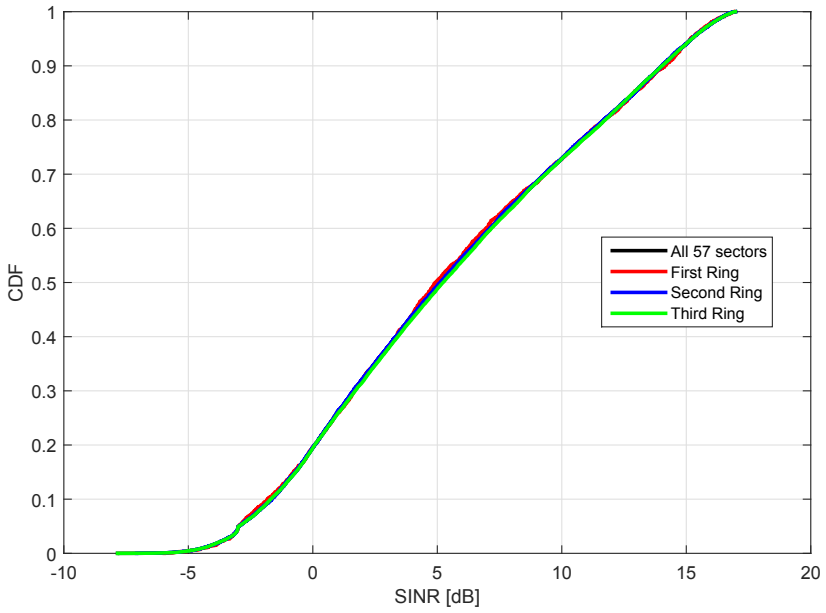

Figure 2.2: CDFs of SINR for different rings of sectors for the network layout in Fig. 2.3, to check the effectiveness of the wrap-around in avoiding the edge-effect.

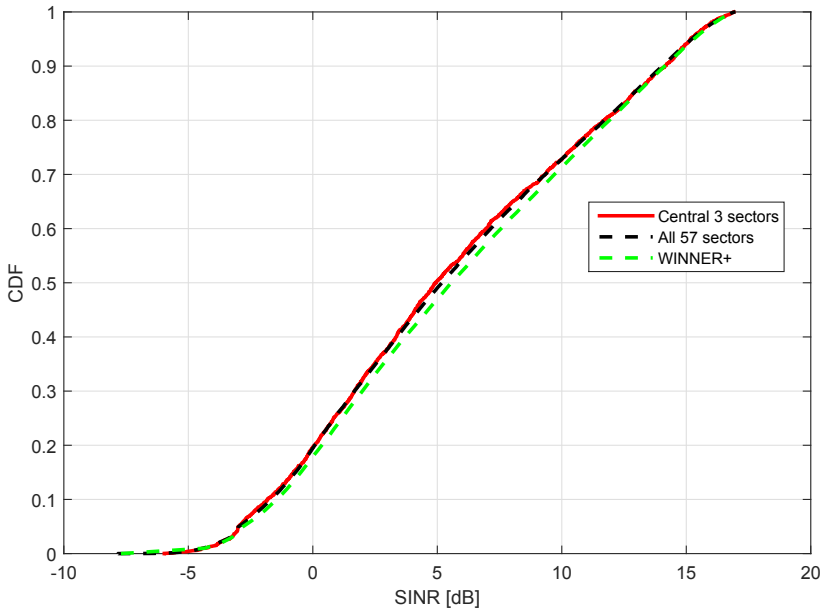

Figure 2.3: CDF of SINR for the network layout in Fig. 2.1 for the UMi scenario, with WINNER+ calibration.

Chapter 3

Mathematical Tool: Facility Location Problem

In order to formulate the CSO problem, we found a well-studied optimization problem that is very similar to CSO. This problem is called the facility location problem (FLP) and is well-known in the fields of operation research and decision making [27]. We introduce the FLP in this chapter and highlight its different types with possible application in cellular networks. We used two of the FLP model formulation in Chapters 4 and 6. We then made the analogy between FLP and CSO in Section 3.3.

The FLP is a combinatorial optimization problem that has been used in several problems, ranging from the traditional application of optimizing warehouse locations, to a modern application like microchip manufacturing [27].

The general FLP is formulated as choosing a subset of the facilities to be open, given a set $\mathcal{S} = \{s_1, .., s_m\}$ of potential facility locations and a set of demand points (*customers*) $\mathcal{U} = \{u_1, .., u_n\}$ which are served by the facilities. The objective is to minimize the total cost of serving all customers, while solving the assignment problem of which customer should be served by which facility. Fig. 3.1 is a graphical representation of the FLP and a possible assignment between facilities and customers. Each facility has an *opening cost* f_j. There is also the *connection cost* c_{ij}, which is the cost of connecting a customer i to the serving facility j, e.g., transportation cost.

Table 3.1: List of Symbols in FLP.

Symbol	Description
$\mathcal{U}$	set of customers
$\mathcal{S}$	set of candidate facility locations
f_j	fixed cost of opening a facility at site j
d_{ij}	distance between customer i and facility j
c_{ij}	cost of connecting customer i to facility j
D_{c}	cover distance (maximum distance a facility can serve a customer)
$\mathcal{G}_i$	$\{j \mid d_{ij} \leq D_{\mathrm{c}}\}$, set of facilities that can cover customer i
K	maximum distance between any customer and its serving facility
y_j	$= \begin{cases} 1 & \text{if a facility is opened on location } j \\ 0 & \text{otherwise} \end{cases}$
x_{ij}	$= \begin{cases} 1 & \text{if customer } i \text{ is assigned to facility } j \\ 0 & \text{otherwise} \end{cases}$
R_i	demand of customer i
p	required number of facilities to be open
z_i	$= \begin{cases} 1 & \text{if customer } i \text{ is covered} \\ 0 & \text{otherwise} \end{cases}$
D_M	a large constant ($\geq \max\{D_{ij}\}$)
D	minimum separation distance between any pair of facilities
W_j	capacity of facility j
C	cost per unit demand per unit distance
h_{ij}	number of units of flow between nodes i and j

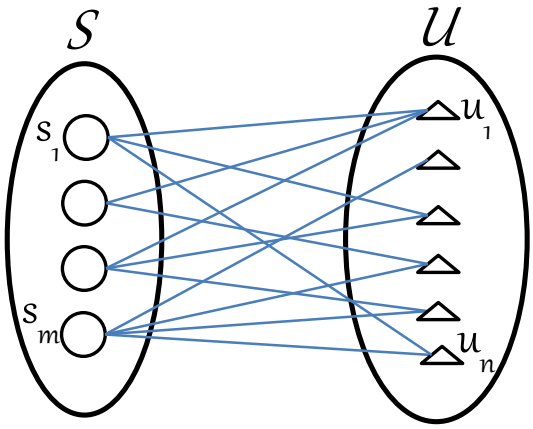

Figure 3.1: Bipartite graph represents the FLP, showing the set of facilities $\mathcal{S}$ and the set of customers $\mathcal{U}$, and a possible assignment.

The mathematical symbols for the FLP are introduced in Table 3.1, and the generalized problem is formulated as:

$$\text{minimize} \quad \sum_{j \in \mathcal{S}} f_j y_j + \sum_{j \in \mathcal{S}} \sum_{i \in \mathcal{U}} c_{ij} x_{ij}, \tag{3.1a}$$

$$\text{subject to} \quad \sum_{j \in \mathcal{S}} x_{ij} \geq 1, \quad \forall i \in \mathcal{U}, \tag{3.1b}$$

$$y_j - x_{ij} \geq 0, \quad \forall i \in \mathcal{U}, j \in \mathcal{S}, \tag{3.1c}$$

$$x_{ij} \in \{0, 1\}, \quad \forall i \in \mathcal{U}, j \in \mathcal{S}, \tag{3.1d}$$

$$y_j \in \{0, 1\}, \quad \forall j \in \mathcal{S}. \tag{3.1e}$$

Usually, a natural extension of the general FLP is the weighted case, where not all the facilities are assigned the same weight (cost). Another extension is the capacitated FLP, where facilities have limited resources; and hence might not be able to serve all customers within their geographical area.

3.1 Basic Facility Location Models

Different FLP models are available for different location problems. The variety of models is due to differences in the objective functions, the constraints, the chosen cost functions, and a number of other parameters [27]. The FLP aims in general

at finding the optimal value for some objective. The fundamental measure in such problems is usually the distance, or a function that is directly related to the distance, such as cost or time. Thus, FLP classification is based on the distance point of view. There are two general FLP categories, the *maximum distance models* and the *total (or average) distance models* [27]. Another factor that can be considered is the prior knowledge of the number of facilities to be opened. In all of the following models, it is assumed that all the locations of the customers and the candidate facilities are given. For simplicity, all the models we introduce in this section are un-capacitated cases of the FLP.

3.1.1 Maximum Distance Models

In this category, there is a maximum coverage distance D_c, usually known in advance, beyond which a customer can not be served by a particular facility. The first and simplest model is the SCP which is introduced hereafter. The SCP formulation is used as the basis of formulating other FLP models.

3.1.1.1 Set Cover Problem (SCP):

The SCP is a fundamental problem in combinatorial optimization; therefore, it has a wide range of applications. In this model, a cover distance is given and the objective is to minimize the number of open facilities required to cover (serve) all customers. The SCP is NP-hard [30].

The SCP can be formulated as:

$$\text{minimize} \quad \sum_{j \in \mathcal{S}} y_j, \tag{3.2a}$$

$$\text{subject to} \quad \sum_{j \in \mathcal{S}} x_{ij} \geq 1, \quad \forall i \in \mathcal{U}, \tag{3.2b}$$

$$y_j \in \{0, 1\}, \quad \forall j \in \mathcal{S}. \tag{3.2c}$$

In this formulation is called the unweighted SCP, where all facilities are assumed to have the same opening cost, so the objective becomes minimizing the number of open facilities. If facilities have different opening costs, then the cost (weight) of the facility is included in the objective function.

3.1.1.2 Maximal Covering Location Problem (MCLP):

In the SCP, there is no upper bound on the number of facilities to open; One can open as many facilities as required to satisfy all customers. However, the MCLP is useful in situations when there is a maximum number of facilities p that can be opened due to budget constraints. With those p facilities, the objective of the MCLP is to select p facilities to open in such a way that maximizes the coverage of customers. In other words, if not all customers can be covered, the MCLP model tries to cover the most demand possible. The MCLP is also NP-hard [30].

The MCLP can be formulated as:

$$\text{minimize} \quad \sum_{i \in \mathcal{U}} h_i z_i, \tag{3.3a}$$

$$\text{subject to} \quad \sum_{j \in \mathcal{G}_i} y_j - z_i \geq 0, \quad \forall i \in \mathcal{U}, \tag{3.3b}$$

$$\sum_{j \in \mathcal{S}} y_j = p, \tag{3.3c}$$

$$y_j \in \{0, 1\}, \quad \forall j \in \mathcal{S}, \tag{3.3d}$$

$$z_i \in \{0, 1\}, \quad \forall i \in \mathcal{U}. \tag{3.3e}$$

3.1.1.3 *p*-Center Problem (PCP):

In the SCP and MCLP, the coverage distance D_c is a fixed predetermined value. But what if, for equity reasons, D_c becomes the target? The PCP has the objective of minimizing the maximum distance K that a customer is from its serving facility, constraint by a predetermined number p of facilities that can be open. Given the previous definitions, and these new variables:

The PCP is formulated as :

$$\begin{aligned}
\text{minimize } & K, && && (3.4a)\\
\text{subject to } & \sum_{j\in\mathcal{S}} y_j = p, && && (3.4b)\\
& \sum_{j\in\mathcal{S}} x_{ij} = 1, && \forall i \in \mathcal{U}, && (3.4c)\\
& x_{ij} - y_j \leq 0, && \forall i \in \mathcal{U}, j \in \mathcal{S}, && (3.4d)\\
& K - \sum_{j\in\mathcal{S}} R_i d_{ij} x_{ij} \geq 0, && \forall i \in \mathcal{U}, && (3.4e)\\
& y_j \in \{0,1\}, && \forall j \in \mathcal{S}, && (3.4f)\\
& x_{ij} \in \{0,1\}, && \forall i \in \mathcal{U}, j \in \mathcal{S}. && (3.4g)
\end{aligned}$$

For fixed values of p, the PCP can be solved in $\mathcal{O}(Np)$ time; whereas for variable values of p, the problem is NP-hard [30].

3.1.1.4 *p*-Dispersion Problem (PDP)

While in the previous models the concern was on the distances between customers and facilities, the concern of the PDP is on the mutual distances between open facilities, with the objective of maximizing the minimum distance between any two open facilities.

To formulate this model, an extra input D_M, which is a large constant, and a decision variable v are introduced:

$$\begin{aligned}
\text{maximize } & v, && && (3.5a)\\
\text{subject to } & \sum_{j\in\mathcal{S}} y_j = p, && && (3.5b)\\
& v \leq D_{ij} + D_M(1-y_i) + D_M(1-y_j), && && \\
& && \forall i,j \in \mathcal{S}, i<j, && (3.5c)\\
& y_j \in \{0,1\}, && \forall j \in \mathcal{S}. && (3.5d)
\end{aligned}$$

3.1.2 Total or Average Distance Models

In several cases, the objective is to minimize the total or average distance instead of minimizing the maximum distance. This category can be considered as min-sum

problems, as opposed to the min-max problems in the previous category.

3.1.2.1 *p*-Median Problem (PMP):

The objective here is to find the locations of p facilities that minimize the total distance between customers and their associated facilities. The PMP can be formulated as follows:

$$\text{minimize} \quad \sum_{i\in\mathcal{U}}\sum_{j\in\mathcal{S}} R_i d_{ij} x_{ij}, \tag{3.6a}$$

$$\text{subject to} \quad \sum_{j\in\mathcal{S}} y_j = p, \tag{3.6b}$$

$$\sum_{j\in\mathcal{S}} x_{ij} = 1, \qquad \forall i \in \mathcal{U}, \tag{3.6c}$$

$$x_{ij} - y_j \leq 0, \quad \forall i \in \mathcal{U}, j \in \mathcal{S}, \tag{3.6d}$$

$$y_j \in \{0,1\}, \qquad \forall j \in \mathcal{S}, \tag{3.6e}$$

$$x_{ij} \in \{0,1\}, \quad \forall i \in \mathcal{U}, j \in \mathcal{S}. \tag{3.6f}$$

3.1.2.2 Un-capacitated Fixed Charge Location Problem (U-FCLP):

The PMP has some limitations and it might not be applicable to some problems. Those limitations are associated with its assumptions. First, the opening cost is the same for all facilities. Secondly, a priori knowledge of how many facilities to open, p, is assumed. To avoid these two assumptions, the objective of the U-CFLP is to jointly minimize the total facility and connection costs. The result of solving the U-FCLP is the optimal number and locations of facilities and a mapping that connects each customer to a facility.

$$\text{minimize} \quad \sum_{j\in\mathcal{S}} f_j y_j + C\sum_{i\in\mathcal{U}}\sum_{j\in\mathcal{S}} R_i d_{ij} x_{ij}, \tag{3.7a}$$

$$\text{subject to} \quad \sum_{j\in\mathcal{S}} x_{ij} = 1, \qquad \forall i \in \mathcal{U}, \tag{3.7b}$$

$$y_{ij} - x_j \leq 0, \qquad \forall i \in \mathcal{U}, j \in \mathcal{S}, \tag{3.7c}$$

$$y_j \in \{0,1\}, \qquad \forall j \in \mathcal{S}, \tag{3.7d}$$

$$x_{ij} \in \{0,1\}, \qquad \forall i \in \mathcal{U}, j \in \mathcal{S}. \tag{3.7e}$$

3.1.2.3 Hub Location Problem (HLP):

This model is concerned with locating distribution points (*hubs*), not the original facilities. In some logistics scenarios, hubs are needed, especially when distributing goods. For cost efficiency, it is better to use larger trucks to deliver the goods to the hubs and then use smaller trucks to deliver the goods to the final destination. The objective here is to locate hubs and delivery routes in order to minimize the total cost.

Different from previous formulations, the decision variables y_j and x_{ij} refers to hub j not facility j, and constant c_{ij} refers to the cost of connecting customer i to hub j. The HLP is formulated as follows:

$$\text{minimize} \quad \sum_{i\in\mathcal{U}}\sum_{j\in\mathcal{S}} b_{ij}\left(\sum_{k\in N} c_{ik}y_{ik} + \sum_{m\in N} c_{jm}y_{jm} + \sum_{k\in N}\sum_{k\in N} c_{km}y_{ik}y_{jm}\right), \tag{3.8a}$$

$$\text{subject to} \quad \sum_{j\in\mathcal{S}} y_j = p, \tag{3.8b}$$

$$\sum_{j\in\mathcal{S}} x_{ij} = 1, \qquad \forall i \in \mathcal{U}, \tag{3.8c}$$

$$y_{ij} - x_j \leq 0, \qquad \forall i \in \mathcal{U}, j \in \mathcal{S}, \tag{3.8d}$$

$$y_j \in \{0,1\}, \qquad \forall j \in \mathcal{S}, \tag{3.8e}$$

$$x_{ij} \in \{0,1\}, \qquad \forall i \in \mathcal{U}, j \in \mathcal{S}. \tag{3.8f}$$

3.2 Solution Approaches for FLP

The FLPs are mainly formulated as a mixed integer linear programming (MILP) problems as seen in the previous section. The fact that all the location models are NP-hard excludes the use of the standard optimization approaches such as *branch-and-bound*. In particular, for large-scale networks, the execution time is prohibitive, with no guarantee of finding a solution (even a poor one). Several methods have been introduced to find a solution for FLP problems, if not the optimal, at least a very good one [27].

Table 3.2: FLP Models Summary Table

	Model	Objective	Assumptions	Possible Applications in Cellular Networks
Maximum Distance Models	SCP	Minimize the number of open facilities required to cover all customers.	- All customers must be covered.	- dynamic CSO (see Ch. 4) - interference minimization
	MCLP	Locate *p* facilities, in such a way as to maximize the covered demand.	- Upper limit on the number of facilities. - Some customers may not be covered.	- cell planning - CSO with QoS guarantee
	PCP	Minimize the maximum distance between each customer and their nearest open facility.	- Predetermined number of facilities.	- power control
	PDP	Maximize the minimum mutual distance between any pair of facilities.	- Predetermined number of facilities. - Concerned only with the mutual distances between open facilities.	- CSO for irregular BS placement (see Ch. 6)
Total/Average Distance	PMP	Minimize the total distance between customers and their serving facilities.	- Predetermined number of facilities.	
	U-FCLP	Minimize total of facility cost plus transportation costs.	- Consider the transportation cost.	- CSO + power control
	HLP	Locate distributing points (hubs) to minimize total cost.	- Each node is assigned to exactly one hub. - Customers may be assigned to a farther hub.	- relay placement problem - drone (UAV) placement

3.2.1 Greedy Algorithms

Greedy algorithms are designed to find a good solution to the FLP with no guarantee of finding the optimal solution. After a first step of creating disjoint sets of customers each facility can cover, the algorithm calculates the effectiveness of each set, and choses the facility with the greatest impact on the objective function and marks it as open. The same procedure is repeated to open (add) facility sequentially in a matter known as *greedy-add*. There exists a reverse algorithm called *greedy-drop* that starts with all the facilities open and then closes (drops) the facility that yield the least impact on the objective function [27].

3.2.2 Improvement Heuristics

Although greedy approaches can generate results fast, they might not yield good results consistently. Several algorithms have been proposed to start with an initial point and try to improve it. A preliminary algorithm, such as a greedy-add, can be used to obtain a good initial solution. Some examples of these algorithms are *neighborhood search*, *heuristic concentration*, and *fast interchange*. A common problem with heuristic algorithms is that they might fail to find the global optima and find local optima instead. A *metaheuristic* is an intelligent way to guide heuristics to escape from local optima and search for better solution in the whole region. An example of a metaheuristic is the *Tabu search*, which restricts some types of moves after a certain number of iterations [27].

3.2.3 Lagrangian Relaxation

A key purpose of heuristics is to reduce the execution time in exchange for the solution quality. Therefore, it is difficult to ensure any performance guarantee (i.e., we don't know how far the solution is from the optimum.) A good way to evaluate the quality of the solution is by finding upper and lower bounds, which can be obtained by using the *Lagrangian relaxation* method. Lagrangian relaxation formulation modifies the original objective function by adding one of the constraints multiplied by an associated Lagrange multiplier in order to find a bound. This new formulation is referred to as a relaxed problem, and is usually much easier to solve optimally. The difficulty here is in finding optimal values for the Lagrangian multipliers [27].

customers	← user
facilities	← BSs
candidate facility locations	← all BSs in the network
open facilities	← BSs that remain active
fixed cost	← energy consumption at a BS
capacity	← bandwidth
connection cost	← transmit power or required bandwidth

Figure 3.2: Analogy between CSO and FLP

3.3 Modeling the CSO Approach as a FLP

The CSO approach is used to save energy by switching off some BSs during periods of light traffic. Switching off BSs is not as simple as it seems; it includes a lot of planning, decision making, and signal exchanging to ensure that active users are satisfied. We need to optimize the number and choice of switched-off BSs, and hand-over users to other active BSs in a way that maximizes the overall network performance and results in the most energy saving. The objectives of the CSO approach (minimize the number of active BSs and find the user-to-cell assignment) are similar to that of the FLP; however, the two problems are not identical. We need to be very careful when modeling the CSO as a FLP.

The FLPs are application-specific; therefore, we first clarify the terminology of the FLP in the context of cellular networks, with the analogy made in Fig. 3.2. Based on this analogy, we can determine the appropriate model to formulate the CSO approach, and modify its available algorithm to find a solution.

According to the FLP classification, the CSO approach would be a capacitated and weighted FLP with unsplittable demand. Splittable demand means that the demand of a customer can be satisfied by more than one facility. If we restrict the demand to be served by a single facility, then it is unsplittable.

Later, in Chapter 4, we model a dynamic CSO approach using as an unweighted capacitated SCP. We also use PDP to find solutions for the CSO for spatially irregular BS deployments.

Chapter 4

Dynamic Cell Switch-Off: A Set Cover Based Algorithm for Cell Switch-Off

4.1 Introduction

In this chapter, we explore a slow-reaction dynamic (online) CSO approach.

Looking at the different FLP models, we find that the set cover problem (SCP) is the most suitable one to model the CSO approach. The objective of the SCP is to minimize the number of open facilities (active BSs). The connection cost between a customer and its serving facility is ignored in the SCP, this matches the CSO problem well, because we assume that the BS transmission power is a small portion of its total power consumption. We formulate the CSO approach as a SCP after modifying it to include the special characteristics of cellular networks. Consequently, we propose an algorithm to solve the CSO problem, and show that it outperforms the benchmark algorithm in terms of the amount of saved energy.

The SCP is usually denoted as $(\mathcal{U}, \mathcal{S}, \mathcal{C})$, where $\mathcal{U}$ is a universe of n elements, $\mathcal{S} = \{\mathcal{S}_1, ..., \mathcal{S}_m\}$ is a set of m subsets of $\mathcal{U}$, and $\mathcal{C} = \{c_1, ..., c_m\}$ is the set giving the cost associated to each subset $S_k \in \mathcal{S}$. A *set cover* is a collection of subsets from $\mathcal{S}$ such that all elements in $\mathcal{U}$ are included in at least one subset. The objective of the SCP is to find the set cover $\mathcal{S}^* \subseteq \mathcal{S}$ that minimizes the cost [30]. If all subsets have the same cost, the problem becomes the unweighted SCP case $(\mathcal{U}, \mathcal{S}, 1)$: find the $\mathcal{S}^*$ that contains the least number of sets that cover all the elements of $\mathcal{U}$. Fig. 4.1 illustrates an example of the SCP, with both $\{\mathcal{S}_1, \mathcal{S}_2, \mathcal{S}_3\}$ and $\{\mathcal{S}_4, \mathcal{S}_5\}$ can cover all the customers. If all sets have the same weight (cost), then the cover set that minimizes

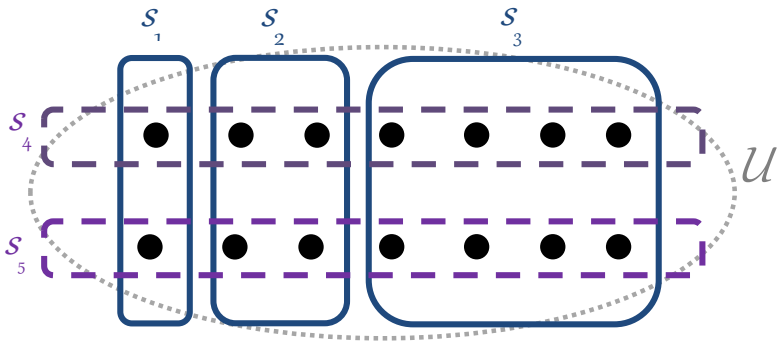

Figure 4.1: A SCP example with two cover sets: $\{\mathcal{S}_1, \mathcal{S}_2, \mathcal{S}_3\}$ and $\{\mathcal{S}_4, \mathcal{S}_5\}$. Black circles represent customers and the rectangles are subsets of users.

the cost is the one with the smallest number of sets, which is $\{\mathcal{S}_4, \mathcal{S}_5\}$ in this example.

From the capacity point of view, there are two versions of the problem: un-capacitated and capacitated SCP. In the un-capacitated version, every subset $\mathcal{S}_k$ is assumed to have unlimited resources and can serve all the elements in the set, while in capacitated SCP, each element i has a demand b_i and each subset has limited resources to distribute among its elements.

4.1.1 Applications in Wireless Networks

The SCP has already been used to solve various problems in wireless networks, as highlighted in this subsection. In wireless mesh networks, the SCP was used in the planning phase to optimally locate the gateways, in order to minimize the deployment cost while covering all the routers [31, 32]. It was used in ad hoc networks to solve the problems of broadcasting [33] and energy saving [34]. Minimizing the interference is another application of the SCP in both wireless sensor networks (WSNs) [35] and cellular networks [36]. Yet the most common application of the SCP in wireless networks is to solve the coverage problem in WSNs [37–46]. According to the survey papers [34, 47], the coverage problem in WSNs is classified into two categories: area coverage and discrete point coverage. The objective of the former category is to monitor a geographical area, while in the latter it is to cover a set of points. The SCP in WSNs is somewhat similar to the CSO approach. Hence, the objective in both of them is to cover some points with the minimum number of sets. This objective corresponds to maximizing energy saving by minimizing the number of active BSs.

However, modeling the CSO approach as a SCP cannot follow the exact same procedure as for WSNs. This is because of three major differences that should be carefully addressed. The first and key difference is the capacity constraint. While in CSO the cell capacity is a vital factor, it is not as important in WSNs because only low data rates are transmitted. The second difference is the coverage pattern. The coverage area in WSNs is usually assumed to be circular [37], whereas in CSO, it is not circular, due to the shadowing effect caused by obstacles, reflection, and diffraction. The third difference is the type of requirements for energy saving.

4.1.2 Problem Formulation

The objective of the CSO approach is to switch off as many cells as possible while providing users with their required rates. Our formulation is based on the observation that this objective can be achieved using the SCP. Moreover, there are several algorithms to solve the SCP and they provide a very good solution with polynomial time complexity [30]. The SCP formulation is a consistent strategy to implement the CSO approach, while its available solutions can be modified to address the special characteristics of the CSO. The results shown later in this section demonstrate the efficacy of the proposed CSO algorithm based on a SCP formulation.

The CSO approach is formulated as a $(\mathcal{U}, \mathcal{S}, 1)$ SCP, where $\mathcal{U}$ is the set of user equipments (UEs) in the network, $\mathcal{S}$ is the set of subsets of UEs belonging to each cell, and 1 corresponds to the unweighted SCP. In the CSO context, unweighted means that all cells have the same cost, where the cell cost is equal to the consumed energy when the cell is active[1].

One possible formulation of the CSO approach as a SCP is the following:

$$\text{minimize} \quad \sum_{j \in \mathcal{S}} y_j \tag{4.1a}$$

$$\text{subject to} \quad \sum_{j \in \mathcal{S}} x_{ij} y_j = 1, \quad \forall i \in \mathcal{U}, j \in \mathcal{S}, \tag{4.1b}$$

$$x_{ij}, y_j \in \{0, 1\}, \quad \forall i \in \mathcal{U}, j \in \mathcal{S}. \tag{4.1c}$$

The notations used in the formulation and algorithms are introduced in Table 4.1.

[1]This formulation can easily be extended to the case of cells with different costs, e.g., in HetNets scenarios with macro, micro, or pico cells.

Table 4.1: Symbols for Dynamic CSO

Symbol	Description
$\mathcal{U}$	universe of n users (elements)
$\mathcal{S}$	set of m subsets of $\mathcal{U}$
$\mathcal{C}$	set of the cost associated to each subset $\in \mathcal{S}$
y_j	binary variable, = 1 if cell j is active
x_{ij}	binary variable, = 1 if UE i is connected to cell j
$\mathbf{X}$	$= [x_{ij}]$: UE-to-cell assignment matrix
R_i	rate required by UE i
β_{ij}	SNR of UE i when connected to cell j
η_{ij}	spectral efficiency between UE i and cell j
η_{th}	spectral efficiency of a central UE
W_j	bandwidth of cell j
b_{ij}	$= \frac{R_i}{\eta_{ij}}$ required bandwidth for UE i if served by cell j
$\mathbf{B}$	$= [b_{ij}]$: required bandwidth matrix
$\mathcal{N}_j$	set of UEs covered by cell j
$\mathcal{M}_j$	set of UEs currently served by cell j
$\mathcal{S}_j$	set of UEs can be served by cell j
$\mathcal{V}$	set of connected/served UEs
$\mathcal{L}$	set of active cells

This un-capacitated SCP (4.1) can be solved by a simple greedy-add algorithm [30, Algorithm 2.2] which provides a good solution. Despite the similarities, the CSO approach has distinct characteristics that should be considered when formulating it as a SCP. To accommodate these characteristics, we made three modifications to the simple greedy-add algorithm.

The first modification is the following capacity constraint

$$\sum_{i \in \mathcal{U}} b_{ij} x_{ij} \leq W_j, \quad \forall j \in \mathcal{S}. \tag{4.2}$$

The input of the original algorithm is the cover set $\mathcal{N}_j$, which is the set of all

UEs that are covered by cell j. Instead of complicating the formulation in (4.1) by adding an extra constraint, the constraint in (4.2) is enforced by running a preliminary algorithm to obtain the *service set* $\mathcal{S}_j$, which is the set of UEs that can be served by cell j without exceeding the cell capacity. Only a subset of UEs covered by cell j will be included in its service set $\mathcal{S}_j$ so that the sum of the demand does not exceed the total bandwidth W_j. In other words, a cell may not be able to serve all UEs in its cover set, i.e., the service $\mathcal{S}_j$ set is a subset of the cover set $\mathcal{N}_j$. Using the service set as an input to the main algorithm instead of the cover set allows the use of [30, Algorithm 2.2] that is originally designed for un-capacitated SCP. The term *served UEs* is used instead of *covered UEs* to emphasize the capacity aspect.

The second modification is regarding the possibility of splitting the demand. If the demand (*required bandwidth* b_i) of UE i can be satisfied by more than one cell, then the demand is referred to as *splittable* demand. In the original SCP formulation, the splittable demand is introduced by the constraint

$$\sum_{j \in \mathcal{U}} x_{ij} y_j \geq 1, \quad \forall i \in \mathcal{U}, j \in \mathcal{S}. \tag{4.3}$$

However, in traditional cellular networks, the UE demand is usually satisfied by a single cell; this is referred to as *un-splittable* demand. This was achieved by replacing constraint (4.3) with constraint (4.1b) in the original CSO formulation (4.1).

The third modification is due to the type of demand. In the capacitated SCP, UE i requires the same demand b_i from any cell. However, in the context of cellular networks, the required bandwidth of UE i differs based on which cell is providing the service: we referred to this as *dissimilar* demand. Therefore, the notation b_{ij} is needed to differentiate between the different required bandwidths when served by different cells. Although there are algorithms to solve the the capacitated SCP [48], we were not able to use them because they are very specific and not designed for dissimilar demand.

4.1.3 The Proposed Algorithm

A centralized two-stage algorithm is proposed here to solve the CSO problem. The first stage, described in Algorithm 1, is used to obtain the service set that enforces the capacity constraint of (4.2). To find the service set $\mathcal{S}_j$ for cell j, we first start with an empty set $\mathcal{S}_j$, and then the set $\mathcal{M}_j$ of UEs that are currently served is are added

Algorithm 1: Obtain Service Set

input :
$\mathbf{B}$, $\mathbf{X}$, $\mathcal{V}$, W_j
output :
$\mathcal{S} = \{\mathcal{S}_1, \mathcal{S}_2, ..., \mathcal{S}_m\}$ service set, $\forall j \in \mathcal{S}$

```
for each cell j do
    S_j ← S_j ∪ {M_j \ V}
    Z = Σ_{∀r∈S_j} b_rj, utilized bandwidth
    while Z < W_j do
        find i* = argmin_{i*∈{N_j \ V}} b_{i*j}
        if Z + b_{i*j} < W_j then
            Z ← Z + b_{i*j}
            S_j ← S_j ∪ {i*}
            else
                Terminate while loop
            end
        end
    end
end
return S
```

to $\mathcal{S}_j$. After that, the cell bandwidth W_j is filled up by adding new UEs from set $\mathcal{N}_j$ starting with UE i^* that requires the least bandwidth b_{i^*j}. The algorithm terminates after obtaining the service sets $\mathcal{S} = \{\mathcal{S}_1, \mathcal{S}_2, ..., \mathcal{S}_m\}$, where m is the number of cells in the network.

The second stage (the main algorithm) is described in Algorithm 2. The input of this algorithm is the set of service sets $\mathcal{S}$ obtained from Algorithm 1. This algorithm is a modified version of the simple greedy-add algorithm for the un-capacitated SCP [30, Algorithm 2.2]. The algorithm starts with the initial condition that all cells are switched off and all UEs are unconnected. In each iteration, the algorithm selects a cell j^* to be switched on. The order in which cells are selected (cell sorting) highly impacts future cell switch-off decisions. The common practice is to select a cell based on its current load. However, switching off a cell does not depend solely on the cell's own load but also on several factors such as the available bandwidth of neighbour cells

Algorithm 2: Greedy_add Algorithm

input :
$\mathcal{M}_j$, **X, B**
$\mathcal{U} = \{e_1, e_2, ..., e_n\}$, the set of all UEs

output :
$\mathcal{L}$ **X**

$\mathcal{L} \leftarrow \phi$, the set of active cells
$\mathcal{V} \leftarrow \phi$, the set of connected UEs
while $\mathcal{V} \neq \mathcal{U}$ **do**
    Call Algorithm 1, to obtain service set $\mathcal{S}$
    switch *Sorting Criteria* **do**
        case *MaxLoad*
            find $j^* = \text{argmax}_{j^* \in \{\mathcal{S} \backslash \mathcal{L}\}} (\sum_{\forall i \in \{\mathcal{M}_{j^*} \backslash \mathcal{V}\}} b_{ij^*})$
        end
        case *MaxUsers*
            find $j^* = \text{argmax}_{j^* \in \{\mathcal{S} \backslash \mathcal{L}\}} |\mathcal{S}_{j^*}|$
        end
        case *MaxCentres*
            $\mathcal{T}_j = \{a \in \{\mathcal{M}_j \backslash \mathcal{V}\} | \eta_{aj} \geq \eta_{th}\} \quad \forall j \in \mathcal{S}$
            find $j^* = \text{argmax}_{j^* \in \{\mathcal{S} \backslash \mathcal{L}\}} |\mathcal{T}_{j^*}|$
        end
    endsw
    $\mathcal{L} \leftarrow \mathcal{L} \cup \{j^*\}$
    $\mathcal{V} \leftarrow \mathcal{V} \cup \{\mathcal{S}_{j^*}\}$
    Update **X**
end
return $\mathcal{L}$, **X**

and the channel quality between its UEs and other cells. Therefore, we investigate three different cell sorting criteria and analyze their effect on the final number of switched off cells. The cell selection procedure is explained in steps 6-16 of Algorithm 2. Furthermore, the three different cell sorting criteria are introduced as follows:

1. *MaxLoad*: In this case, the next cell to be selected is the cell with the highest load. Selecting cells based on their loads is the common practice in literature.

2. *MaxUsers*: In this case, the next cell to be selected is the cell that can serve the most unconnected UEs.

3. *MaxCentres*: In this case, the next cell to be selected is the cell that has the most number of cell-central UEs (UEs with good channel quality). A UE i is a cell-central UE for cell j if $\eta_{ij} \geq \eta_{\text{th}}$, where η_{th} is the spectral efficiency of a central UE and is achieved when SNR is 30 dB or more.

After selecting a cell j^* to switch on, all UEs in its service set $\mathcal{S}_{j^*}$ are added to the set $\mathcal{V}$ and the assignment matrix $\mathbf{X}$ is updated accordingly. The service set is updated at each iteration, by calling Algorithm 1, based on the updated values of $\mathcal{V}$ and $\mathbf{X}$. The algorithm terminates when all UEs are connected to a BS. Finally, the cells in set $\mathcal{V}$ will stay active while all other cells are switched off.

4.1.4 Simulation Results

We evaluate the proposed algorithms for the UMi scenario, for a square network layout of 100 BSs with omni-directional antennas. The number of UEs per cell and their required rates are selected to simulate a lightly-loaded network, which is the normal operating situation of the CSO approach. For highly-loaded networks, all cells are expected to be active, and hence the CSO approach is not applicable.

In our simulations, we assume that all UEs in the network area are included in the cover set of each cell. This assumption is valid because of the natural dense cell deployment of the UMi scenario. To make the problem tractable, we assume that the inter-cell interference is managed by some interference management techniques. Therefore, the spectral efficiency η_{ij} is calculated based on β_{ij} the signal-to-noise ratio (SNR) between UE i and cell j is using Shannon's formula:

$$\eta_{ij} = \log_2(1 + \beta_{ij}). \tag{4.4}$$

The proposed algorithm represents a centralized approach where all cells are connected to a central entity (cloud) that has global information about SNR values between all UEs and all cells. The average number of switched-off cells is obtained by taking the average over 100 realizations. The energy saving is assumed to be proportional to the number of switched-off cells. This is because of the fact that cells are consuming a significant amount of energy even when not serving any users; therefore, the energy consumed for transmission and processing can be neglected.

The proposed algorithm is compared with the benchmark greedy-drop algorithm from [18], and the results are illustrated in Fig. 4.2. This figure presents the energy saving (y-axis) for different numbers of UEs per cell (x-axis). For the sake of a fair comparison, we compare both algorithms using the same cell sorting criterion, *MaxLoad*. For a very small number of UEs per cell (5) the benchmark algorithm performs slightly better. However, when the number of UEs per cell increases to 10 or more, our algorithm outperforms the benchmark algorithm by achieving up to 20% more energy saving (in the case of 25 UEs per cell). This improvement might be credited to the fundamental difference between the greedy-add and the greedy-drop approaches. In greedy-drop approaches, UEs of a cell are handed over before the cell is switched off it off. This may not result in using 100% of the bandwidth of other cells. Hence, the focus is to get rid of the cell load, and not to maximize the load in some cells. On the other hand, our greedy-add algorithm concentrates the load in a cell before switching it on by trying to load it to the maximum. This maximum cell loading results in an increased number of switched off cells when using our greedy-add algorithm.

Fig. 4.3 demonstrates the energy saving when applying different cell sorting criteria: *MaxLoad*, *MaxUsers* and *MaxCentres*. As shown in the figure, the selection of the cell sorting criterion affects the achieved energy saving. Both *MaxLoad*, and *MaxCentres* criteria performed very close to each other regardless of the number of UEs per cell. However, the *MaxUsers* criterion outperformed the other two sorting criteria in terms of energy saving: A gain of about 5% was constant throughout all the different numbers of UEs per cell. This improvement can be explained as follows: in *MaxUsers*, the next cell to switch on is determined based on the number of UEs that a cell can serve. Thus the selection includes the future contribution of this particular cell to accommodate unconnected UEs. However, in *MaxLoad*, the selection is based on the current load of the cell without any indication of how much it can contribute

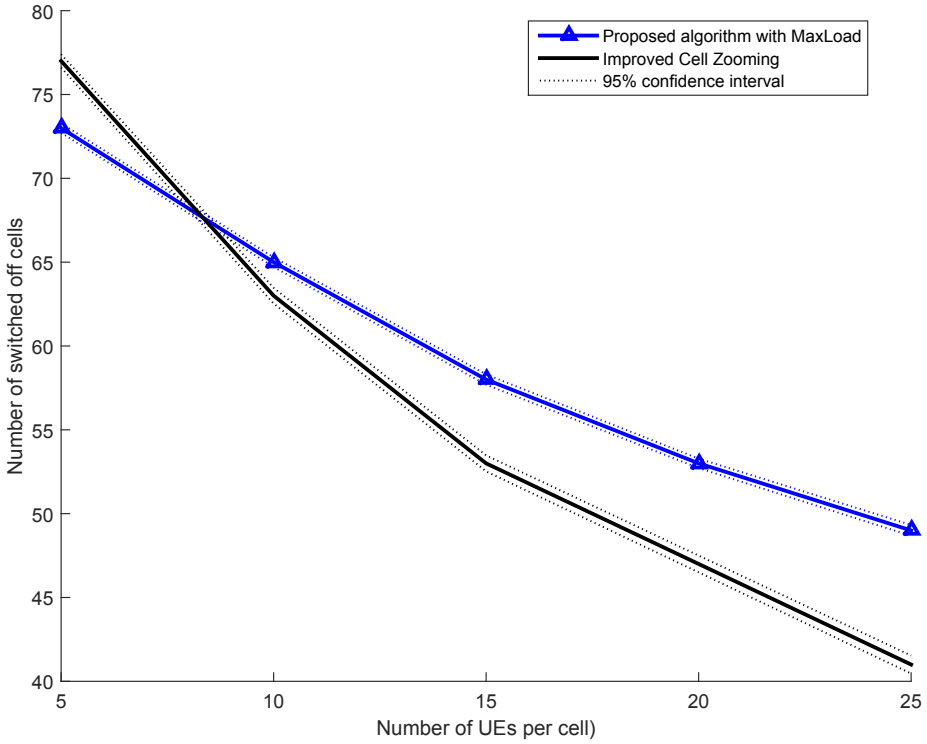

Figure 4.2: The average number of switched-off BSs for the proposed algorithm vs the benchmark algorithm from [18] using the *MaxLoad* cell sorting criterion.

to the unconnected UEs. In this latter case, the selected cell might not be the best cell to select as it cannot contribute much to the unconnected UEs.

Fig. 4.4 shows a realization for 5 UEs per cell to demonstrate the impact of the the cell sorting criterion on the CSO procedure and the resulting UE-to-cell assignments. Fig. 4.4(a) shows the initial UE-to-cell assignment before applying the proposed CSO algorithm. Figs. 4.4(b) and 4.4(c) illustrate the difference in UE-to-cell assignment after applying different sorting criteria *MaxLoad* and *MaxUsers* respectively. As shown in Fig. 4.4, the set of active cells highly depends on the cell sorting criterion.

Fig. 4.5 shows the load distribution of BSs after applying CSO. We find that most cells are very highly loaded, however, there remain some cells that are very lightly loaded (as light as 10%). Some opportunities for extra energy saving may come from switching off those cells through multi-carrier cooperation or user-assisted CSO.

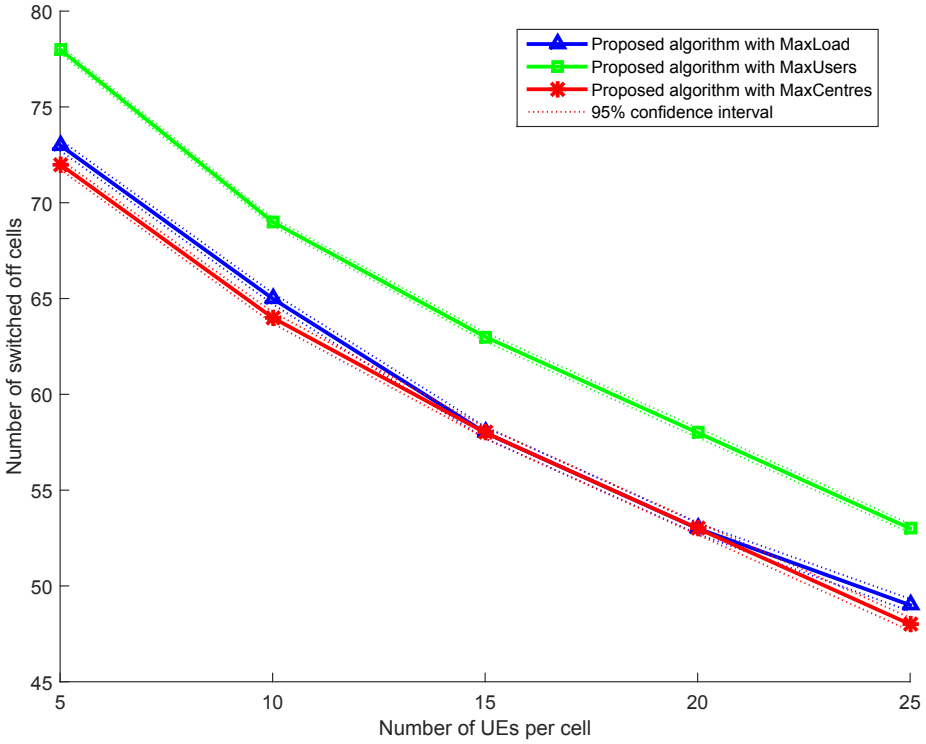

Figure 4.3: Comparing different cell sorting criteria in terms of The average number of switched-off BSs.

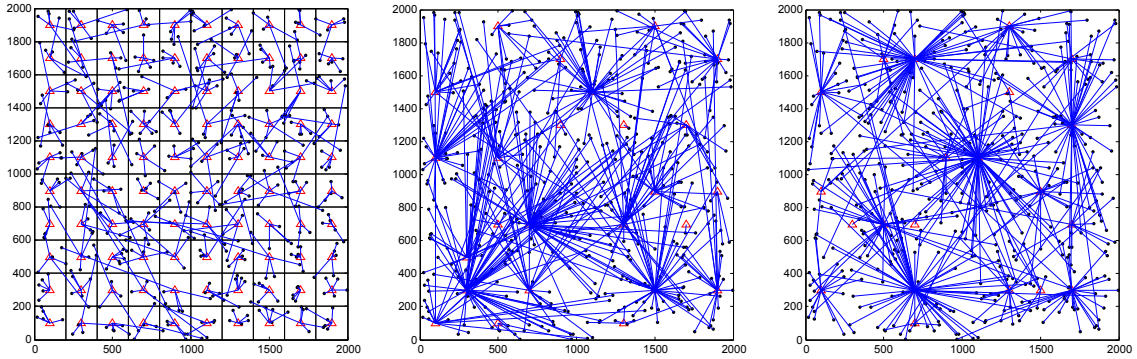

(a) Before CSO (100 active cells).

(b) CSO with *MaxLoad* (25 active cells).

(c) CSO with *MaxUsers* (21 active cells).

Figure 4.4: A visualization of the UE-to-cell assignments for the case of 5 UEs per cell; to show the impact of cell sorting criterion.

4.2 Conclusion

Dynamic CSO is a promising approach for energy saving in cellular networks through switching off some appropriate cells. Most of the existing algorithms for implementing the CSO approach switch off cells based on their current load. However, the switch-off procedure is affected by the order in which cells are switched off (cell sorting). Therefore, three different cell sorting criteria were investigated and compared to show their impact on the total energy saving. Simulations showed that switching off cells based on the number of UEs they can serve provided the best performance among the investigated cell sorting criteria.

Furthermore, we formulated the CSO approach as a SCP. Using this formulation, we proposed a greedy-add algorithm for dynamic CSO. This proposed algorithm was shown to outperform the benchmark algorithm, improved cell-zooming, when the number of UEs per cell is large.

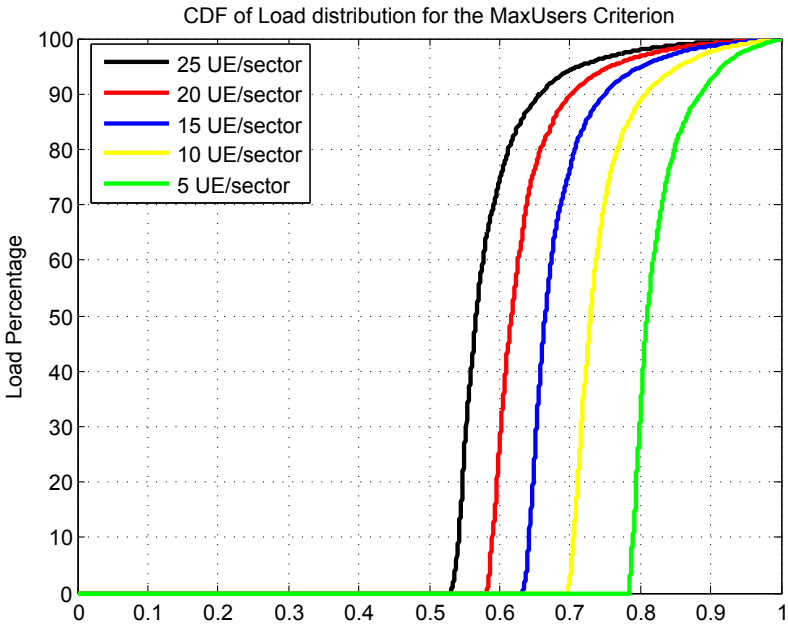

Figure 4.5: Load CDF of cell after applying CSO approaches.

Chapter 5

Sector-Level and Site-Level Regular Switch-Off Patterns

5.1 Introduction

Regular CSO is a special case of static CSO, also known as *CSO patterns*. A *pattern* refers to the configuration of active sectors. Besides being predetermined offline, the set of active sectors is selected according to a periodic spatial pattern [9]. It has been shown that, for the same number of BSs, the best SIR distribution can be achieved when the BSs are located on a regular grid [49]. Therefore, CSO patterns were introduced in literature to make the interference tractable and to avoid coverage holes at the same time.

By applying regular CSO, the choice of active cells minimizes coverage holes. This aspect is usually overlooked in the literature [23]. Also, regular CSO is more energy-efficient for UEs in the uplink, as there is always a nearby active cell [24, 25]. Regular CSO patterns reduce the interference between cells due to the careful selection of BS locations so that the are as far from each other as possible. The patterns are conceptually simple and can be described in a systematic way. Regular Static CSO is useful when the UEs' distribution is approximately uniform in space.

Regular CSO patterns resemble the intuitive and well-known frequency reuse[1] patterns [11].

[1]Regular CSO patterns have conceptual similarities with frequency reuse. Here we can make a contrast with the performance of frequency reuse schemes, in which the average SINR increases with the frequency reuse factor [50, Table I]. This is because the distance to the nearest interfering BS is increased, while the cell size remains about the same. In regular static CSO, however, the cell grows with the decrease of the proportion of active sectors [15], which is analogous to the frequency reuse factor. The current practice in LTE is to employ a frequency reuse of one.

Table 5.1: Regular CSO Patterns in the Literature.

Ref.	Site-level	Sector-level		
		$\frac{3}{3}$	$\frac{2}{3}$	$\frac{1}{3}$
[10]	$\frac{1}{4}$	Omni-directional		
[11]	$\frac{2}{3}$, $\frac{2}{4}$, $\frac{3}{7}$	Omni-directional		
[14]	$\frac{1}{3}$, $\frac{1}{4}$ $\frac{1}{7}$, $\frac{1}{9}$	Omni-directional		
[16]	$\frac{1}{3}$, $\frac{2}{3}$, $\frac{1}{4}$, $\frac{2}{4}$, $\frac{3}{4}$	Omni-directional		
[13]	$\frac{1}{4}$, $\frac{1}{7}$	Omni-directional		
[15]	$\frac{1}{4}$, $\frac{1}{7}$, $\frac{1}{9}$	Yes	No	No
[17]	$\frac{1}{4}$, $\frac{2}{4}$, $\frac{3}{4}$	Yes	No	No
Our work [51]	$\frac{1}{3}$, $\frac{2}{3}$, $\frac{1}{4}$, $\frac{2}{4}$, $\frac{3}{4}$, $\frac{1}{7}$, $\frac{1}{9}$	Yes	Yes	Yes

CSO patterns are already under consideration by several research groups. Table 5.1 summarizes the existing work on regular CSO patterns. The effect of different CSO patterns on the outage probability is investigated in [10, 11], while the effect of the blocking probability is studied in [12, 14]. Authors in [16] introduce a set of CSO patterns and propose a scheduler to jointly ensure full coverage for both downlink and uplink.

The patterns in the literature [10–17] we will call *site-level* patterns, since only entire sites (BSs) are switched off. We introduce *sector-level* patterns, where a certain number of sectors is switched off at each site. Sector-based regular CSO patterns are based on a logical AND combination of site-level and sector-level patterns. We compare the performance of these patterns using only one parameter, abstracting from bandwidth and required rate. Results show that regular CSO patterns with individual sector switch-off can be efficient in several interesting cases. In our simulations, each BS site has three 120°-sectors and the azimuth orientation of the sectors is the same for all sites.

Table 5.2: List of Symbols for Static CSO Patterns.

W	total system bandwidth
N	number of UEs that can be served per active sector
$\bar{N}(w)$	renewal process
γ_i	SINR between UE i and its serving sector
$\gamma_{\min}$	minimum SINR at which a UE can receive information
$\gamma_{\max}$	maximum SINR that can be supported
η_i	spectral efficiency of UE i,
	$= \log_2(1+\gamma_i)$ [bps/Hz]
R_i	rate required by UE i
b_i	bandwidth required by UE i,
	$= R_i/\eta_i$ [Hz]
η_{eq}	equivalent spectral efficiency (ESE),
	$= 1/\mathbb{E}\{1/\eta\}$ [bps/Hz/Sector]
$\mathsf{P}_{\text{X}}(n/m, k/3)$	CSO pattern where n out of m BSs are active,
	k out of 3 sectors are active, and
	X is to distinguish between different rotations
ρ	proportion of active sectors in the network,
	$= \lvert\mathsf{P}(n/m, k/3)\rvert = \frac{nk}{3m} \in [0,1]$
P_{site}	total power consumed at a fully active site
P_{pattern}	power consumed per system site for the selected pattern
P_{S}	power consumed per sector
P_{C}	common power consumed at a site
α	$= P_{\text{C}}/P_{\text{S}}$
δ	ratio of ESEs of two patterns
P_o	probability of signal outage (when $\gamma_i < -7$ dB)
$\mathbb{C}\text{oV}\{X\}$	coefficient of variation of a random variable X
	$= \sqrt{\mathbb{V}\text{AR}\{X\}}/\mathbb{E}\{X\}$

5.2 Methodology

In this section, we explain the analysis for estimating the average number of supported users, introduce the two levels of CSO patterns (site-level and sector-level), and then compare the sector-based versus site-based CSO patterns in terms of energy efficiency. The symbols used are provided in Table II.

5.2.1 Analysis of the Number of Supported Users

In this subsection, we study the distribution of the number N of UEs served by an active sector, and derive expressions for the mean number $\mathbb{E}\{N\}$ of UEs, as well as for the distribution and variance of N.

In our system, UEs are uniformly and independently distributed. The UE-to-cell assignment is such that UE i is connected to the sector that provides it with the best SINR γ_i. Hence, the spectral efficiency of UE i is calculated as

$$\eta_i = \log_2(1 + \gamma_i) \text{ [bps/Hz]}. \tag{5.1}$$

Some UEs might have a very weak SINR ($< \gamma_{\min}$). When this happens, a UE cannot receive any useful signal and as a result will be in outage (considered when estimating the outage probability P_o). Other UEs will have a very high SINR ($> \gamma_{\max}$), to the extend that it might be higher than what the current constellations can utilize. As a result, these SINRs are truncated. For LTE networks, typical values for $\gamma_{\min}$ and $\gamma_{\max}$ are -7 dB and 18 dB, respectively [28], [29].

In order to find the number of UEs N that can be served by an active sector, we formulate the problem as a renewal process (RP) [52, Chapter 7]. We assume that the UEs are admitted to the network on a first-come, first-served basis. This is regardless of their bandwidth demand b_i, where

$$b_i = \frac{R_i}{\eta_i}, \tag{5.2}$$

which depends on the UE's downlink rate requirement R_i, and its downlink spectral efficiency η_i. At each sector, UEs are admitted one-by-one; their bandwidth requirements are added up until the next UE exceeds the sector's downlink bandwidth W. Thus we have

$$\begin{aligned} &\sum_{i=1}^{N} b_i \leq W, \text{ and} \\ &\sum_{i=1}^{N+1} b_i > W. \end{aligned} \tag{5.3}$$

Since $\{b_1, ..., b_N, b_{N+1}\}$ is a sequence of positive independent and identically distributed (iid) random variables (RVs), the RP $\bar{N}(w)$ is defined in terms of N, b_i, and

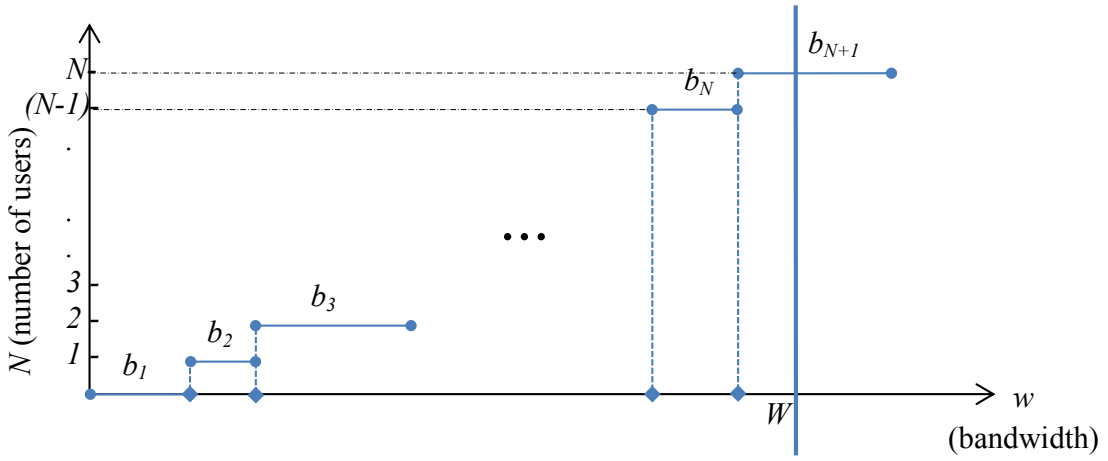

Figure 5.1: A renewal process used to find the number of users N that can be supported by one sector with a bandwidth W, where b_i is the bandwidth required from UE i to satisfy its rate R_i.

a bandwidth w as

$$\bar{N}(w) = \max\left\{N \in \mathbb{N} : \sum_{i}^{N} b_i \leq w\right\}. \tag{5.4}$$

Fig. 1 illustrates the RP, where UEs are admitted until there is no more bandwidth available in that sector for the next user UE_{N+1}. If we consider W as the stopping time of this RP, we find that $\bar{N}(W) = N$ is the number of UEs that will be admitted by one active sector.

5.2.1.1 Mean Number of Users

From the Central Limit Theorem for RPs (RP-CLT)[2]: for large W, the distribution of $\bar{N}(W)$ is approximately Gaussian [52, Chapter 7] with mean

$$\mathbb{E}\{N\} = W/\mathbb{E}\{b\}. \tag{5.5}$$

[2]The RP-CLT for renewal processes is very different from the ordinary Central Limit Theorem (CLT): In the CLT, it is the sum of the RVs that is approximately Gaussian [52, Chapter 2], while in the RP-CLT, it is the number N of the summed RVs that is approximately Gaussian [52, Chapter 7].

To find $\mathbb{E}\{N\}$, we first calculate $\mathbb{E}\{b\}$ as

$$\mathbb{E}\{b\} = \mathbb{E}\left\{\frac{R}{\eta}\right\} = \mathbb{E}\{R\}\mathbb{E}\left\{\frac{1}{\eta}\right\}, \tag{5.6}$$

since R_i and η_i are independent RVs. Then, substituting $\mathbb{E}\{b\}$ in (5.5),

$$\mathbb{E}\{N\} \cong \frac{W}{\mathbb{E}\{R\}}\eta_{\text{eq}}\,, \tag{5.7}$$

where we call η_{eq} the equivalent spectral efficiency (ESE), and is calculated as:

$$\eta_{\text{eq}} = \frac{1}{\mathbb{E}\{1/\eta\}}\ \text{(bps/Hz/Sector)}. \tag{5.8}$$

The ESE η_{eq} is an interesting metric, as it predicts the pattern performance abstracting from the bandwidth and the rate. It is obtained by simulating many UEs in the network and considering their spectral efficiency.

5.2.1.2 Variance and Distribution of Number of Users

Similarly, again from the RP-CLT [52, Chapter 7], the variance of $\bar{N}(W)$ is approximated by

$$\begin{aligned}\mathbb{VAR}\{N\} &\cong \frac{W\,\mathbb{VAR}\{b\}}{\mathbb{E}^3\{b\}} \\ &\cong \frac{W\,\mathbb{VAR}\{b\}}{\mathbb{E}^3\{R\}\mathbb{E}^3\{1/\eta\}}.\end{aligned} \tag{5.9}$$

First, we find $\mathbb{VAR}\{b\}$ as

$$\begin{aligned}\mathbb{VAR}\{b\} &= \mathbb{VAR}\left\{\frac{R}{\eta}\right\} \\ &= \mathbb{VAR}\{R\}\mathbb{VAR}\left\{\frac{1}{\eta}\right\} \\ &+ \mathbb{VAR}\{R\}\mathbb{E}^2\left\{\frac{1}{\eta}\right\} \\ &+ \mathbb{E}^2\{R\}\mathbb{VAR}\left\{\frac{1}{\eta}\right\}.\end{aligned} \tag{5.10}$$

After plugging (5.10) into (5.9), and doing some simplifications, we obtain

$$\begin{aligned}\mathbb{VAR}\left\{N\right\} \cong \mathbb{E}\left\{N\right\}\mathbb{CoV}^2\left\{\frac{1}{\eta}\right\} \\ \times\left(\mathbb{CoV}^2\left\{R\right\}+\frac{\mathbb{CoV}^2\left\{R\right\}}{\mathbb{CoV}^2\left\{1/\eta\right\}}+1\right),\end{aligned} \tag{5.11}$$

where the coefficient of variation of a random variable X is defined as $\mathbb{CoV}\left\{X\right\} = \sqrt{\mathbb{VAR}\left\{X\right\}}/\mathbb{E}\left\{X\right\}$.

For a constant UE rate requirement R, $\mathbb{CoV}\left\{R\right\} = 0$. Therefore, the variance simplifies to

$$\mathbb{VAR}\left\{N\right\} \cong \mathbb{E}\left\{N\right\}\mathbb{CoV}^2\left\{\frac{1}{\eta}\right\}. \tag{5.12}$$

Since the distribution of $\bar{N}(W)$ is approximately Gaussian [52, Chapter 7], we now know the approximate distribution of N. Thus, for example, the number of UEs we can support 97.5% of the time is approximately

$$\begin{aligned}&\mathbb{E}\left\{N\right\} - 1.96\sqrt{\mathbb{VAR}\left\{N\right\}} \\ =&\mathbb{E}\left\{N\right\} - 1.96\sqrt{\mathbb{E}\left\{N\right\}}\mathbb{CoV}\left\{\frac{1}{\eta}\right\},\end{aligned} \tag{5.13}$$

where 1.96 comes from the Gaussian table for the 97.5% area of the normal distribution.

5.2.2 Site-Level CSO Patterns

We consider 14 different site-level regular CSO patterns, where only entire BSs are switched off (i.e., there is no individual sector switch-off). Most of these patterns appear in the regular CSO patterns literature (see Table 5.1).

The pattern for which all BSs are active (without CSO) is called $\mathsf{P}(1)$. Then $\mathsf{P}(n/m)$ is the pattern where n out of every m BSs are active; the proportion of active cells in these patterns is $\rho = \frac{n}{m}$. For some patterns with the same $\frac{n}{m}$ there are several distinct rotations. To differentiate between those rotations, patterns are referred to as $\mathsf{P}_{\mathrm{X}}(n/m)$, where the subscript X denotes a particular rotation.

Fig. 5.2 shows the different possible patterns we investigate at the site-level. Those patterns are based on the well-known frequency reuse patterns, where m is the number of BSs in the reuse cluster. The patterns are assumed to be periodic, i.e.,

they expand to infinity. However we limited the simulation region, keeping in mind that there should be enough BSs to model all the dominating interferers.

5.2.3 Combining Sector-Level and Site-Level Patterns

Previous papers on regular CSO patterns focus on site-level patterns only, i.e., there is no individual sector switch-off. For the first time, we investigate the effect of using sector-level regular CSO patterns; these patterns are denoted as $\mathsf{P}(1, k/3)$, where k is the number of active sectors per site. The proportion of active sectors is $\rho = \frac{k}{3}$. There are three different patterns at this level: all sectors are active: $\mathsf{P}(1)$; two sectors are active: $\mathsf{P}(1, 2/3)$; and only one active sector: $\mathsf{P}(1, 1/3)$. No rotations are necessary at this level, as site-level patterns already contain all possible rotations. Fig. 5.3 illustrates the sector-level patterns that can be combined with each site-level pattern to form new patterns.

Sector-level CSO patterns become more interesting when combined with site-level CSO patterns. Any site-level pattern can be combined with any sector-level pattern, in which case the active sectors are those resulting from the logical-AND operation of the two patterns (there are 14×3 combinations). These patterns are denoted as $\mathsf{P}_{\mathrm{X}}(n/m, k/3)$, where the subscript X denotes the rotation of the pattern, the first term inside parenthesis denotes the site-level pattern, and the second term denotes the sector-level pattern. The proportion of active sectors is $\rho = |\mathsf{P}(n/m, k/3)| = \frac{nk}{3m} \in [0, 1]$.

In order to further illustrate this idea, we focus on two interesting examples. These examples introduce different patterns with the same proportion of active sectors.

5.2.3.1 One-Third of the Sectors are Active

In this example, we illustrate all the CSO patterns where One-third of the sectors are active (i.e., $\rho = \frac{1}{3}$), namely: $\mathsf{P}(1, 1/3)$, $\mathsf{P}(1/3)$, $\mathsf{P}_{\mathrm{A}}(2/4, 2/3)$, $\mathsf{P}_{\mathrm{B}}(2/4, 2/3)$, and $\mathsf{P}_{\mathrm{C}}(2/4, 2/3)$. These patterns are illustrated in Fig. 5.4. It is worth mentioning that there are different rotations for the case of $\mathsf{P}(2/4, 2/3)$. Two of them, $\mathsf{P}_{\mathrm{A}}(2/4, 2/3)$ and $\mathsf{P}_{\mathrm{B}}(2/4, 2/3)$, represent different sectors in the same pattern, whereas $\mathsf{P}_{\mathrm{C}}(2/4, 2/3)$ is a different pattern.

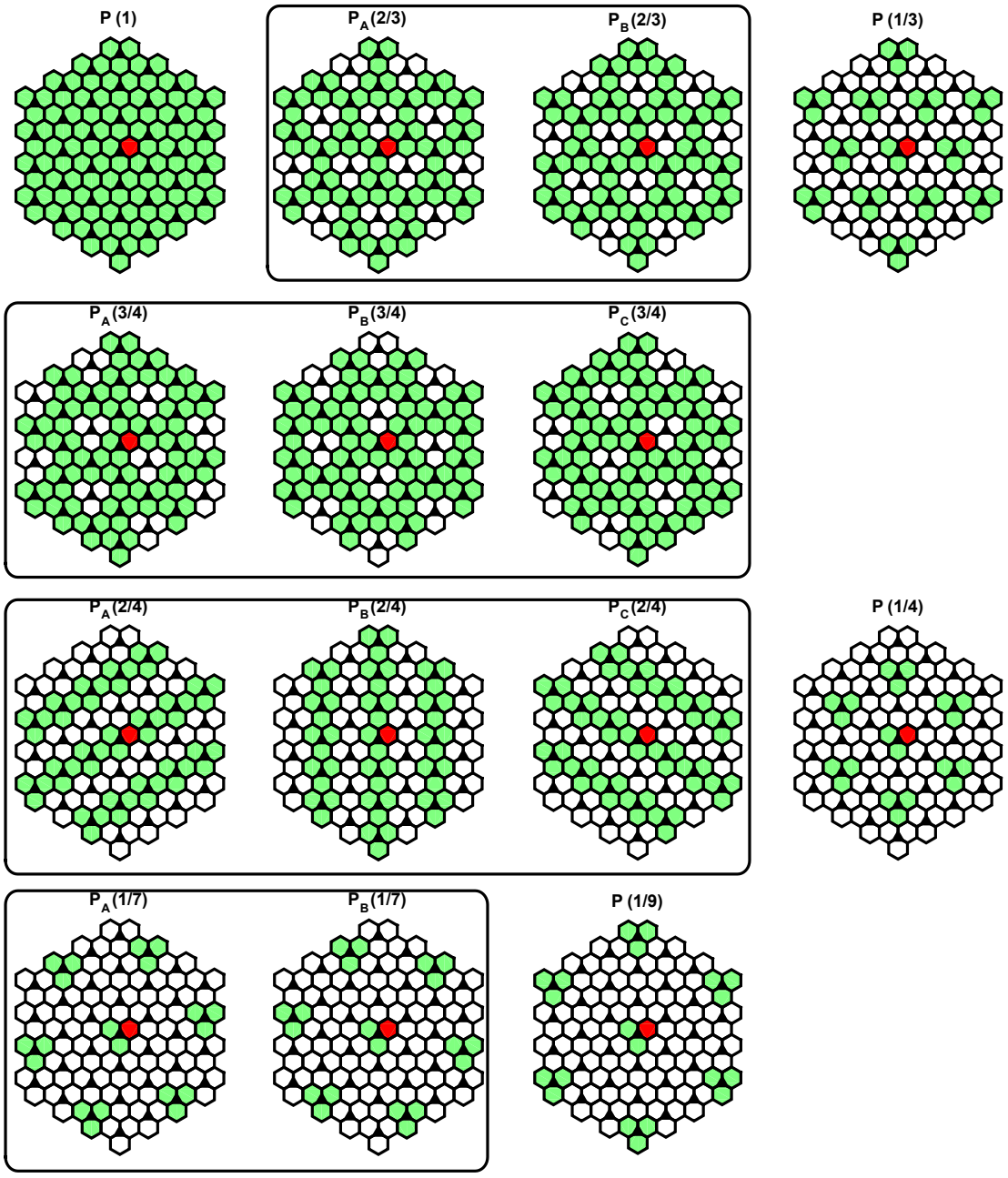

Figure 5.2: Site-level patterns. Black triangles are site locations, each site having three sectors. The red hexagon is sector 1, to which the UE is connected; green hexagons are active sectors which cause interference to the UE; while white hexagons are switched-off sectors. Patterns with the same number of active BSs but having different rotations are enclosed in a rectangle.

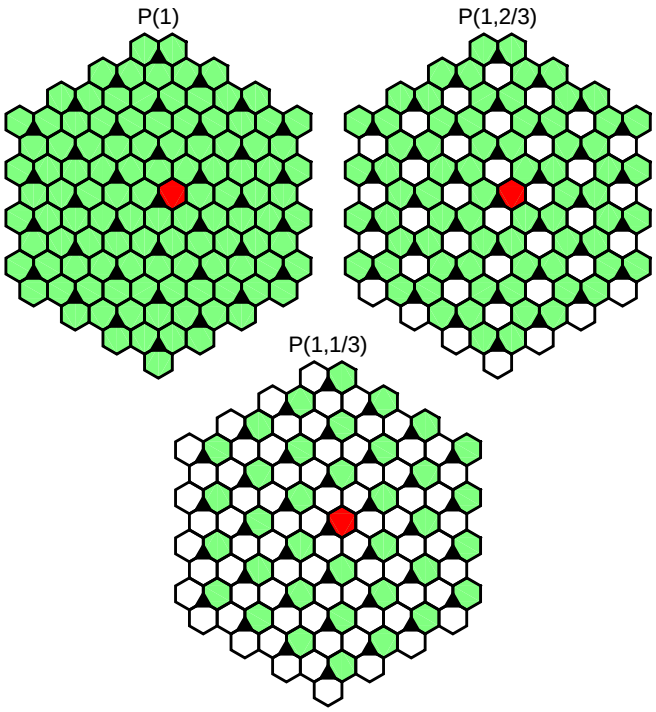

Figure 5.3: Sector-level patterns. All BSs are active and only the number of active sectors per BS is different.

5.2.3.2 One-Sixth of the Sectors are Active

In this example, we illustrate all the CSO patterns where one-sixth of the sectors are active (i.e., $\rho = \frac{1}{6}$), namely: $\mathsf{P}(1/4, 2/3)$, $\mathsf{P}_{\mathrm{A}}(2/4, 1/3)$, $\mathsf{P}_{\mathrm{B}}(2/4, 1/3)$ and $\mathsf{P}_{\mathrm{C}}(2/4, 1/3)$. These patterns are illustrated in Fig. 5.5. It is worth mentioning that there are different rotations for the case of $\mathsf{P}(2/4, 1/3)$. Two of them, $\mathsf{P}_{\mathrm{B}}(2/4, 1/3)$ and $\mathsf{P}_{\mathrm{C}}(2/4, 1/3)$, are the same patterns, whereas $\mathsf{P}_{\mathrm{A}}(2/4, 1/3)$ is a different pattern.

We will investigate the first example in detail in Section 5.4.

5.2.4 Number of Supported Users in the Network

The total number of supported UEs over the total number of sectors in the network is found by multiplying (5.7) by ρ:

$$\mathbb{E}\{\rho N\} \cong \frac{W}{\mathbb{E}\{R\}} \eta_{\mathrm{eq}} \rho. \tag{5.14}$$

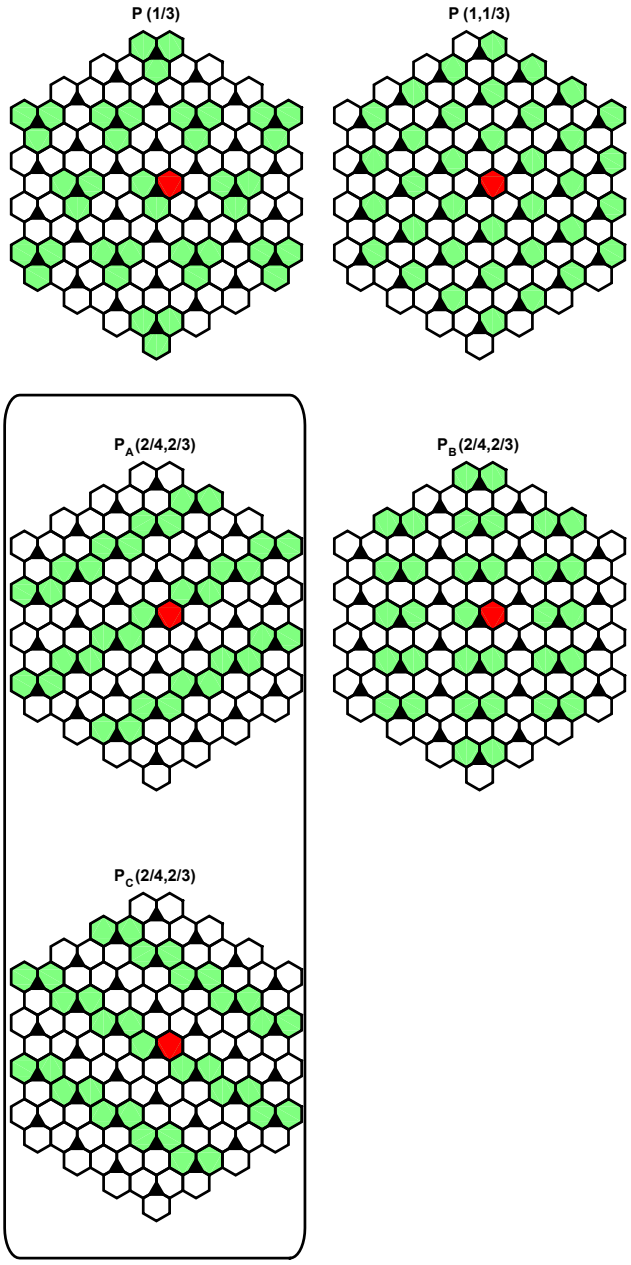

Figure 5.4: All patterns with $\rho = 1/3$. Patterns inside the rectangle are parts of the same overall pattern.

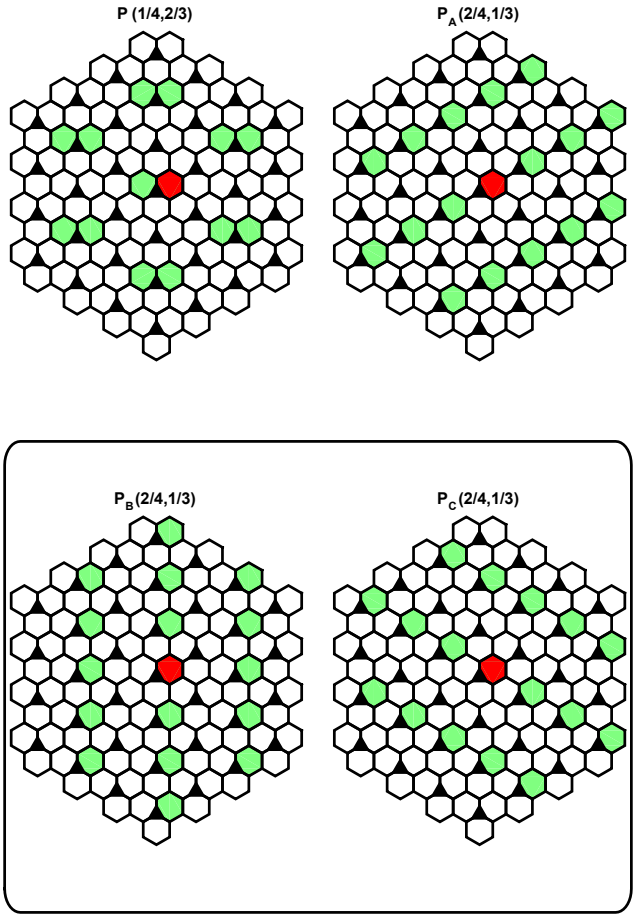

Figure 5.5: All patterns with $\rho = 1/6$. Patterns inside the rectangle are the same.

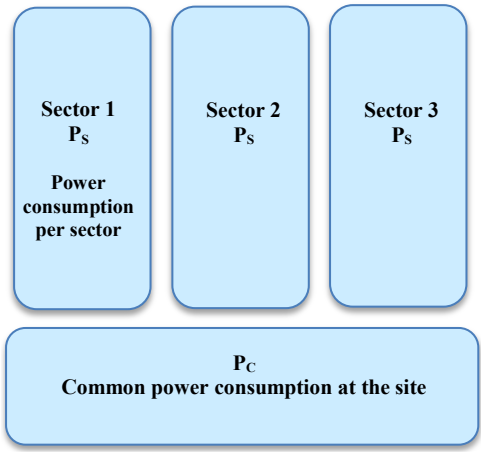

Figure 5.6: Power consumption at a site $P_{\text{site}} = P_{\text{C}} + 3P_{\text{S}}$ when all sectors are active.

In order to find the average number of UEs supported by the network, one simply multiplies (5.14) by the total number of sectors in the network. Thus, $\eta_{\text{eq}}\,\rho$ is proportional to the average number of UEs supported by the network for a given pattern. Conversely, (5.14) allows us to choose the CSO pattern that can support a given user density based on $\eta_{\text{eq}}\,\rho$.

5.2.5 Sector-Based vs. Site-Based Energy Efficiency

In some CSO literature, the amount of energy saving is assumed to be directly proportional to the number of switched-off BSs [5, 6, 53]. This is a valid assumption, especially as the power consumption of a BS is highly independent of its load [5, 6]. It is worth investigating the relationship between site-level switch-off and sector-level switch-off energy in terms of energy efficiency. In a typical LTE network, each BS has three sectors; however, switching off one sector per BS does not necessarily result in one-third of energy saving. This is because there is common hardware that is shared among the three sectors at each site, such as cooling and baseband processing equipment. This is summarized in Fig. 5.6.

The average power consumption at each system site of pattern $\mathsf{P}(n/m, k/3)$ is

$$P_{\text{pattern}} = \frac{n}{m}(P_{\text{C}} + kP_{\text{S}}), \tag{5.15}$$

where P_{C} is the common power consumption at the site; and P_{S} is the power consumption per sector. This equation is useful to determine which pattern to choose when considering two patterns with the same ρ.

In this subsection, we provide the analysis to compare the energy efficiency of site-level CSO pattern $\mathsf{P}(n/3m)$; with that of the sector-level CSO pattern $\mathsf{P}(n/m, 1/3)$. Both patterns have the same proportion of active sectors $\rho = \frac{n}{3m}$. Then, for pattern $\mathsf{P}(n/m, 1/3)$, we have

$$P_{\text{pattern,1}} = \frac{n}{m}(P_{\mathrm{C}} + 1P_{\mathrm{S}}), \tag{5.16}$$

and for pattern $\mathsf{P}(n/3m)$, we have

$$P_{\text{pattern,2}} = \frac{n}{3m}(P_{\mathrm{C}} + 3P_{\mathrm{S}}). \tag{5.17}$$

We compare the energy efficiency in terms of power consumption per user as

$$\frac{P_{\text{pattern,1}}}{N_1} = \frac{P_{\text{pattern,2}}}{N_2}. \tag{5.18}$$

The average number of users N is found from (5.7) and we substitute in (5.18) to get

$$\frac{P_{\text{pattern,1}}}{\eta_{eq,1} W/\mathbb{E}\{R\}} = \frac{P_{\text{pattern,2}}}{\eta_{eq,2} W/\mathbb{E}\{R\}}, \tag{5.19}$$

which simplifies to

$$\frac{P_{\text{pattern,1}}}{P_{\text{pattern,2}}} = \frac{\eta_{eq,1}}{\eta_{eq,2}}. \tag{5.20}$$

Then, substituting (5.16) and (5.17) in (5.20), we obtain

$$\frac{(1+\alpha)}{(1+\frac{\alpha}{3})} = \frac{1}{\delta}, \tag{5.21}$$

where, $\delta = \eta_{eq,2}/\eta_{eq,1}$ and $\alpha = P_{\mathrm{C}}/P_{\mathrm{S}}$.[3]

Finally, we can find the breakpoint as

$$\alpha^* = \frac{1-\delta}{\delta - \frac{1}{3}}. \tag{5.22}$$

If $\alpha < \alpha^*$ then the site-level pattern $\mathsf{P}(n/3m)$ is more energy efficient; otherwise, the

[3]The value of α would be known by the network operator.

pattern $\mathsf{P}(n/m, 1/3)$ with 1/3 active sectors is preferred.

Similar calculations can be done for the case of 2/3 active sectors; however, we will find in the next section that those patterns are not favourable in terms of energy efficiency, regardless of α.

5.3 Simulation Evaluation of Patterns

We consider the downlink of a cellular network with a hexagonal layout. We simulate two ITU scenarios, the Urban Micro-cell (UMi) and the Urban Macro-cell (UMa), according to the evaluation guidelines of [26]. The simulation parameters are listed in Table 2.1.

Sector 1 (the red hexagon) is chosen as a typical sector; we consider all UEs that get the best downlink SINR when connected to sector 1. Other active sectors (green hexagons) will cause interference to those UEs. All UEs are uniformly and independently distributed over the entire network area.

For each CSO pattern, we simulate a large number of UEs to estimate the ESE according to (5.8), as well as P_o and $\mathbb{C}\text{oV}\{1/\eta\}$. Results are summarized in Table 5.3 for both the UMi and the UMa scenarios.

Fig. 5.7 compares the performance of different CSO patterns. The x-axis is proportional to the average number of UEs that can be supported by the network, as given by (5.14), and hence is also proportional to the aggregate rate. The y-axis is the proportion of active sectors ρ. The energy consumption of the network when configured to a particular pattern is computed from both ρ and the marker type; different markers indicate the number of active sectors per BS site. The reference line indicates where the performance of the network is scaled proportionally with respect to the fully active network $\mathsf{P}(1)$. The trend is that patterns with all sectors active fall close to the reference line, while patterns with two active sectors per BS fall to the left of the reference line (i.e., perform worse). Interestingly, patterns with one active sector per BS fall to the right of the line (i.e., perform better). Notably, consider the case of $\rho = 1/3$: the number of active sectors is reduced to One-third; however, the average number of UEs that can be supported by pattern $\mathsf{P}(1, 1/3)$ is only reduced to 48.5%. This means that almost half of full capacity is achieved using only 1/3 of the sectors. The yellow staircase curve shows the operational region based on the best

Table 5.3: Characteristic Values of CSO Patterns.

	UMi				UMa			
Pattern	η_{eq}	$\eta_{\text{eq}}.\rho$	$P_o\%$	$\mathbb{C}\text{oV}\left\{\frac{1}{\eta}\right\}$	η_{eq}	$\eta_{\text{eq}}.\rho$	$P_o\%$	$\mathbb{C}\text{oV}\left\{\frac{1}{\eta}\right\}$
$\mathsf{P}(1)$	1.53	1.53	0.00	0.75	1.37	1.37	0.00	0.63
$\mathsf{P}(1, 2/3)$	1.36	0.91	0.10	0.75	1.36	0.91	0.00	0.66
$\mathsf{P}(1, 1/3)$	2.22	0.74	0.00	0.82	2.06	0.69	0.08	0.86
$\mathsf{P}_{\text{A}}(2/3)$ $\mathsf{P}_{\text{B}}(2/3)$	1.53	1.02	0.00	0.75	1.32	0.88	0.05	0.70
$\mathsf{P}_{\text{A}}(2/3, 2/3)$ $\mathsf{P}_{\text{B}}(2/3, 2/3)$	1.36	0.61	0.057	0.73	1.31	0.59	0.07	0.73
$\mathsf{P}_{\text{A}}(2/3, 1/3)$ $\mathsf{P}_{\text{B}}(2/3, 1/3)$	2.08	0.46	0.01	0.94	1.72	0.39	0.67	0.95
$\mathsf{P}(1/3)$	1.44	0.48	0.76	0.84	1.36	0.45	0.82	0.83
$\mathsf{P}(1/3, 2/3)$	1.28	0.29	0.15	0.78	1.17	0.26	1.35	0.80
$\mathsf{P}(1/3, 1/3)$	1.92	0.21	0.14	0.95	1.48	0.16	3.41	0.97
$\mathsf{P}_{\text{A}}(3/4)$ $\mathsf{P}_{\text{B}}(3/4)$ $\mathsf{P}_{\text{C}}(3/4)$	1.54	1.15	0.01	0.74	1.33	1.0	0.07	0.69
$\mathsf{P}_{\text{A}}(3/4, 2/3)$ $\mathsf{P}_{\text{B}}(3/4, 2/3)$ $\mathsf{P}_{\text{C}}(3/4, 2/3)$	1.36	0.68	0.05	0.74	1.31	0.66	0.09	0.72
$\mathsf{P}_{\text{A}}(3/4, 1/3)$ $\mathsf{P}_{\text{B}}(3/4, 1/3)$ $\mathsf{P}_{\text{C}}(3/4, 1/3)$	2.14	0.55	0.01	0.91	0.78	0.44	0.46	0.95
$\mathsf{P}_{\text{A}}(2/4)$ $\mathsf{P}_{\text{B}}(2/4)$ $\mathsf{P}_{\text{C}}(2/4)$	1.51	0.76	0.01	1.75	1.35	1.67	0.08	1.71
$\mathsf{P}_{\text{A}}(2/4, 2/3)$ $\mathsf{P}_{\text{C}}(2/4, 2/3)$	1.30	0.44	0.08	0.74	1.18	0.40	0.75	0.76
$\mathsf{P}_{\text{B}}(2/4, 2/3)$	1.41	0.47	0.01	0.73	1.42	0.47	0.09	0.75
$\mathsf{P}_{\text{A}}(2/4, 1/3)$	1.75	0.29	0.30	1.03	1.36	0.23	2.64	0.97
$\mathsf{P}_{\text{B}}(2/4, 1/3)$ $\mathsf{P}_{\text{C}}(2/4, 1/3)$	2.02	0.34	0.01	0.90	1.63	0.27	1.29	0.96
$\mathsf{P}(1/4)$	1.55	0.39	0.00	0.69	1.45	0.36	0.39	0.75
$\mathsf{P}(1/4, 2/3)$	1.26	0.21	0.35	0.76	1.14	0.19	2.80	0.83
$\mathsf{P}(1/4, 1/3)$	1.74	0.14	0.54	0.98	1.42	0.12	5.66	0.98
$\mathsf{P}_{\text{A}}(1/7)$ $\mathsf{P}_{\text{B}}(1/7)$	1.24	0.18	0.84	0.77	1.15	0.17	5.82	0.82
$\mathsf{P}_{\text{A}}(1/7, 2/3)$ $\mathsf{P}_{\text{B}}(1/7, 2/3)$	1.08	0.10	2.63	0.78	1.05	0.10	9.57	0.81
$\mathsf{P}_{\text{A}}(1/7, 1/3)$ $\mathsf{P}_{\text{B}}(1/7, 1/3)$	1.46	0.07	4.66	1.05	1.37	0.07	14.45	1.03
$\mathsf{P}(1/9)$	1.20	0.13	1.21	0.78	1.16	0.13	8.53	0.84
$\mathsf{P}(1/9, 2/3)$	1.08	0.08	4.65	0.79	1.04	0.08	13.26	0.82
$\mathsf{P}(1/9, 1/3)$	1.41	0.05	8.46	1.06	1.32	0.05	18.68	1.01

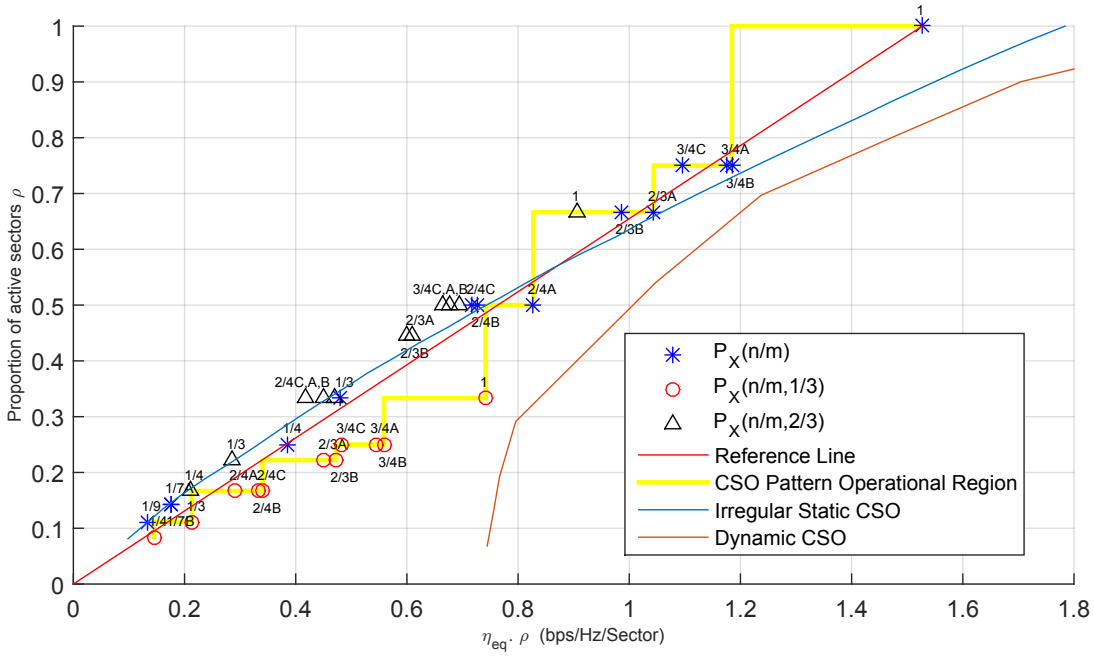

Figure 5.7: Performance comparison of different patterns and other CSO schemes for the UMi scenario. The x-axis is proportional to the average number of UEs supported by the network. The y-axis is the proportion of active sectors. The reference line gives locations where the performance of the network is scaled proportionally with respect to the fully active network $\mathsf{P}(1)$. The operational region curve follows the best performing pattern for any given ρ. The irregular static CSO is a benchmark from [23], while the dynamic CSO is a benchmark from [21]. Patterns with outage $P_o > 2\%$ are not included.

performing pattern for any given ρ. This curve can be used by operators to select the best pattern that can support a given user density demand. The operational region (yellow staircase), could be used directly only for the specific case of $\alpha = 0$ (no common power).

In order to make the study complete, we compare the performance of regular CSO patterns with irregular static (offline) CSO [23] and also with dynamic (online) CSO [21]. Note that the values for irregular static CSO are obtained according to the simulation parameters indicated in [23], but with a uniform UE distribution. As we can conclude from the figure, regular CSO patterns perform comparably and even better at some points, to the irregular static CSO. For the case of dynamic CSO, the values in the curve are obtained according to the simulation parameters indicated in [21], but with a uniform UE distribution. It is worth mentioning that the simulation parameters used in [21] are not entirely compliant with our simulation parameters. One fundamental difference is that in [21], UEs are served in a way that maximizes the aggregate network capacity, i.e., UEs with high spectral efficiency are provided with large bandwidth, while UEs with low spectral efficiency might be blocked. In contrast, in our simulation, UEs are served on a first-come, first-served basis. Thus [21] can be considered as an upper bound for both CSO and admission control design.

Fig. 5.8 shows a similar comparison for the UMa scenario, with similar trends.

5.4 Case Study

In this section, we further investigate all the CSO patterns with $\rho = 1/3$, shown in Fig. 5.4 (the first example from Section 5.2.3). All the figures in this section are for the UMi scenario; however, we find that the UMa scenario results in a similar trend [54].

5.4.1 SINR Distribution

Each CSO pattern results in a different spatial distribution of the SINR of a typical UE conditioned to be connected to sector 1, as seen in Fig. 5.9.

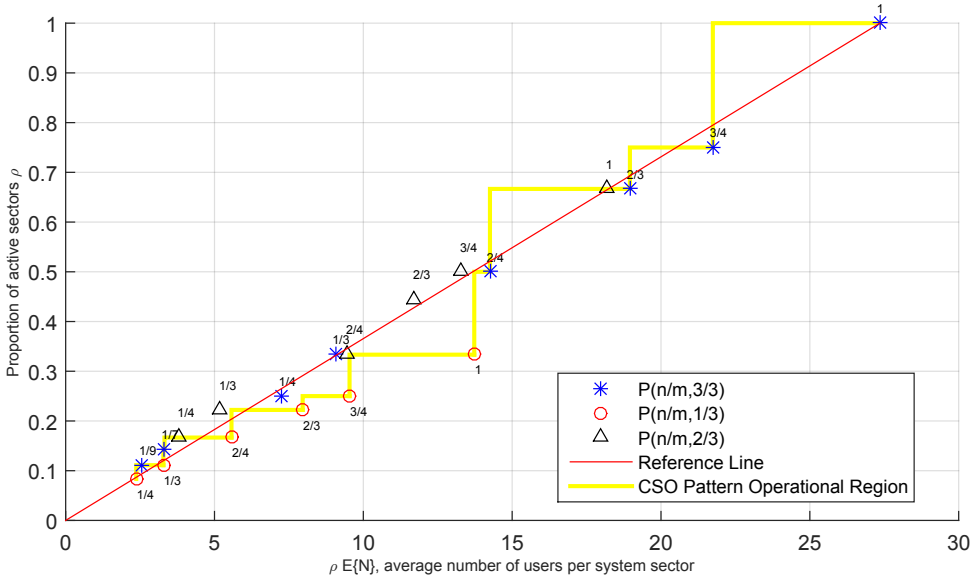

Figure 5.8: Performance comparison of different patterns for UMa scenario. The x-axis is the average number of UEs supported per system sector when $W/R = 20$. The y-axis is the proportion of active sectors. The trend is similar to that of the UMi scenario.

Fig. 5.10 shows the effect of the chosen patterns on the resulting cumulative distribution function (CDF) of the downlink SINR for UEs connected to sector 1. To validate our simulation platform, we also included the average CDF results obtained from the WINNER+ project using multiple simulation tools [28]. As shown in the figure, the SINRs obtained from pattern $\mathsf{P}(1)$ have a CDF that closely matches the WINNER+ results. Note that pattern $\mathsf{P}(1)$ is the case where all cells are active, i.e., without CSO.

It is worth mentioning that there is a high improvement in the SINR in pattern $\mathsf{P}(1, 1/3)$, where only one sector is active per site. This improvement is due to the significant reduction in the number of nearby interferers. Moreover, the SINR values are truncated at 18 dB [29]; these higher SINR values might be of interest in future systems that allow for higher constellations.

5.4.2 Number of Users per Sector

We now compare the number of supported UEs per active sector for all patterns with $\rho = 1/3$. After finding η_{eq} and $\mathbb{C}\text{oV}\{1/\eta\}$ for each pattern, we assume a constant rate

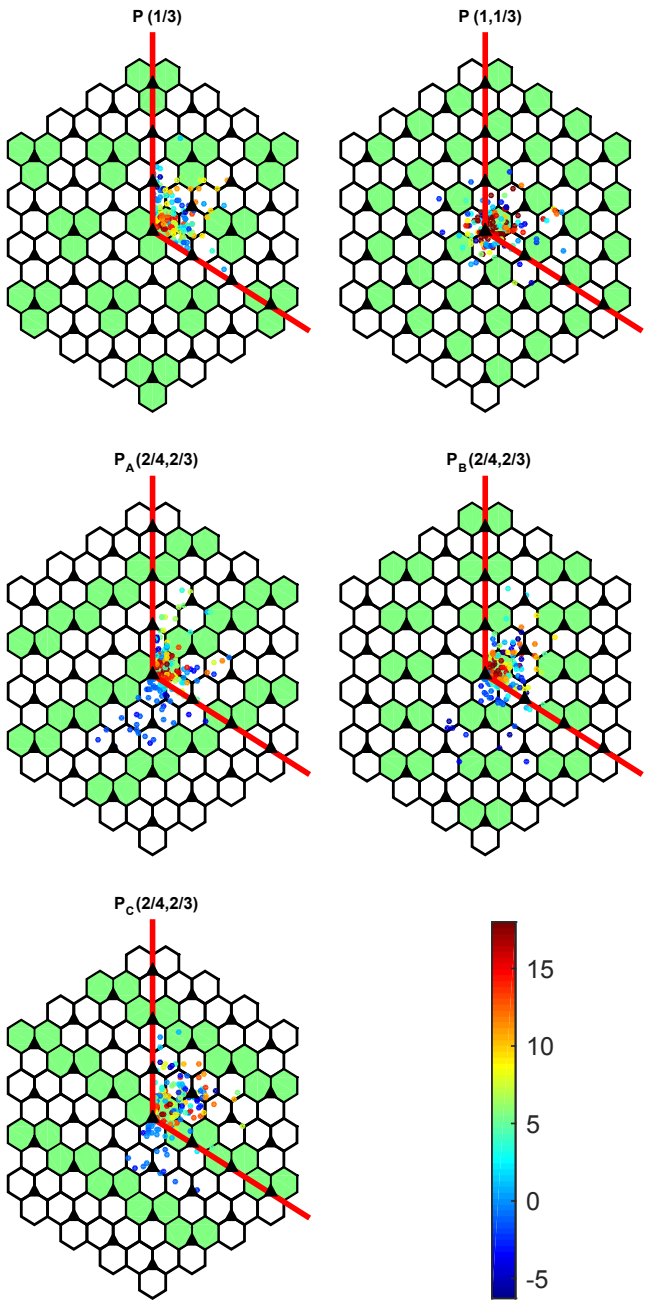

Figure 5.9: Conditional spatial distribution of the SINR (in dB) of a typical UE when connected to sector 1, for patterns in Fig. 5.4, for the UMi scenario (the UMa scenario shows a similar trend). The UE is connected to the sector that results in the highest downlink SINR.

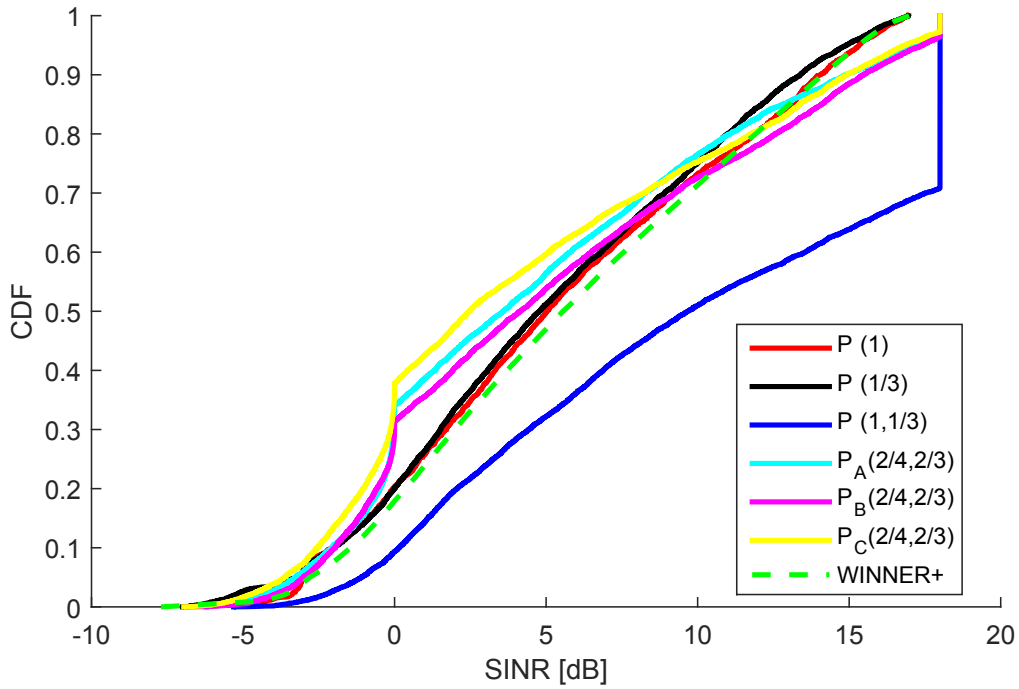

Figure 5.10: CDFs of SINR for patterns in Fig. 5.4 for the UMi scenario, with WINNER+ calibration for the fully active network (pattern $\mathsf{P}(1)$).

demand of 500 kbps and a system bandwidth of 10 MHz, resulting in $W/\mathbb{E}\{R\} = 20$ and $\mathbb{C}\mathrm{oV}\{R\} = 0$. We also find the number of UEs that a typical sector can support, and show both the simulated and the closely matching analytical CDFs (from Section 5.2.1.2) in Fig. 5.11. Analytical calculations show that the $\mathsf{P}(1, 1/3)$ pattern can support the most UEs (44.5 UEs) per sector on average - this is also approximately the median (50%), since N is close to Gaussian- and about 33 UEs 97.5% of the time (according to (5.13)). The distribution of the number of UEs closely follows a Gaussian distribution, as expected from the analysis in Section 5.2.1.2.

5.4.3 Energy Efficiency Aspects

Based on the calculations in Section 5.2.5, we can find the breakpoint that indicates which pattern is better in terms of energy efficiency per UE. While the patterns with 2/3 active sectors are never advantageous, the pattern $\mathsf{P}(1, 1/3)$ is advantageous over

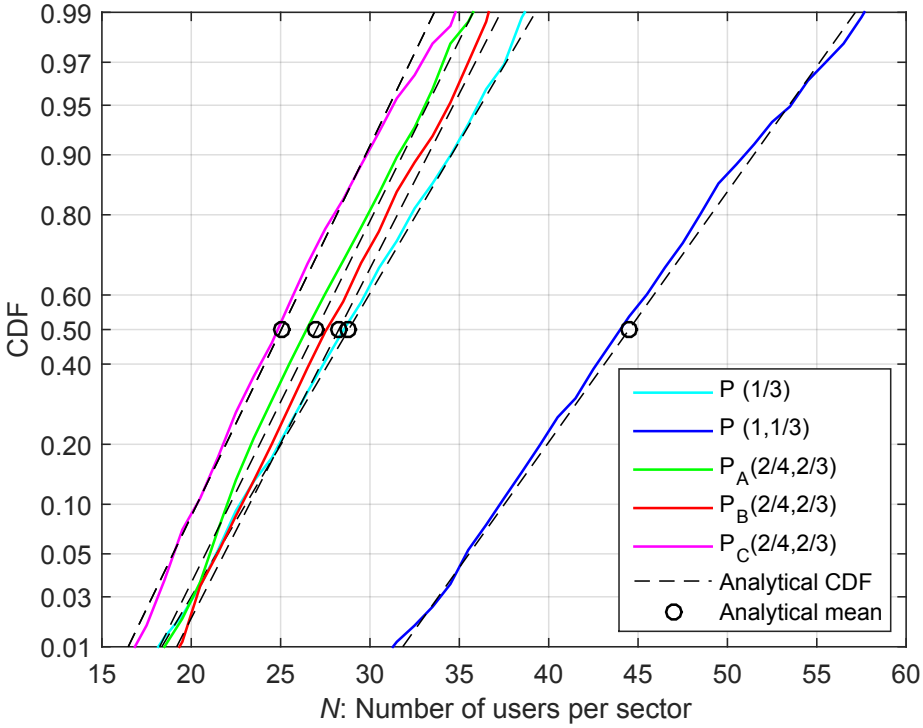

Figure 5.11: CDFs of the number N of UEs supported for patterns in Fig. 5.4, when R is constant and $W/R = 20$, for the UMi scenario. The y-axis is transformed so that all and only Gaussian distributions appear as straight lines. The coloured curves are simulated CDFs, which closely match the analytical CDFs. Black circles are the analytical means, which are close to the simulation medians (50%).

pattern $\mathsf{P}(1/3)$, as long as $P_{\mathrm{C}}/P_{\mathrm{S}} > \alpha = 1.114$, as found from (5.22).

5.5 Conclusion

CSO is a promising approach for more energy-efficient cellular networks. In this chapter, classified and investigated 26 different regular CSO patterns in detail, and presented them using a systematic nomenclature. Furthermore, this paper was the first to investigate sector-based regular CSO patterns. The performances of different CSO patterns were compared using only one parameter. The distribution of the number of users supported was found to be close to Gaussian with a variance estimated using one additional parameter. The maximum number of supported users was usually obtained from patterns where one sector out of three is active at a site. In many cases, the performance of regular CSO patterns is comparable to that of a benchmark irregular static CSO. Moreover, although a benchmark dynamic CSO outperforms the regular CSO patterns, it is still reasonable to employ the regular CSO patterns because of their simplicity and scalability.

Regular CSO patterns are conceptually simple and can be characterized systematically both statistically and geometrically. Location regularity of CSO patterns provides the advantages of: 1) ensuring that interferer cells are as far away as possible, 2) allowing for realistic interference modelling, 3) minimizing the coverage holes, and 4) being more energy-efficient for users in the uplink transmission, since users do not need to transmit at full power because there is always a nearby active cell.

The advantages of the regularity of CSO pattern are very encouraging. In the next chapter, we studied the possibility of benefit from CSO in making the cellular layout to be more regular even for networks with irregular BS placements.

Chapter 6

Evaluating Cell Switch-Off Algorithms for Networks with Spatially Irregular BS Deployments

6.1 Introduction

In Chapters 4 and 5, we introduced the CSO approach and its potential for energy saving in cellular networks in periods of light traffic. We found that regular CSO patterns are advantageous in terms of modeling interference properly, reducing coverage holes, and making the uplink transmissions more energy-efficient for UEs. These advantages came without much compromise of the performance of the CSO patterns over dynamic CSO, as investigated in detail in Chapter 5.

In most of the CSO literature, BSs are placed according to a triangular lattice (TL). The geographical cell boundary is a function of the Euclidean distance that correspond to a hexagonal Voronoi tessellation. Hexagonal cell shapes are preferred because it covers an entire area without gaps or overlaps. Another BS locations model is placing BSs randomly according to a Poisson point process (PPP). For the same number of BSs in the network, the TL model produces an upper bound on he downlink SIR, and SINR performance, whereas the PPP model results in a lower bound [57].

[1]Part of this chapter is a collaboration work that resulted in the submission of two letters [55, 56] and a magazine paper under preparation. The contribution of Quoc-Nam Le-The (a summer student with the NSERC Undergraduate Student Research Award program) was inventing a new algorithm, conducting the programming, and wrote an early draft of [56]. Faraj Lagum (a PhD student in our research group) provided expertise in stochastic geometry, provided simulation code, and introduced the new CSO problem formulation in [55].

6.1.1 BS Location Models in CSO Literature

In CSO literature the common BS location models are

- Manhattan layout: BSs are placed on the vertices of a square grid [58].
- Hexagonal layout: BSs are placed on TL [6, 18, 58].
- Poisson layout: BSs are distributed over the service area according to a two-dimensional homogeneous PPP with density λ_P [58–60].

While the first two models represent a perfect regular grid, the last one represents a totally random layout.

However, due to geographic restrictions of site placement and the network planning, BS locations are neither regular nor completely random [2, 61]. In addition to providing coverage, extra BSs might be located in hot spots to deliver more capacity, making their placement irregular.

While placing BSs based on a TL model results on an upper bound on the SIR, placing them according to a PPP model produces a lower bound. Therefore, there is a need to have a model that can change the BS regularity between these two extremes. The repulsive point processes (RPPs), from the literature of stochastic geometry, are found to be useful to model actual BS locations. Recent work [55, 56] in the context of CSO use RPPs to model BS locations so that they are neither perfect regular nor totally random.

If we combine this irregularity with the observation that the best SIR distribution can be achieved when BSs are located on a regular grid [49, 61], we find a great opportunity for applying CSO to irregular network layouts with the objective of making the active BS locations as regular as possible.

This problem has been introduced only recently in [55]. Therefore, it is worth evaluating CSO algorithms designed for layouts with irregular BS locations.

In this chapter, we evaluate CSO algorithm designed for networks with spatially irregular BS deployment with the extra objective of selecting the set of active BSs so that their locations form a layout with maximum regularity, regardless of the irregularity of the original network layout. This problem is motivated by two observations:

- Regular CSO patterns are simple and perform very well, as discussed in Chapter 5.

Table 6.1: List of Symbols.

M	number of BSs in the network
ρ	fraction of active BSs in the network
ρM	number of desired active BSs
Δ	inter-site distance between BSs
r	hard-core distance
Γ	disc radius for uniform PTL
$\tilde{\Gamma}$	normalized perturbation radius = Γ/Δ
λ	BS density
λ_{P}	BS density of a PPP
D_{ij}	distance between BS i and BS j
D	the minimum distance between any pair of active BSs
C_{D}	coefficient of variation of the Delaunay triangulation edge lengths
k_{D}	normalization factor
μ_{D}	mean of the Delaunay edge lengths
σ_{D}	standard deviation of the Delaunay edge lengths
$G_{\mathrm{SIR}}(X)$	downlink SIR gain for fraction X of users

- The best download SIR is achieved when BSs are located on regular grid [49,61].

In this chapter, we generate irregular BS locations using a perturbed triangular lattice (PTL) model, where we can vary the spatial regularity of BS locations continuously from perfect regular grid to totally random. We test the suitability of several algorithms for applying CSO to irregular network layouts with the objective of making the active BS locations as regular as possible, regardless of the irregularity of the original network layout. Moreover, we also evaluate some of these algorithms on real BS locations obtained from a major cellular operator in Canada.

6.2 Problem Formulation

Consider a network with M BSs. The idea of CSO is that when the users service demand decreases (at night time for example), the demand could be supported by only fraction ρ of BSs. Without loss of generality, we assume that, for a given service level, the required number of active BSs ρM is proportional to the decrease in demand. Moreover, additional BSs might be switched of as the SIR improves. All the symbols used in this chapter are shown in Table 6.1.

Different algorithms result in different sets of combinations of ρM active BSs. We are interested in evaluating these algorithms to find the one that results in the best downlink SIR.

In order to evaluate different algorithms in different spatial regularity levels, we first need a point process that has the ability to vary the spatial regularity regularity of BS locations over the full range between TL and PPP.

6.2.1 Modeling BS Locations

In cellular networks, the actual layout of BS locations lies somewhere in between the perfect TL and the totally random PPP [49, 57, 61–63]. Therefore, we first need to have a point process that can generate BSs locations so that it can sweep the entire regularity spectrum, from perfect regular grid (TL) to totally random deployment (PPP).

The BS density λ (number of BSs per km^2) is the main parameter to describe the layout of the network. However, density by itself cannot describe the the regularity of BS locations, therefore, another parameter is needed to quantify the distance between any pairs of BSs. RPPs can characterize this parameter and it can be classified, based on the strictness of the allowable distance condition r, as soft-core and hard-core models.

6.2.1.1 Soft-Core Point Processes

Points have probabilities of being closer than r to each other. Some examples of soft-core point processes are determinantal point process models [64], and the family of Gibbs point processes [49, 63].

6.2.1.2 Hard-Core Point Processes

A minimum separation (hard-core) distance $r > 0$ is assumed, where points are not allowed to be closer than r to each others. Three different hard-core processes are proposed to model BS locations [65, 66]. The generation of these processes usually starts with a PPP and then some points are eliminated. The type of the hard-core process is determined by the point elimination criterion as follows:

- Matérn Hard-Core Process of Type I: Generate a PPP with density λ_{P} BSs per km^2, and then simultaneously eliminate points that are separated by a distance

that is shorter than r. The resulting density of this model is $\lambda = e^{-\lambda_P \pi r^2}$.

- Matérn Hard-Core Process of Type II: This process starts with a PPP as well. It assigns to each point a mark between [0,1], points with higher marks than their neighbouring are simultaneously eliminated. A neighbour of a point is defined as any point that is within radius r from that point. The resulting density of this model is $\lambda = (1 - e^{-\lambda_P \pi r^2})/\pi r^2$.

- Simple Sequential Inhibition (SSI): Points are generated sequentially according to a PPP. If a point is closer than r to any previously generated point, then it is discarded. This is repeated until the required density λ is reached.

6.2.1.3 Perturbed Triangular Lattice

This is the model we use for irregular BS deployment. We will discuss it in detail in the following subsection.

6.2.2 Chosen BS Location Model: Perturbed Triangular Lattice

A significant limitation of the RPPs is the difficulty of generating a very high regularity with these models because points are generated independently based on their distances. Therefore, we choose to model BS locations using the PTL model which have the capability of sweeping over the full range of regularity from perfect regular TL to totally random PPP (asymptotically). [67].

The PTL process begins with generating a TL, where BSs are located on a hexagonal layout with inter-site distance Δ.

The PTL is obtained by displacing each point by an independent random vector. Depending on the distribution of this random vector, there are two PTL models: uniform PTL, and Gaussian PTL. The two models results in similar SIR [67]. We model BS locations using a uniform PTL, in which, in which the displacement vector has a uniform distribution over a disc of radius Γ. The most interesting parameter is the normalized radius $\tilde{\Gamma} = \Gamma/\Delta$, which controls the amount of regularity.

Fig. 6.1 shows visualizations of cell layouts of BSs deployed with different spatial regularities. Fig. 6.1(a) visualizes a layout of BSs deployed with TL (perfect regularity). Fig. 6.1(d) visualizes a layout with BSs deployed according to PPP. Fig. 6.1(b)

Table 6.2: Relationship between normalized perturbation radius $\tilde{\Gamma}$ and regularity metric C_{D} [67].

C_{D}	0.1	0.2	0.3	0.4	0.5
$\tilde{\Gamma}$	0.059	0.129	0.202	0.278	0.360
C_{D}	0.6	0.7	0.8	0.9	≈ 1
$\tilde{\Gamma}$	0.450	0.562	0.729	1.063	≥ 2

and Fig. 6.1(c) visualize layouts that are neither regular nor totally random.

6.2.3 Spatial Regularity Metrics

In order to compare the performance of different algorithms, we first define the metrics.

6.2.3.1 Geometry-Based Metrics for Spatial Regularity

The first geometry-based metric is the distance between the two nearest BSs. Our objective is to maximize the minimum distance D between any pair of BSs.

The second geometry-based metric is C_{D}. This metric was proposed in [61, 68], and is used to measure the spatial regularity of the locations of all BSs in the network. It is the normalized coefficient of variation of the Delaunay triangulation edge lengths of a set of points. It is called C_{D}, and can be found by:

$$C_{\mathrm{D}} = \frac{1}{k_{\mathrm{D}}} . \frac{\sigma_{\mathrm{D}}}{\mu_{\mathrm{D}}}, \tag{6.1}$$

where μ_{D} and σ_{D} are the mean and the standard deviation of the Delaunay edge lengths, respectively; and $k_{\mathrm{D}} \cong 0.492$ is the normalization factor such that for a PPP $C_{\mathrm{D}} = 1$ on average [61]. C_{D} is thus a measure of spatial regularity of points, where TL is a perfectly regular layout with $C_{\mathrm{D}} = 0$ and PPP is the totally random (irregular) layout with $C_{\mathrm{D}} = 1$ [67].

The C_{D} metric is a bijective function of $\tilde{\Gamma}$ [67] with values shown in Table 6.2.

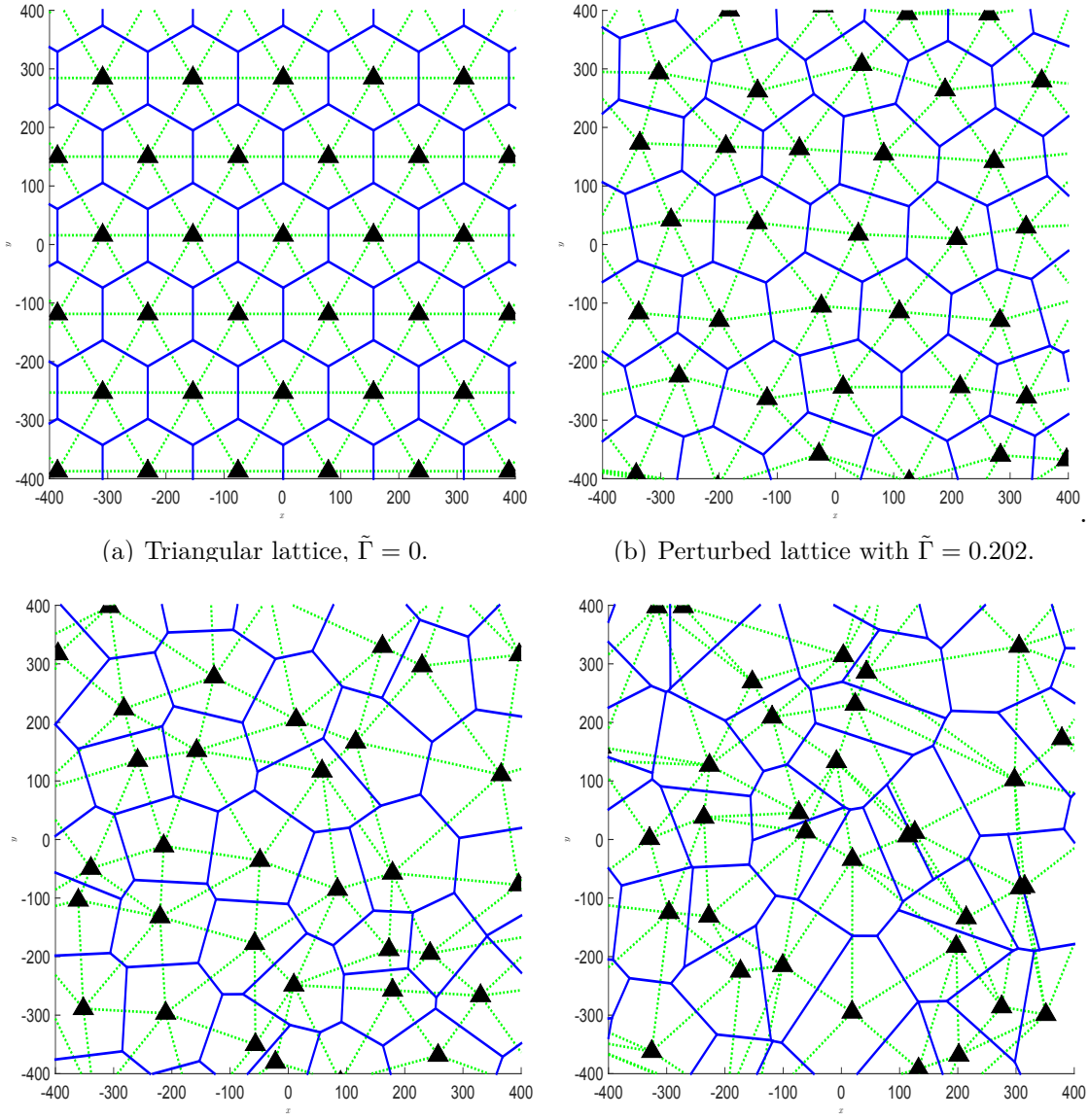

(a) Triangular lattice, $\tilde{\Gamma} = 0$.

(b) Perturbed lattice with $\tilde{\Gamma} = 0.202$.

(c) Perturbed lattice with $\tilde{\Gamma} = 0.450$.

(d) PPP with $\tilde{\Gamma} \geq 2$.

Figure 6.1: BSs (black triangles) located according to random point processes, with their Delaunay triangulation (dashed green lines) and Voronoi tessellation (solid blue lines).

6.2.3.2 SIR-Based Metric

It is known that the best downlink SIR is achieved when BSs are placed on a regular grid [49, 61]. Also, from the UE perspective, it is more energy efficient for UEs to have regular grid, which guarantees not only having a nearby BS, but also insures that interfering BSs are carefully located far away.

The metric used to evaluate different CSO algorithms is the downlink SIR gain $G_{\mathrm{SIR}}(X\%)$ in dB, which is the difference between the SIR for the best $X\%$ of users when the active BSs are selected according to a given algorithm, and the SIR in a network with the same number of BSs but deployed randomly (according to a PPP). We measure the SIR gain for 50% and 95% of users.

Although the objective of the problem in hand is to maximizing the minimum distance between active BSs, measuring the SIR is a good indicator of the algorithm performance. A problem with the same objective exist in literature of operation research known as the PDP which is a simple version the FLP.

6.2.4 *p*-Dispersion Problem

The PDP concerns about the mutual distances between open facilities, with the objective of maximizing the minimum distance between any two open facilities [27]. The PDP has the objective of maximizing the minimum mutual distance between any pair of facilities for a given number of active facilities. The distance between BS i and BS j is given by D_{ij}. The objective is to maximize the minimum separation distance D between any pair of active BSs.

$$\begin{aligned}
&\text{maximize } && v, && && \text{(6.2a)}\\
&\text{subject to } && \sum_{j\in\mathcal{S}} y_j = \rho M, && && \text{(6.2b)}\\
& && v \le D_{ij} + D_M(1-y_i) + D_M(1-y_j), && && \\
& && && \forall i,j \in \mathcal{S}, i<j, && \text{(6.2c)}\\
& && y_j \in \{0,1\}, && \forall j \in \mathcal{S}. && \text{(6.2d)}
\end{aligned}$$

The first constraint is to have exactly ρM active BSs. The second constraint defines the minimum distance between pairs of active BSs [69]; this constraint is binding only when both BSs i and j are active then the constraint is equivalent to

$v \leq D_{ij}$. Therefore, maximizing D has the effect of forcing the minimum pairwise distance to be as large as possible. The last constraint is the binary constraint that a BS j should be either on or off.

6.3 Algorithms for Maximizing Spatial Regularity

The PDP is well-studied problem that has different proposed algorithms. Given that the PDP is NP-hard, heuristic algorithms are encouraged. Authors in [70, 71] compared the performance of ten heuristic algorithms to solve the PDP. The pseudo-codes for all these algorithms can be found in [70].

In this chapter, we evaluate the performance of nine of these algorithms, plus one proposed in [56], to solve the CSO problem with the aim of maximizing the SIR by switching of some BSs to improve the regularity of the remaining active BSs.

6.3.1 Triangular Lattice Fit (TLF) Algorithm

This algorithm is proposed in [56]. As known from the literature, the best SIR is achieved with regularly placed BSs; therefore we propose the TLF as a novel algorithm for the CSO problem at hand. For a given CSO percentage, the TLF algorithm starts by creating a regular TL with the required number of active BSs. This generates the theoretical locations of BSs that would maximize regularity. These theoretical points are transformed (rotated and/or shifted) to best fit the real BS locations. This is done by overlaying the theoretical points on top of the real BS locations. To find the best fit, we calculate the distance from each BS to its nearest theoretical point. For each transformation of the theoretical points, we find the sum of those distances. The transformation that yields the minimum sum distance is chosen to be the best fit.

6.3.2 Greedy Algorithms

These algorithms start with a set of BSs and then iteratively select one BS to add to or remove from the solution set. The two common varieties are *greedy construction* (GC) and *greedy deletion* (GD). GC starts with the two furthest BSs and iteratively activates the BS that maximizes the minimum distance to other BSs already in the solution set. GD initializes with all BSs active and finds the nearest two active BSs then switches off the one that has the shortest distance to its second nearest

neighbour, doing so iteratively. The *semi-greedy deletion* (SG) is similar to the GD but the selection among the two nearest BSs being random. The algorithms terminate when the desired number of active BSs is achieved. The three greedy algorithms were implemented in [55]. While GC and GD result in good performance, SG was found to perform poorly, and hence we excluded it from the discussion.

6.3.3 Neighbourhood Algorithms

The neighbourhood algorithms are similar to GC as they iteratively add one BS to the solution set at each step [70]. However, they have a restriction that any added point must be outside of the *neighbourhood* of all of the existing points in the solution set. A neighbourhood of an active BS is defined as a circle with radius r centered at the BS. All other BSs in the circle are switched off. The objective of the neighbourhood algorithms is to generate a solution with a guaranteed separation distance of radius r.

Each neighbourhood algorithm has a different criterion for selecting the new BS to add to the solution set. The three neighbourhood algorithms are *first point outside the neighbourhood* (FP), *closest point outside the neighbourhood* (CS) and *furthest point outside the neighbourhood* (FS). The name of the algorithms specify the criteria used for BS selection. We exclude the FP algorithm due to its poor performance.

6.3.4 Interchange Algorithms

The interchange algorithms initialize with a solution set that contains the desired number ρM of BSs, randomly selected to be active. Then BSs from the solution set are repeatedly interchanged with BSs from outside the set (inactive BSs) if the new BSs increase the objective function. The algorithm terminates when no more interchanges result in an increase in the regularity metric. The three interchange algorithms are *first pairwise interchange* (IF), *best pairwise interchange* (IM), and *simulated annealing* (SA). Whereas IF interchanges an active BS with the first inactive BS that would increase the minimum distance, IM interchanges with the inactive BS that would increase the minimum distance the most. A disadvantage of both IF and IM is that the algorithm could get stuck in a local maximum. SA was proposed in [70] to escape the local maximum by allowing some interchanges that decrease the performance metric in order to eventually hopefully reach the global maximum [72]. Therefore, we were tempted to apply the SA to our problem.

6.3.5 Simulated Annealing

The probability of accepting a worse solution is proportional to the solution quality compared to the current incumbent solution. The probability of accepting a worse solution decreases as the time passes. SA plays an important role in the metaheuristic field. The probability of changing from the current network configuration to a new one is specified by the acceptance function $P(e, T)$ which depends on two factors: the error value e (the difference between the objective function) and the temperature T (the length of the simulation); this probability decreases as the time increases or the difference decreases. The pseudo code of the SA algorithm is shown in Algorithm 3.

However, we did not implement the SA here due to its prohibitive computational time, its several parameters that were complicated to tune correctly, and the high variability (instability) of its output solutions.

6.3.6 Bounds

We place ρM BSs according to a PPP, which is known to give the worst SIR performance [55]: We consider this as the base-line. The algorithms' performance is compared in terms of the SIR gain G_{SIR} (with respect to a PPP deployment). For the same number of BSs, the best SIR is achieved with a TL placement, which is known to have a G_{SIR} of 3.4 dB (compared to the PPP) [73]; this value is considered as the upper bound on the algorithm performance [55]. As a lower bound, we switch off BSs randomly: any reasonable algorithm should at least perform better than this.

6.4 Simulation Setup

First we place 600 BSs in a square area according to a PTL and vary the spatial regularity from TL to PPP to obtain different amounts of spatial regularity C_{D}, by tuning $\tilde{\Gamma}$ according to Table 6.2. All BSs are assumed to have the same transmit power, operating frequency, and are equipped with an omni-directional antenna.

The performance is measured in terms of downlink SIR gain. Users are uniformly distributed inside the central area of the network. The received power is calculated assuming a pathloss exponent of 4 and no shadowing. Users are connected to the BS with the strongest received signal and all of the links experience independent Rayleigh fading. After finding the SIR values of all users, the SIR gain G_{SIR} is then calculated

Algorithm 3: Simulated Annealing

input : The set of candidate BS, and the SA parameters: $FreezeLimit$, $SizeFactor$, $CutOff$, $TempFactor$, and $MinPercent$
output : A set S with ρM BSs

$S \leftarrow$ random solution
$T \leftarrow \max d(p_i, p_j) : p_i, p_j \in P, p_i \neq p_j$
$iterations \leftarrow 0$
while $iterations < FreezeLimit$ **do**
    $trials \leftarrow 0$
    $changes \leftarrow 0$
    while $trials < SizeFactor$ **and** $change < CutOff$ **do**
        $trials \leftarrow trials + 1$
        $p_i \leftarrow$ a random point in S
        $p_i \leftarrow$ a random point in $P \setminus S$
        $S' \leftarrow S \setminus \{p_i\} \cup \{p_j\}$
        $e \leftarrow f(s') - F(s)$
        $r \leftarrow$ a random point in [0,1]
        if $e > 0$ **or** $r < \exp(e/T)$ **then**
            $S \leftarrow S'$
            $changes \leftarrow changes + 1$
        end
    end
    $T \leftarrow T * TempFactor$
    if $f(S)$ has increased **then**
        $iterations \leftarrow 0$
    end
    if $change/trials < MinPercent$ **then**
        $iterations \leftarrow iterations + 1$
    end
end
return $\mathcal{S}$

for 50% and 95% of users. We compare the algorithms at different values of initial network regularity C_{D}. We vary the CSO percentage from 5% to 90%.

6.5 Algorithm Comparison Results

In this section, we compare the results obtained from different CSO algorithms.

6.5.1 SIR Gain

The performance of the algorithms is illustrated in Fig. 6.2 for selected C_{D} values of the initial deployment. We show the SIR gains $G_{\mathrm{SIR}}(0.50)$ and $G_{\mathrm{SIR}}(0.95)$, for 50% and 95% of users, respectively. For both threshoulds, the ordering of the algorithms is similar.

Based on both CSO percentage and C_{D} values, we can choose the best performing algorithm as illustrated in Fig. 6.4. The three dominating algorithms are GD, FS and TLF. Although, the main factor is the CSO percentage, C_{D} also has a moderate effect on the choice of algorithm.

For low CSO percentages ($< 50\%$), GD is the best algorithm for any input C_{D} value. For very high CSO percentages ($> 75\%$), the TLF is the best algorithm. For CSO percentages between 50% and 75%, the best performing algorithm is chosen based on the following formula:

$$C_{\mathrm{D}} \gtrless 1.875 - 3.5\rho, \qquad 0.50 < (1-\rho) < 0.75, \tag{6.3}$$

where ρ is the fraction of active BS, i.e., $=\ 1\ -$ (CSO Percentage), and C_{D} can be estimated for a given point set using (6.1). Based on (6.3) and Fig. 6.4, we have three regions, each having a preferred algorithm:

1. above the line $(C_{\mathrm{D}} + 3.5\rho < 1.875)$: TLF,
2. below the line $(C_{\mathrm{D}} + 3.5\rho > 1.875)$: GD,
3. on the line $(C_{\mathrm{D}} + 3.5\rho \approx 1.875)$: FS.

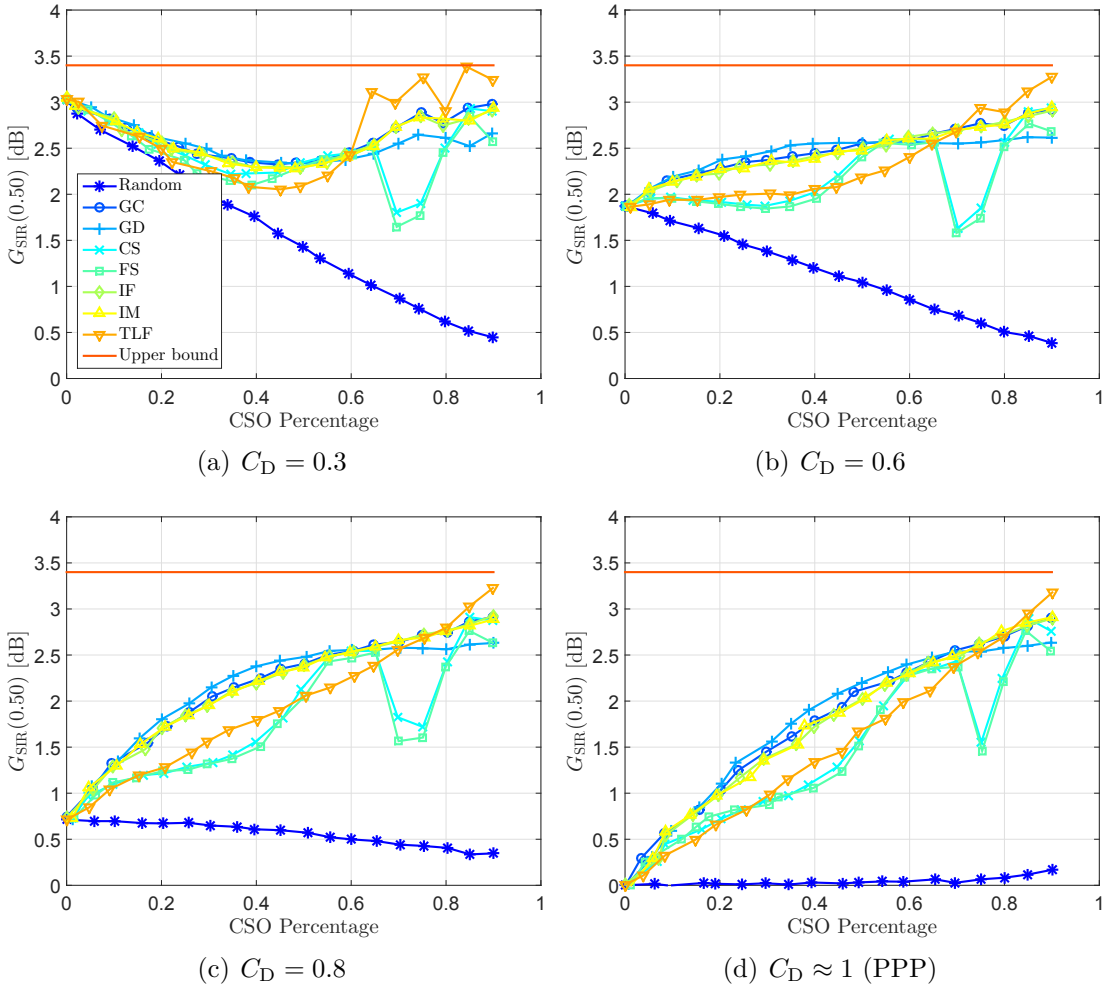

(a) $C_{\mathrm{D}} = 0.3$ (b) $C_{\mathrm{D}} = 0.6$

(c) $C_{\mathrm{D}} = 0.8$ (d) $C_{\mathrm{D}} \approx 1$ (PPP)

Figure 6.2: The SIR gain G_{SIR} for 50% users as a function of the CSO percentage $(1 - \rho)$, for different deployment regularity (C_{D}) of the initial BSs.

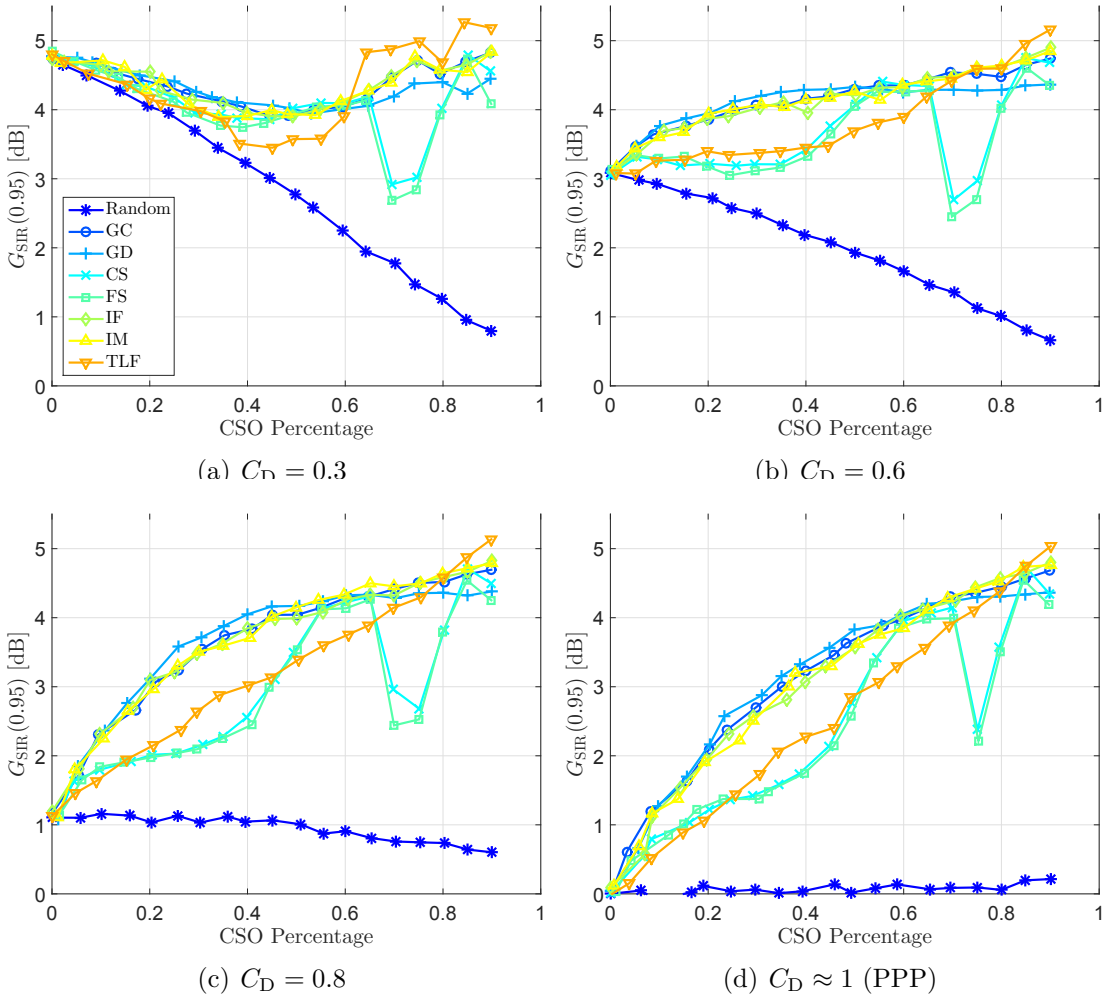

(a) $C_{\mathrm{D}} = 0.3$ (b) $C_{\mathrm{D}} = 0.6$

(c) $C_{\mathrm{D}} = 0.8$ (d) $C_{\mathrm{D}} \approx 1$ (PPP)

Figure 6.3: The SIR gain G_{SIR} for 95% users as a function of the CSO percentage $(1 - \rho)$, for different deployment regularity (C_{D}) values.

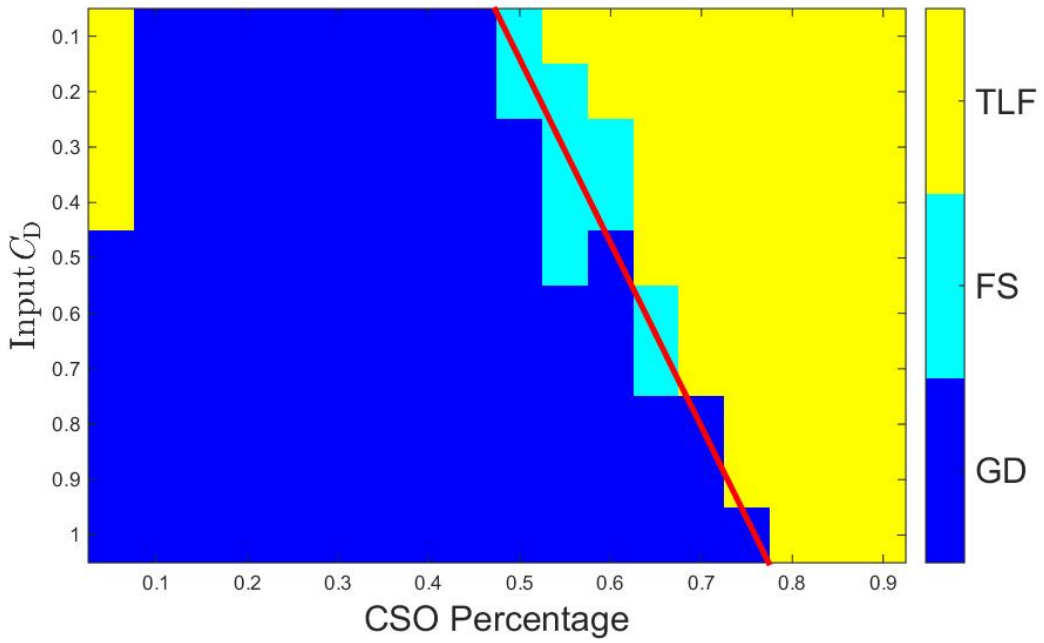

Figure 6.4: Map of the best performing algorithms. The selection of the algorithm can be approximately based on the location with respect to the red line.

Finally, algorithms GC and IF are nowhere optimal, but they are still good overall choices.

It is worth mentioning that the TLF algorithm outperforms all other algorithms for very high CSO percentages (within 1 dB SIR of the upper bound). This is because the number of active BSs decreases as the CSO percentage increases, which results in a greater probability of finding a subset of the BSs that almost matches a regular hexagonal layout. However, for very low CSO percentages the TLF do not perform as well, especially for the case of high spatial regularity, where it performs as poorly as the random algorithm. This is because, when the BSs are already close to regular, switching off some of them often results in a less regular layout.

A summary of all the algorithms and their relative performance is included in Table 6.3.

Table 6.3: Algorithm Summary

Initial	Name	Performance
Recent Algorithm [56]		
TLF	Triangular lattice fit	Performs the best for high CSO percentages; it is not so well for low CSO percentages
Greedy Algorithms [55,70]		
GC	Greedy construction	Performs well in all regions.
GD	Greedy deletion	Performs well in all regions and it is best for low CSO percentages ($< 55\%$).
SG	Semi-greedy deletion	Performs poorly compared to other algorithms.
Neighbourhood Algorithms [70]		
FP	First point outside	Performs well in low CSO percentages ($< 40\%$).
CS	Closest point outside	Performs fairly well in high CSO percentages($> 80\%$).
FS	Furthest point outside	Performs well in all regions and it is the best among the neighbourhood algorithms.
Interchange Algorithms [70]		
IM	Best pairwise	Performs well in all regions but best in none.
IF	First pairwise	Performs well in all regions but best in none. it is faster than IM.
SA	Simulated annealing	Has prohibitive computational time, several parameters to tune, and high variance (instability) of performance.

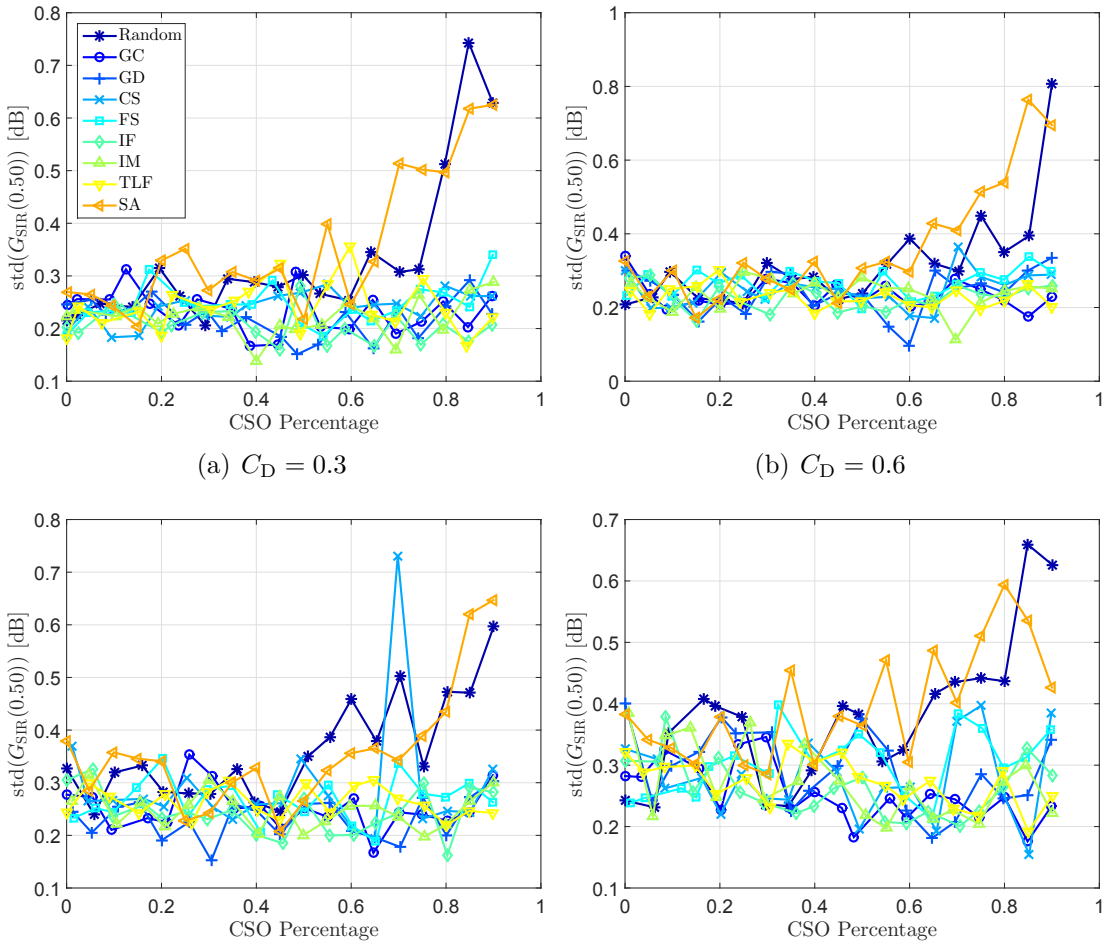

(a) $C_{\mathrm{D}} = 0.3$ (b) $C_{\mathrm{D}} = 0.6$

(c) $C_{\mathrm{D}} = 0.8$ (d) $C_{\mathrm{D}} \approx 1$ (PPP)

Figure 6.5: The standard deviation (std) of the SIR gain G_{SIR} for 50% users as a function of the CSO percentage $(1-\rho)$, for different deployment regularity (C_{D}) values.

6.5.2 SIR Standard Deviation

We also compare the standard deviation of the SIR of 50% of users after applying different algorithms, as illustrated in Fig. 6.5. Both the random CSO and the simulated annealing (SA) have a very high standard deviation up to 0.8 dB, especially in the case of higher CSO percentages. For this reason, we prefer not to study the SA algorithm, and leave it for future study where a comprehensive parameter calibration would be necessarey before considering it for CSO.

6.6 Visualization of Algorithms

In this section, we visualize the effect of applying different algorithms on the cellular layout and how the algorithms try to maximize regularity.

6.6.1 Simulated Networks

We simulate networks with initial BS density of $\lambda = 100$ BSs per km^2, deployed for two spatial irregularity values of $C_{\mathrm{D}} = 0.3$ and $C_{\mathrm{D}} = 0.6$ shown in Fig. 6.1(b) and Fig. 6.1(c), respectively. We select four algorithms – Random, TLF, IF and GC – to visualize the change on the cellular layout as a result of applying each CSO algorithms. We visualize the active cells after applying CSO algorithms at three different CSO percentages: 25%, 50%, and 75%. As we can see from Figs 6.9, 6.10, and 6.11, the more BSs are to be switched off, the more freedom algorithms have to make the layout more regular. As the CSO percentage increases, we notice an improvement in the regularity (the cells become close to hexagons), and as we reach the case of 75% CSO, we gain more freedom in selecting the set of active cells and hence improve the regularty, and consequently the SIR.

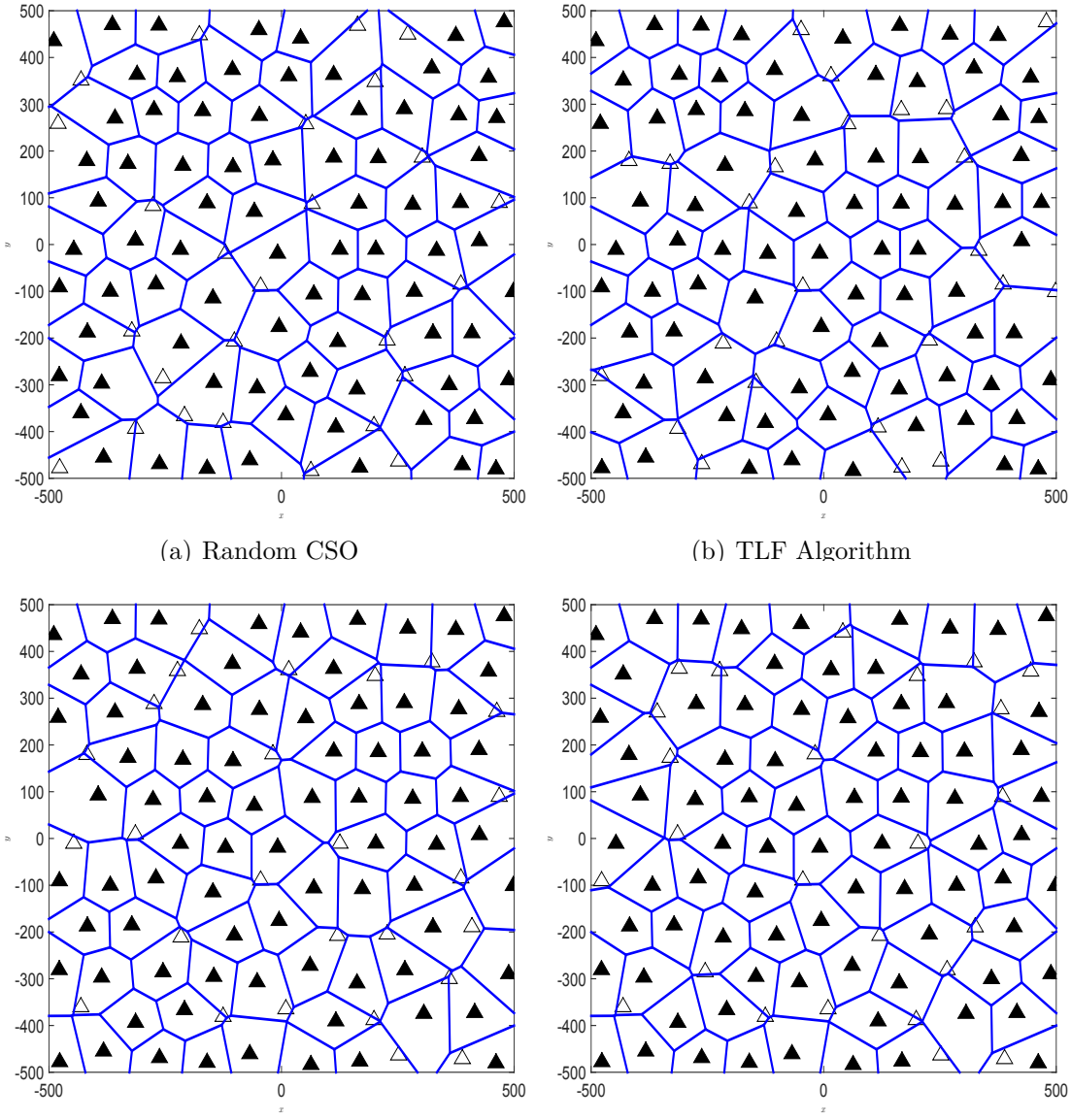

(a) Random CSO

(b) TLF Algorithm

(c) IF Algorithm

(d) GC Algorithm

Figure 6.6: Voronoi tessellation of active BSs (black triangles) after 25% CSO with initial regularity of $C_{\mathrm{D}} = 0.3$; empty triangles are the locations of switched-off cells.

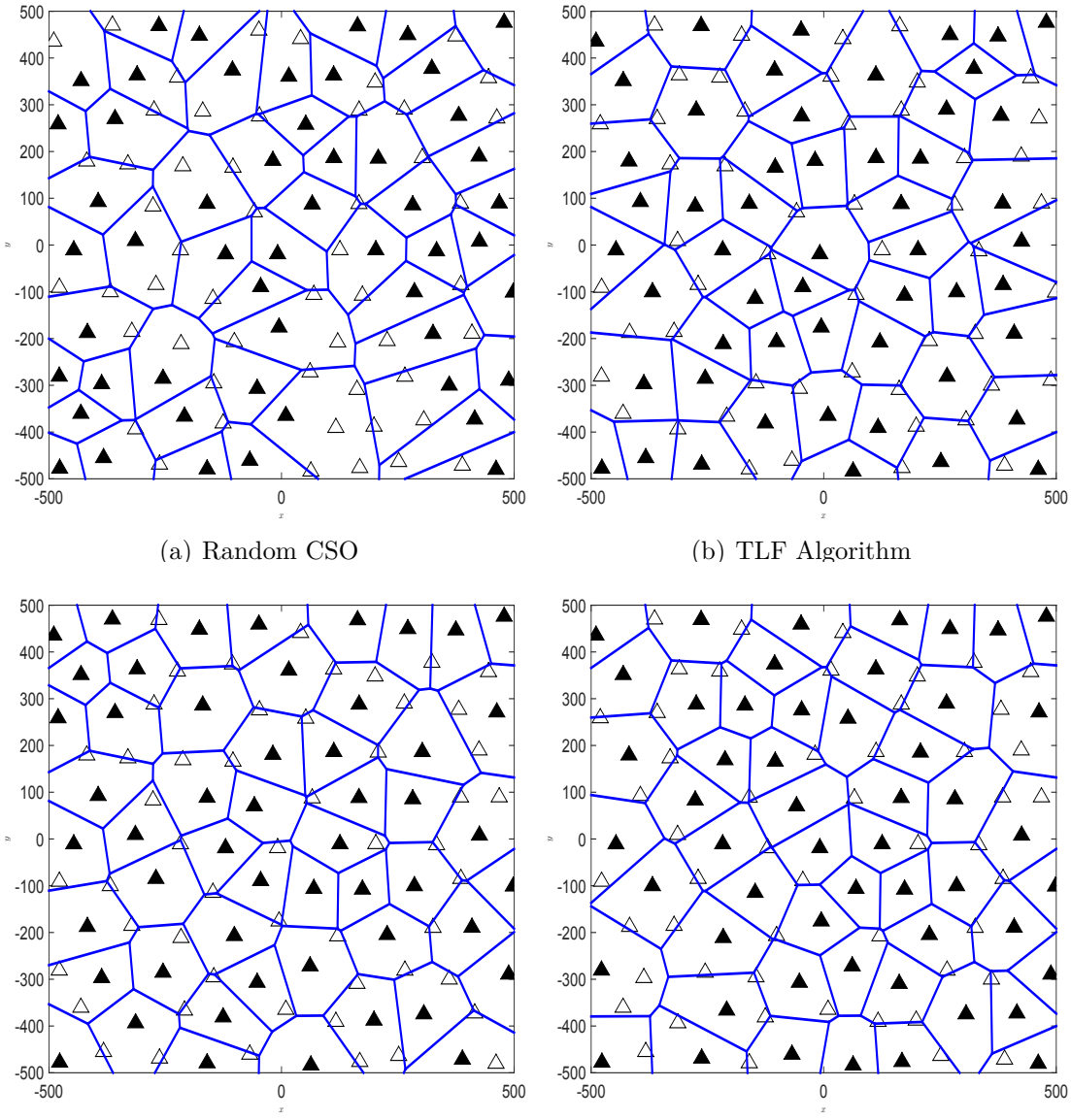

(a) Random CSO

(b) TLF Algorithm

(c) IF Algorithm

(d) GC Algorithm

Figure 6.7: Active cells after 50% CSO with initial regularity of $C_{\mathrm{D}} = 0.3$.

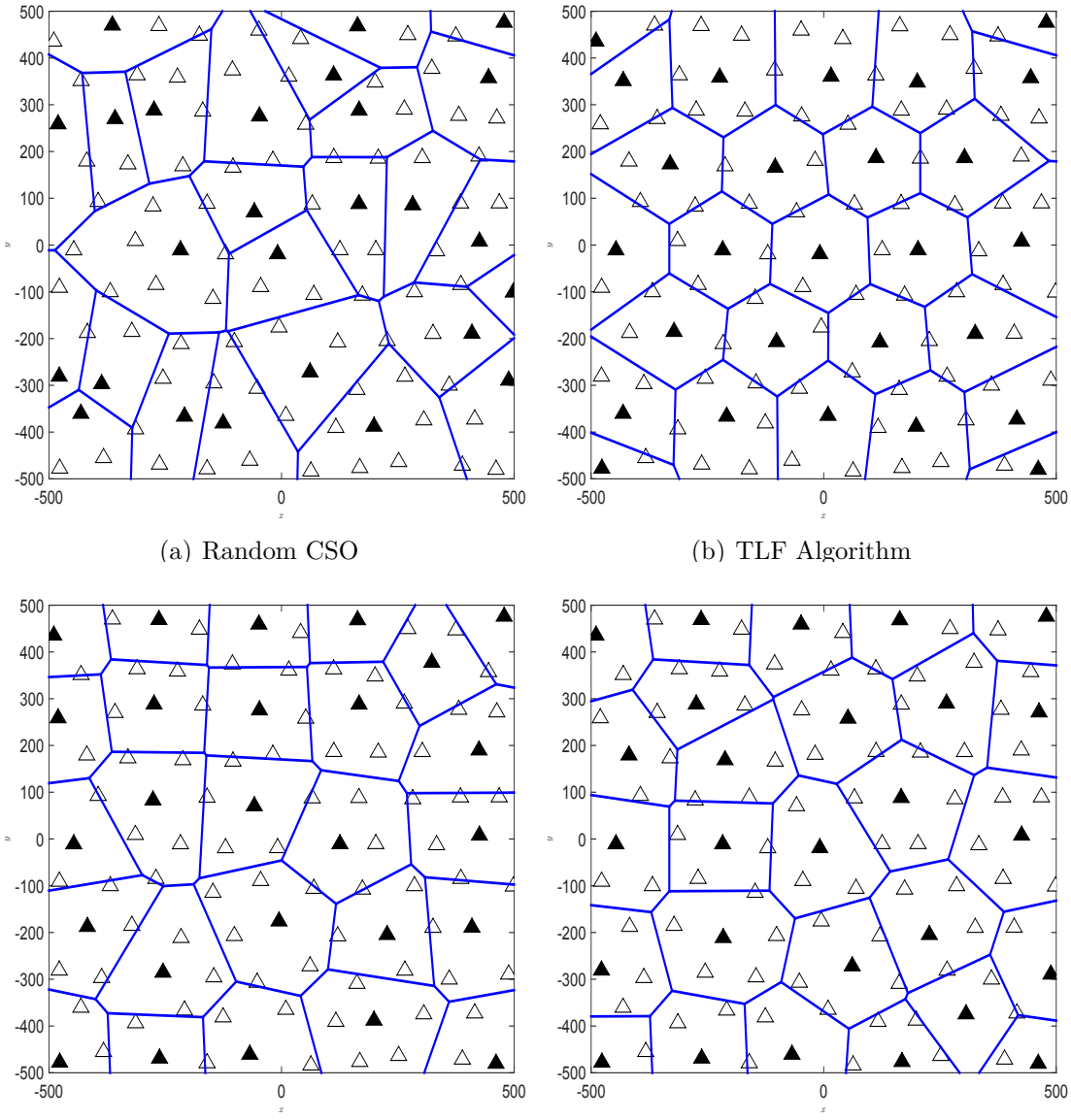

(a) Random CSO

(b) TLF Algorithm

(c) IF Algorithm

(d) GC Algorithm

Figure 6.8: Active cells after 75% CSO with initial regularity of $C_{\mathrm{D}} = 0.3$.

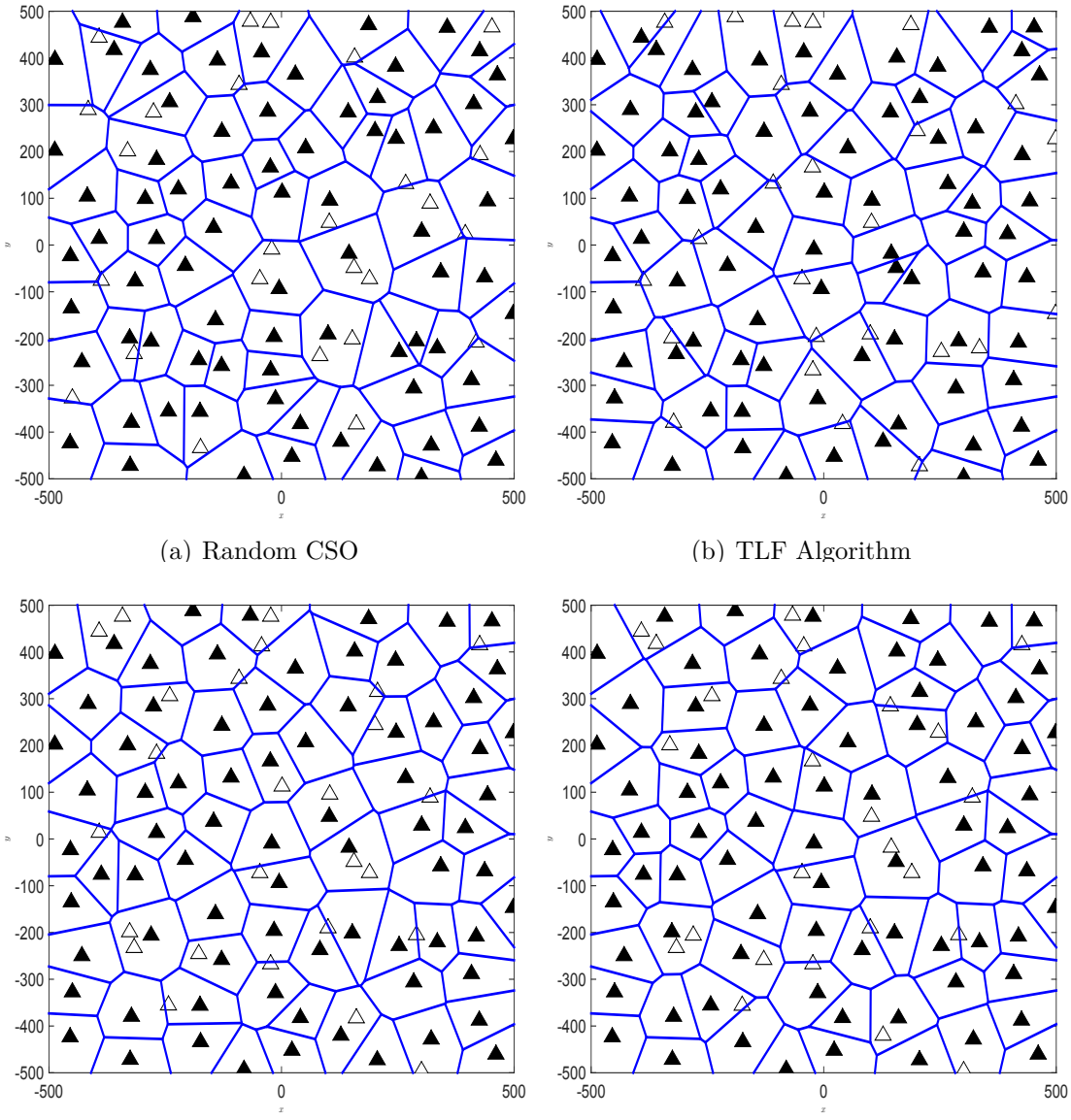

(a) Random CSO

(b) TLF Algorithm

(c) IF Algorithm

(d) GC Algorithm

Figure 6.9: Active cells after 25% CSO with initial regularity of $C_{\mathrm{D}} = 0.6$.

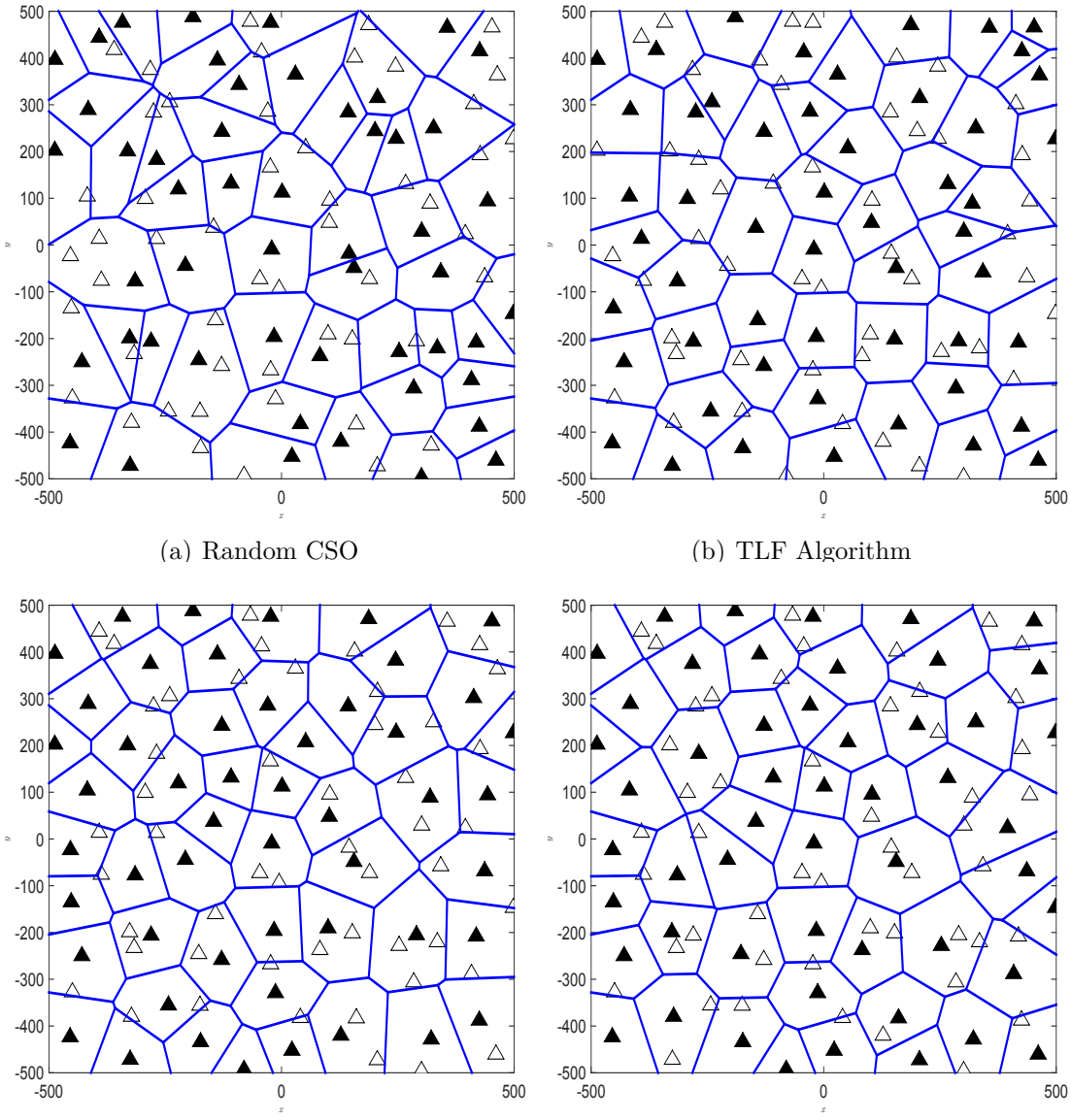

(a) Random CSO

(b) TLF Algorithm

(c) IF Algorithm

(d) GC Algorithm

Figure 6.10: Active cells after 50% CSO with initial regularity of $C_{\mathrm{D}} = 0.6$.

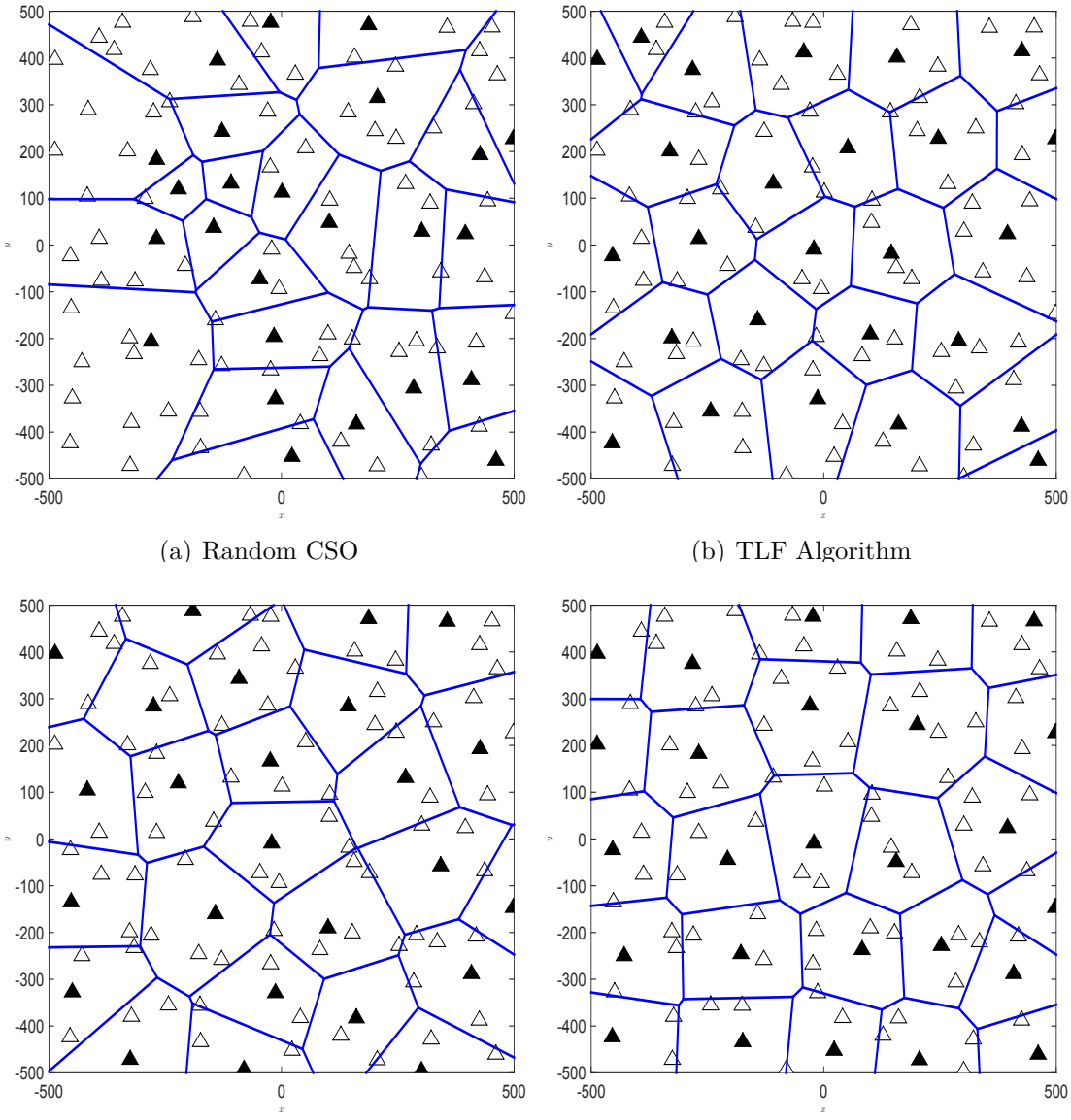

(a) Random CSO

(b) TLF Algorithm

(c) IF Algorithm

(d) GC Algorithm

Figure 6.11: Active cells after 75% CSO with initial regularity of $C_{\mathrm{D}} = 0.6$.

6.6.2 Real BS Locations

Now, we examine the behaviour of some of these CSO algorithms when applied to real networks in different Canadian regions:

1. Richmond, BC: We consider a Telus LTE network in Richmond, BC. This region represents a suburban environment with BSs placed with similar inter-site distances. An illustration of the city map and the data set of this region is shown in Fig. 6.12. We apply different CSO algorithms and show the resulting network layout in Figs. 6.13, 6.14, and 6.15 for CSO percentages of 25%, 50%, and 75%, respectively.

2. Toronto, ON: We consider a Rogers LTE network in the downtown area; this represents an urban environment, where BSs have irregular spatial distribution to cope with the variable user density. An illustration of the city map and the data set of this region is shown in Fig. 6.16. We apply different CSO algorithms and show the resulting network layout in Figs. 6.17, 6.18, and 6.19 for CSO percentages of 25%, 50%, and 75%, respectively.

For real BS locations, we only examine Random, IF and GC algorithms as we discovered a drawback of the TLF algorithm. TLF showed the best performance for regimes in which the number of switched-off cells is high. However, it shows improper results when applied to real networks. This is due to the fact that in real networks, the actual BS density cannot be easily estimated; therefore the TLF needs extra calibration before being applied to real networks.

The Toronto network is clearly designed to serve non-uniform user density (refer to [23] for a study on the effect of non-uniform distribution on the performance of CSO algorithms). All of these algorithms considers the distances between BSs as the sole parameter without considering user distribution. However, since CSO is designed for low traffic period, we can say that making the network regular is acceptable in periods of low traffic density. Nevertheless, further study is needed on how to design algorithm that can couple both the BS irregularity and the non-uniform user distribution.

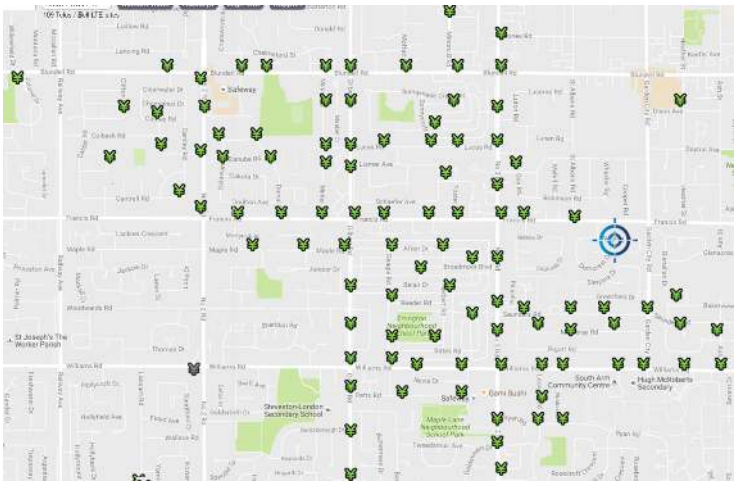

(a) BSs on city map

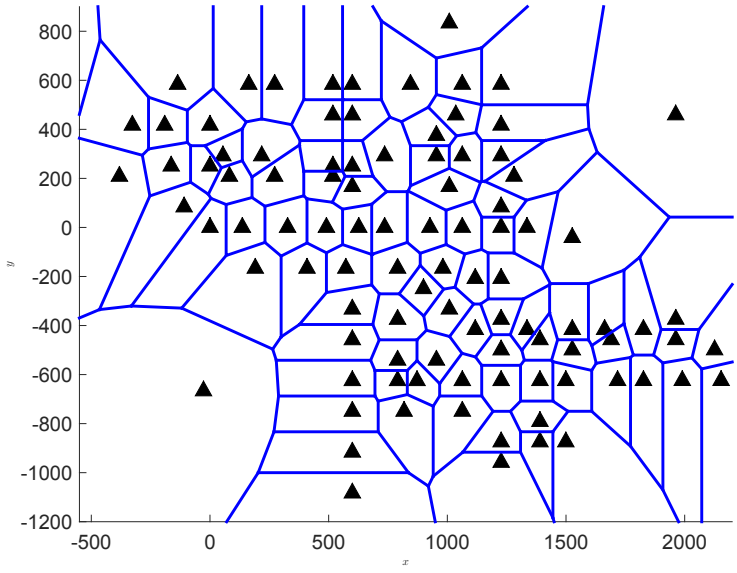

(b) Point set

Figure 6.12: Real BS locations in Richmond, BC of the LTE Telus network, taken from [74].

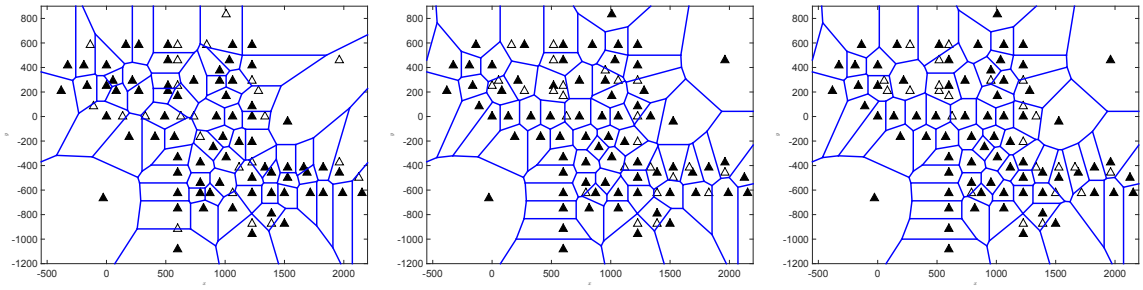

(a) Random CSO (b) IF Algorithm (c) GC Algorithm

Figure 6.13: Active cells after 25% CSO of Richmond BSs.

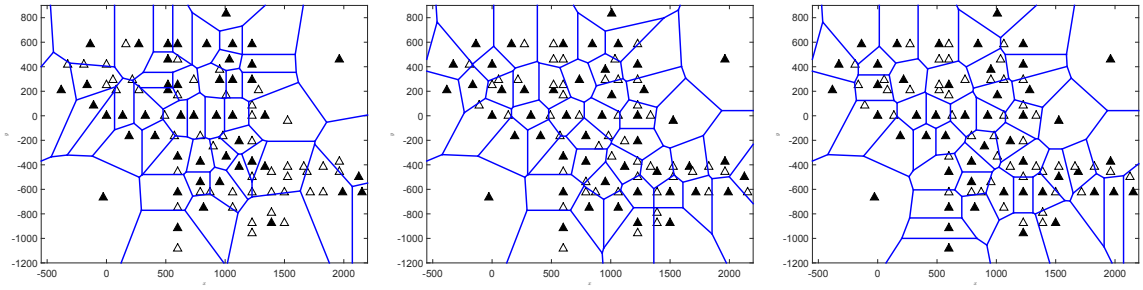

(a) Random CSO (b) IF Algorithm (c) GC Algorithm

Figure 6.14: Active cells after 50% CSO of Richmond BSs.

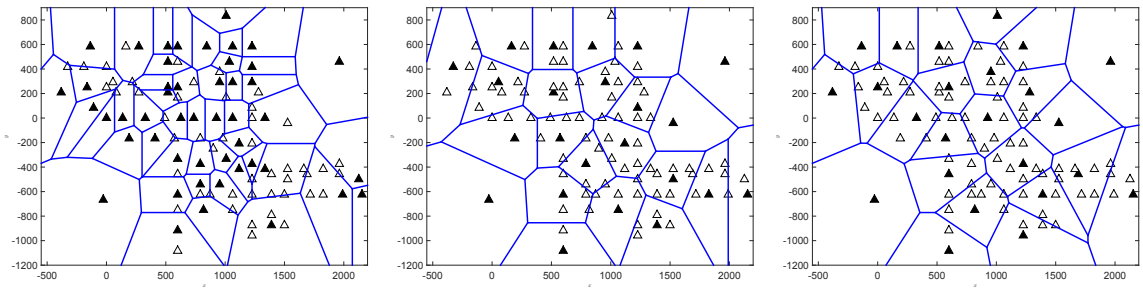

(a) Random CSO (b) IF Algorithm (c) GC Algorithm

Figure 6.15: Active cells after 75% CSO of Richmond BSs.

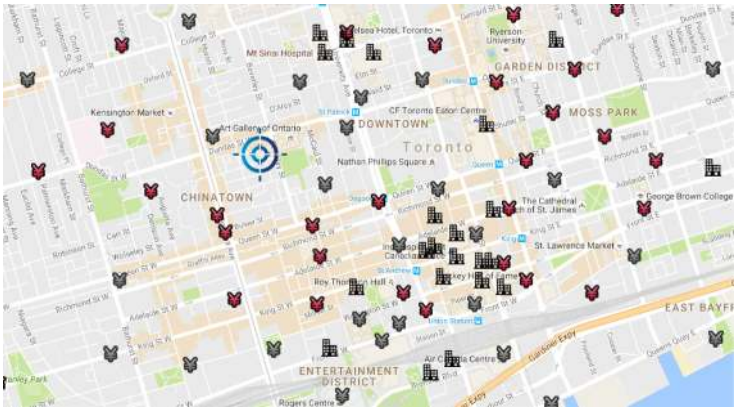

(b) data set

Figure 6.16: Real BS locations Toronto, ON of the LTE Rogers network, taken from [74].

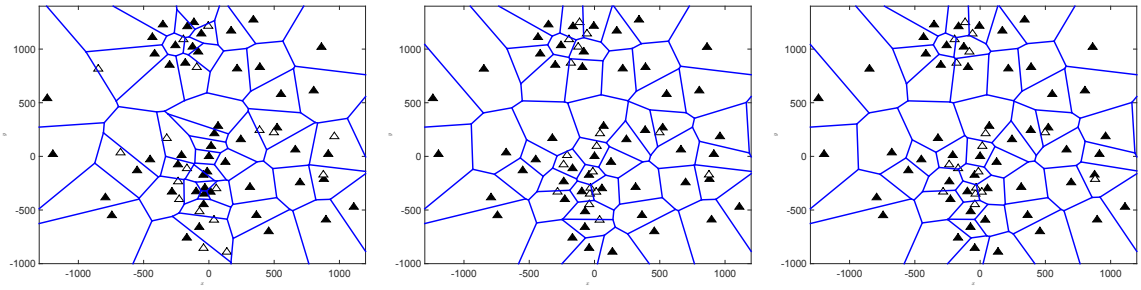

(a) Random CSO (b) IF Algorithm (c) GC Algorithm

Figure 6.17: Active cells after 25% CSO of Toronto BSs.

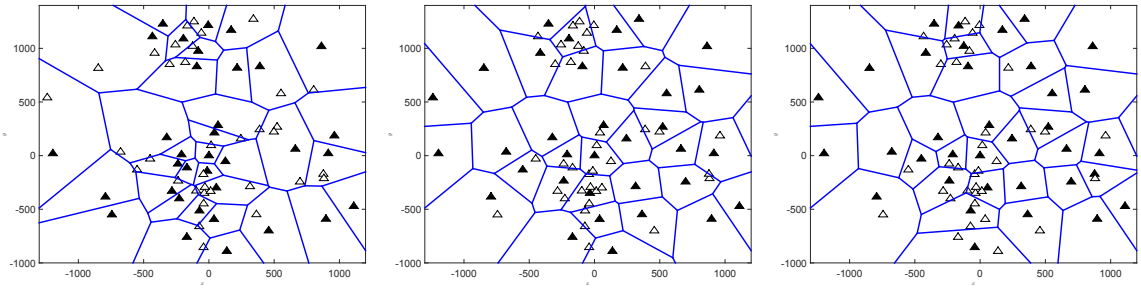

(a) Random CSO (b) IF Algorithm (c) GC Algorithm

Figure 6.18: Active cells after 50% CSO of Toronto BSs.

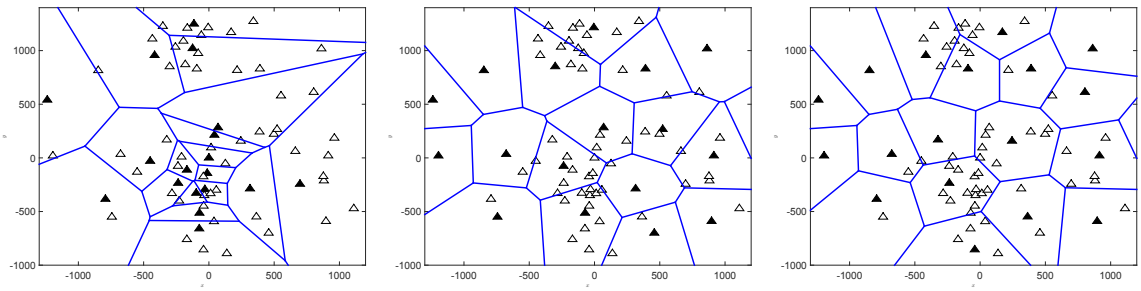

(a) Random CSO (b) IF Algorithm (c) GC Algorithm

Figure 6.19: Active cells after 75% CSO of Toronto BSs.

6.7 Conclusion

We evaluated several algorithms for solving the recently studied problem of cell switch-off that considers spatially irregular BS deployments. Generally, the greedy algorithms GC and GD were found to be good choices overall; we found that for high CSO percentage, all exiting algorithms perform suboptimally. We also examined a recent algorithm (TLF), which performs very well in high CSO percentages, and its performance is close to the known performance upper bound. For low CSO percentages, we found that all algorithms, although very different in design, perform quite similarly.

The optimal choice of algorithm is primarily influenced by the desired CSO percentage, and also by the spatial regularity of the entire network. If implementing only one algorithm is preferable, then the two algorithms GC and IF, although never best, offer a good overall performance.

We evaluated these algorithms in real network deployments for both a suburban and an urban environment. The main observation was that the TLF algorithm failed to perform well because an important input is the BS density which is hard to find for real networks because the area borders can is not clearly defined.

Future research may include:

1. Finding a tighter upper bound for the algorithms.

2. Modifying the TLF so that it is applicable to real networks.

3. Designing algorithms for non-stationary deployments, as these algorithms assume stationary BSs deployments (i.e., the BSs are deployed with the same density in every part of the network).

4. Extending this research to HetNets and non-uniform user distributions.

Chapter 7

Conclusion and Future Works

7.1 Summary and Conclusion

Key aspects of future cellular networks are the ability to support ubiquitous and exponentially increasing data rates, while being energy-efficient at the same time. Operators are striving to implement techniques to make the best use of the scarce radio resources. During the planning phase, cells are deployed in large numbers to cope with the peak traffic. Therefore, some cells become underutilized or even redundant when the demand is low. Despite being underutilized, these cells still consume a major portion of their peak energy. CSO is introduced to strategically switch off cells during off-peak times. The contribution of this thesis is advancing the research of the CSO approach by efficiently switching off cells in space (which cell) and in time (when to switch off).

In Chapter 2, we presented the channel model and simulation setup used to study, evaluate, and compare different CSO algorithms. In order to ensure the reliability of our results, our SINR curves were calibrated against the SINR CDFs obtained from WINNER+ partners. Our results matched closely with those standard results and we are confident about our simulator.

In Chapter 3, we introduced the FLP, which is a location problem concerned with locating service points with the objective of minimizing the total of implementation and transportation cost, while serving demand points. We believe that the FLP is a very diverse and efficient problem formulation that is capable, through its different models, to address several research problems related to cellular networks. Therefore, we introduced those models and provided a summary table. We used two of these models in Chapter 4 and Chapter 6 to design CSO algorithms.

In Chapter 4, we proposed a dynamic CSO algorithm based on the well-known SCP. The proposed algorithm outperformed a benchmark algorithm in terms of overall energy saving, especially as the number of users per BS increased. Dynamic CSO approaches have the advantage of adapting to current traffic situations; however, we faced several problems regarding modelling the interference properly and avoiding the possibility of coverage holes, as well as challenges in adapting to possible sudden changes in user distribution. Therefore, we investigated the other category of CSO: static CSO.

Chapter 5 is dedicated to regular CSO patterns, which is a specific case of static CSO. This chapter provides a systematic characterization of different CSO patterns and serves as a systematic summary of CSO patterns. We identified previous work and proposed a possible way to form new regular patterns. In particular, we were the first to study the sector-based regular CSO patterns. Although CSO patterns are conceptually much simpler, they perform comparably to dynamic CSO approaches. CSO patterns are advantageous in terms of ensuring interfering cells are far away, minimizing coverage holes, and energy-efficiency for users.

In Chapter 6, motivated by the advantages of CSO patterns, we evaluated several CSO algorithms designed for cellular networks with irregular BS placement, which is a better model for real network deployments. We examine some of these algorithms in real networks.

In the Appendix, we focused on the demand side of cellular networks as we studied the impact of the spatially-correlated shadowing on the user-in-the-loop (UIL) which is a user-centric approach that aims at shaping the demand by including users as active participants of the cellular system. Users are encouraged, through financial incentives, to relocate to locations with better SINR, in order to alleviate congestion situations. By doing so, users can achieve the same data rate with fewer radio resources. Operators can benefit from these saved resources by providing higher data rates to current users or accommodating new users. Our results confirmed the increase in cell-average spectral efficiency after applying the UIL, and also showed that the average moving distance increases with the correlation parameters. It would be interesting to investigate a user-assisted CSO approach by considering the UIL concept when designing a CSO algorithm with the aim of switching off extra BSs.

7.2 Future Work

Although the CSO literature is rich, there exist some gaps in the literature that we think need to be addressed. Within each chapter, we provide some future works that can extend that topic of that chapter. Here, we introduce the advantages of applying CSO in a non-traditional cellular structure where several parties may own and share different entities of the network.

7.2.1 Software-Defined Cell Switch-Off for Virtual Cellular Networks.

The architecture of 5G cellular networks is expected to change [2], and several parties may own small parts of the network, unlike the current situation, where one operator may own an entire large network. This opens the door for opportunities to share resources and cooperate. Enabling technologies are network function virtualization (NFV) and software defined networks (SDN); therefore we propose to investigate the CSO approach in future scenarios with multi-operator cooperation in order to reduce the overall energy consumption and benefit from the advantages of NFV and SDN.

The main objective of the CSO approach is to reduce energy consumption in cellular networks by switching off unnecessary cells, which results in concentrating the load (users) in as few cells as possible. After applying CSO, the majority of cells are heavily loaded (more than 70% load); however, there can remain some cells that are very lightly loaded (less than 30% load), Fig. 4.5 illustrates a possible realization.

Different cellular operators can dynamically share physical infrastructure, radio resources to reduce energy consumption without affecting users' QoS. One possible solution for doing so is by offloading the users of the lightly loaded BSs to another operator's BSs (multi-operator cooperation).

We propose the possibility of a novel approach called software-defined CSO for virtual cellular networks to exploit the advantages of network function virtualization (NFV) and software defined networking (SDN), see Fig. 7.1.

7.2.1.1 Challenges of Applying CSO among Multiple Operators

In order to identify enabling technologies, we first need to discuss some possible challenges related to CSO. Here, we emphasize challenges related to applying CSO

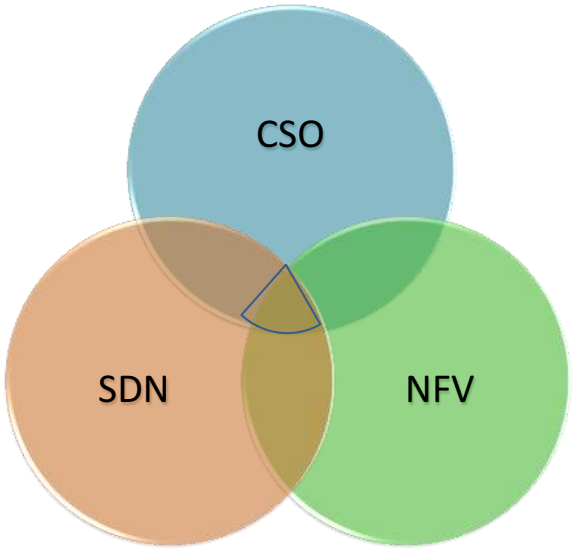

Figure 7.1: This work is the intersection of three topics: CSO, SDN and NFV.

with multi-operator cooperation, see [75] for general challenges in cellular networks. Some possible challenges can be summarized as:

1. Control signaling: A lot of information needs to be exchanged among different operators and entities; therefore it is necessarily to manage these signals.

2. Global information: This information should be available at a central entity, so that different parties can have access to it.

3. Resource discovery and allocation: Before deciding to switch off a cell, an operator should first discover available resources before sending a request to a central entity, which manages and allocates resources accordingly.

4. Inter-operator CSO management: Relying on other operators' resources might pose the possibility of conflict between the decisions of switching-off BSs. Therefore, we need to manage CSO procedures among different operators.

5. Stability: We need to make sure that the CSO procedure is stable and will not affect the original network's operation.

7.2.1.2 Enabling Technologies

In traditional networks, one mobile network operator (MNO), which is the main service provider (SP), usually owns an entire cellular network, including the infrastructure, the radio access network (RAN), the core network (CN), and the transmission network (TN). In future networks, different network entities may be owned and managed by different parties such as infrastructure providers (InPs), mobile virtual network operators (MVNOs), and service providers (SPs) [75].

Future networks are expected to be cloud-enabled, and some research is already available about cloud-RAN [2]. This is a very suitable network topology for CSO approaches as they require global knowledge and need to run centrally. Two important enabling technologies are:

Network Functions Virtualization (NFV): Virtualizing the network simply means abstracting the infrastructure from the function it supports. This allows to divide the physical network into several virtual networks called *slices*. Virtualization should facilitate the CSO cooperation procedure and reduce the execution time.

In NFV, a full knowledge of the network is assumed to be acquired by each operator. Operators who want to apply CSO and want to utilize other operators' RANs are assuming that the RAN resources will be available upon request. However, this might cause a problem when several operators decide to run the CSO concurrently. Therefore, we need SDN to manage the available resources flexibly among different parties, and consequently, it will facilitate the CSO procedures.

Software Defined Networking (SDN): SDN allows for dynamic reconfiguration of the network through the separation of the control plane, data plane, and management plane. The SDN controller has a global view of the network so that it can optimize the resource allocation and avoid any possible conflict of the operators' objectives.

7.2.1.3 Problem Statement

3GPP has recognized the importance of supporting network sharing [76], and five main scenarios were defined:

- Scenario 1: Multiple core networks sharing common RAN;

- Scenario 2: Geographically split networks sharing;
- Scenario 3: Common network sharing;
- Scenario 4: Common spectrum network sharing; and
- Scenario 5: Multiple RANs sharing common core network.

There exist some research on applying CSO for multi-operator cooperation; for example, authors of [77] studied the collaboration among several MNO that serve the same geographical area, and they proposed network switch-off, where the entire network of one operator is switched off to save energy. This might not always be possible or desired, and more sophisticated cooperation scenarios are needed and encouraged, as seen from the growing body of literature [77–81]. However, the previous work is restricted to the physical aspects of sharing BSs among operators, and do not address possible benefits of including SDN nor NFV.

The problem of multi-operator cooperation for CSO is such that an operator could handoff its users to BSs belonging to other operators, as opposed to its own BSs only. This cooperation provides on-demand resources so that operators can share physical BSs to minimize the total number of active BSs in the networks. This can be done in two ways:

- Each operator conducts its own CSO procedure and then communicate with another operator to offload users and switch off extra BSs.
- All operators in the network construct a virtual network, and conduct the CSO procedure jointly.

Although the first is simpler, the latter provides the maximum benefit. However, we need to pay special attention not to fall into the trap of switching off virtual BSs, as the actual energy consumed is from physical BSs.

7.2.1.4 Case Study

As a starting point, examine the simple network-sharing scenario presented in [80] with the following assumptions:

- Two operators, MVNO1 and MVNO2, serve partly-overlapping geographical areas.

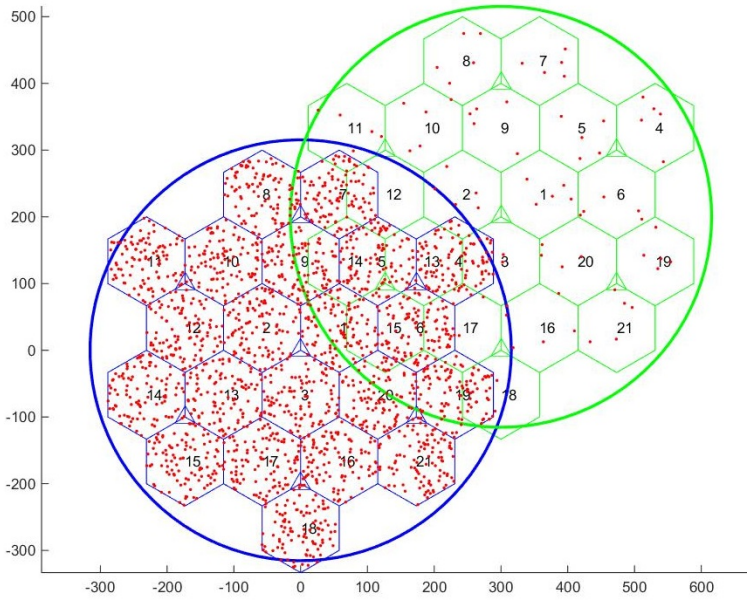

Figure 7.2: Example of two MVNOs, with different user densities, serving partly-overlapping geographical areas. Each MVNO has its own RAN, RAN1 owned by MVNO1 is enclosed in the blue circle, while RAN2 owned by MVNO2 is enclosed in the green circle.

- Operators do not have any shared sites.
- Each MVNO has a different user density.
- Each MVNO provides a single service with rate requirements.
- MVNOs have their own RANs, their individual CNs, and their own licensed spectrum.

In this case study, we assume the following: Figure 7.2 shows a realization of a possible network scenario in which MVNO1 has high user density, while MVNO2 has a very low user density. The performance metric is the number of active BSs after running the CSO procedure. The area of overlap between the two MVNOs can be considered as a variable. Also, the number of users per operator could be another variable. There might or might not be a correlation between the number of users served by each operator. Also, the required rate and the type of service can vary.

Appendix A

Impact of Spatially-Correlated Shadowing on the User-in-the-Loop Concept

The current practice is mainly to improve the performance of cellular networks from the supply side (i.e., by implementing new transmission techniques or installing more BSs); however, the demand side stays unchanged, while users are expecting ubiquitous and very high data rates, which is not always viable. A new user-centric paradigm could be considered to motivate users to be active participants of the system and not just consumers. Some reasons for this consideration are:

- The increase in required data rates leads to an excess of demand over supply. Many of the existing techniques on the supply side are reaching their theoretical limits and further improvements are not expected soon.
- BSs have limited radio resources, bandwidth, that are shared among several users. It is useful to raise users' awareness towards sharing network services and resources to avoid the possibility of the tragedy of the commons [82].
- Users located close to BSs generally receive a much stronger signal power than users located far away. In addition to this distance-dependent power attenuation, there is the shadowing effect that impacts the signal before reaching the receiver and hence users at equal distances from the BS may receive quite different signal powers [26]. If users with weak received powers are willing to move to better locations with higher received power, these users could obtain higher data rates, resulting in an increase in the overall system performance.

Consequently, an approach to encourage users to be active participants in the network by changing their locations is very useful, both for users (they can get financial

incentives) and operators (they can support more users and cope with congestion). The target population for this approach is mainly young healthy individuals with a constrained budget, such as students.

A.1 User-in-the-Loop Concept

The user-in-the-loop (UIL) concept was proposed in 2010 [83–85] and has gained attention in recent years [84–89]. The main idea of UIL is to encourage users to be active participants of the system and not just consumers; in particular, to alleviate network congestion by reducing the demand in periods/locations of high traffic. This is done by providing instantaneous feedback on the cost of the session and a possible financial incentive if users cooperate by changing physical locations (spatial UIL), or by postponing their sessions (temporal UIL).

User terminals (UTs) at low power locations require more radio resources to achieve the same data rate than UTs at locations with a stronger received power. Therefore, a higher overall capacity may be achieved if some users cooperate by moving to better locations. The effect of user relocation on the cell spectral efficiency was discussed in [83]. When users relocate to better signal locations, by moving walkable distances, the cell saves some resources, which can then be used to serve other users or to provide higher data rates for current users. The results in [83] are promising and an increase of more than 100% in the spectral efficiency is achieved without any modification to the current system. This improvement is gained simply from users being active participants of the system. Those results are based on the pathloss calculation only, which is a simplified scenario.

The goal of the UIL approach is to increase the cell spectral efficiency γ, measured in bps/Hz. The cell spectral efficiency is the averaged rate achieved over the cell coverage area and divided by the system bandwidth [90]. The spectral efficiency for each UT depends on its SINR, the higher the SINR the higher the spectral efficiency [83]. UTs with low SINRs have low spectral efficiencies and acquire more radio resource blocks to achieve high data rates. To increase the average cell spectral efficiency, more UTs should receive higher SINRs, which might not be possible because of their bad locations and the limitations on the maximum transmitted power. The relationship between the SINR values and the corresponding spectral efficiency (γ) is summarized in Table 2.2 based on the AMC scheme.

In order to achieve higher SINR, instead of increasing the transmit power, the user is incentivized to assist the network by relocating to better SINR locations. The general idea of including users in the loop is shown in Fig. A.1. The controller provides users with information, and users then decide in return whether to change their locations or not.

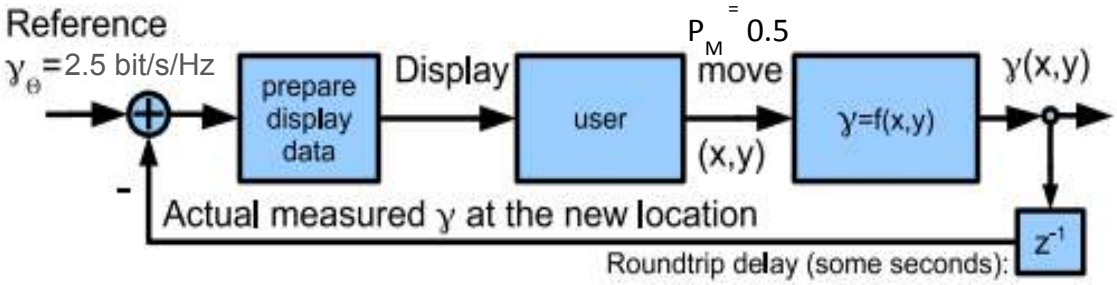

Figure A.1: The user becomes a part of the system (in the loop). Source: [83].

With smartphones widely available, it has become possible to provide users with all the information necessary to make the decision, such as the distance to move and the incentive advertised. Fig. A.2 is an example of a graphical user interface to facilitate the decision of relocating to higher spectral efficiency spots [83].

This cooperation from users may provide advantages for the operators, because fewer radio resources are assigned to users in good SINR locations; consequently they can save resources to better serve current users or accommodate new ones. Users who decided to relocate receive an incentive (reduced prices or higher data rates). Physically relocating to a better spot is well-observed in Wi-Fi (IEEE802.11) networks, where users change their locations to get higher data rates.

Fig. A.2 shows an example of a graphical display that provides directions to better locations and the possible incentive, so users can decide if they want to participate or not.

Users are expected to relocate with a probability p_M which is the probability that a user will move from the current location $\vec{p_1} = (x_1, y_1)$ with spectrum efficiency γ_1 to the new location $\vec{p_2} = (x_2, y_2)$ with spectrum efficiency γ_2, where $\gamma_2 \geq \gamma_\Theta \geq \gamma_1$. This SE γ_Θ is chosen to determine the average cell spectral efficiency to be achieved after the user's movement.

Figure A.2: Example of a map to facilitate the decision of relocating. It shows the direction and distance to walk and the incentive offered. Based on an incentive, users are expected to relocate to a stronger signal location with probability p_M. Source: [83].

A.2 Modeling Spatially-Correlated Shadowing

Shadowing is an important factor that should be considered, to have a more realistic model of the SINR in space. Considering spatially-correlated shadowing is especially important in the context of UIL, as it can affect the average walking distance.

Shadowing results from obstruction of the transmitted signal by buildings, natural obstacles, vehicles, etc. Shadowing plays an important role in determining the received power at a UT from a specific BS.

The shadowing can be modeled as either independent (uncorrelated) shadowing or spatially-correlated shadowing. In the first case, each point is assumed to have an independent shadowing value $Z_n \sim N(0, \sigma)$, a Gaussian random variable with zero mean and a σ [dB] standard deviation [26]. In this model, the shadowing values are taken as independent at each point, i.e., two neighbouring points may have completely different shadowing values despite their adjacency. This independence in shadowing values is a simplified assumption. A more realistic model is correlated shadowing that implies: if a UT is in deep/light shadowing, its neighbours probably have deep/light shadowing as well. The correlation in shadowing can significantly

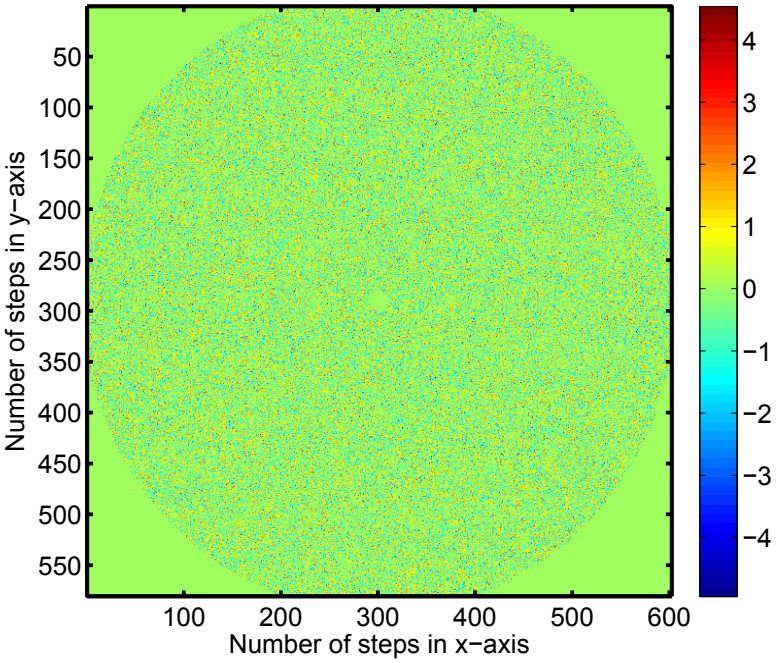

Fig. 2. Example of two-dimensional uncorrelated shadowing field.

Figure A.3: Realization of a 2D uncorrelated shadowing field.

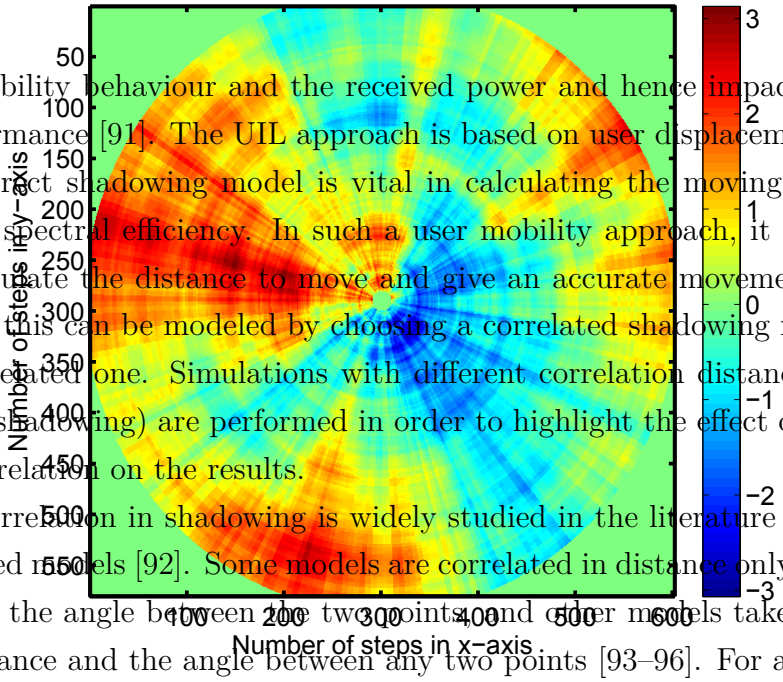

Fig. 3. Example of two-dimensional correlated shadowing field.

affect the mobility behaviour and the received power and hence impacts the overall system performance [91]. The UIL approach is based on user displacement, therefore using the correct shadowing model is vital in calculating the moving distance and the resulting spectral efficiency. In such a user mobility approach, it is essential to correctly calculate the distance to move and give an accurate movement suggestion to users, and this can be modeled by choosing a correlated shadowing model instead of the uncorrelated one. Simulations with different correlation distances (including independent shadowing) are performed in order to highlight the effect of the amount of spatial correlation on the results.

Spatial correlation in shadowing is widely studied in the literature and there are many proposed models [92]. Some models are correlated in distance only, while others consider only the angle between the two points and other models take into account both the distance and the angle between any two points [93–96]. For a visualization of correlated shadowing, see Figs. A.3 and A.4. Both figures show the value of the shadowing on a 2D field representing the coverage area for the given scenario. In Fig. A.3, each point has a shadowing value independent from its neighbours', while it is separable. A separable model is necessary to reduce the simulation complexity especially in this paper to calculate the spectral efficiency all over the coverage area (too many points are considered). Separability means that correlation can be imposed in one dimension first, and then the correlation in the other dimension can be calculated according to (4) [10] as

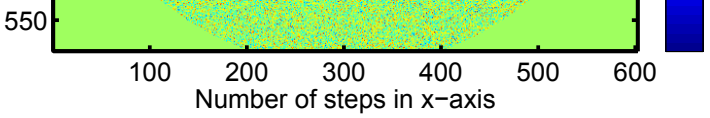

Fig. 2. Example of two-dimensional uncorrelated shadowing field.

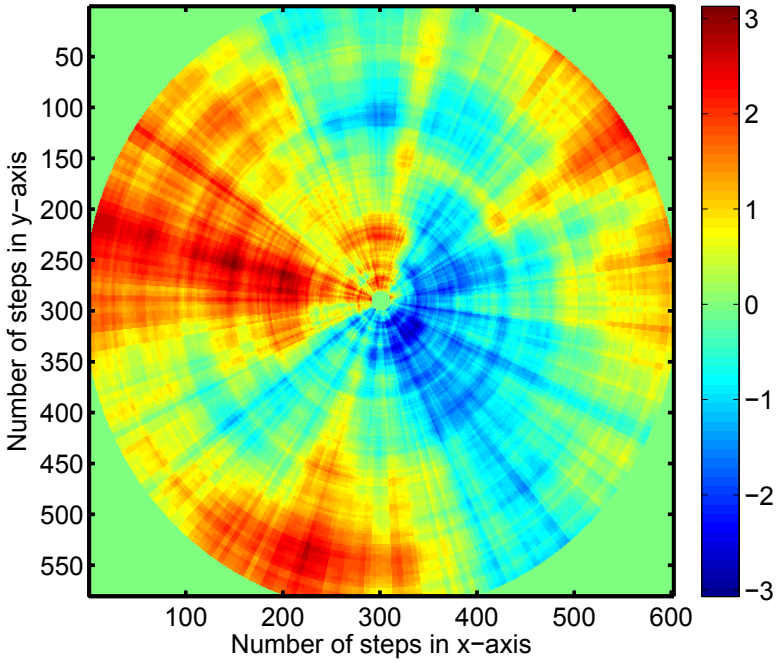

Fig. 3. Example of two-dimensional correlated shadowing field.

Figure A.4: Realization of a 2D correlated shadowing field using model (A.1) with $R_0 = 6$ dB and $\phi_0 = 60°$, as in [91].

it is separable. A separable model is necessary to reduce the simulation complexity especially in this paper to calculate the spectral efficiency all over the coverage area (too many points are considered). Separability means that correlation can be imposed in each dimension first, and then the correlation in the other dimension can be calculated according to (4) [10] as

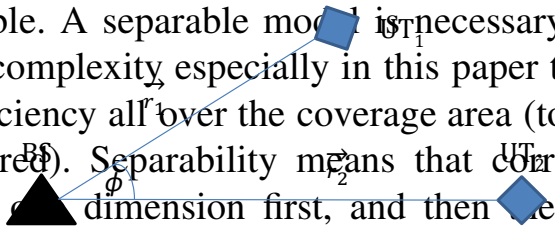

Figure A.5: Two UT positions $\vec{r_1}$ and $\vec{r_2}$, relative to a BS.

$$\phi = |\angle\vec{r_1} - \angle\vec{r_2}| \in [0\,°, 180\,°], \tag{2}$$

in Fig. A.4, the adjacent points have correlated shadowing values.

The correlated shadowing model selected among many others in [92] and studied in [91] is used here. This is a two-parameter model that depends on both the angle ϕ and the distance ratio R (in dB) between any two points $\vec{r_1}$ and $\vec{r_2}$, as shown in Fig. A.5. The calculation of these two parameters is shown in (A.2) and (A.3).

$$R\,[\text{dB}] = |10\log(r_1/r_2)|, R_0 > 0, \tag{3}$$

$$h(\phi, R) = h_\phi(\phi)h_R(R) \tag{4}$$

In the model selected in [91], the correlation coefficient between any two points $\vec{r_1}$ and $\vec{r_2}$ is given by:

Here is the abstract description of this model: If two UTs are located at the same point then they are 100% correlated. This correlation ratio decreases as the distance ratio and/or the angle between the UTs increases [10]. After certain values, the two UTs are considered to be totally uncorrelated. These values are defined as (ϕ_0): the maximum angle after which any two UTs are uncorrelated in angle, and (R_0): the maximum distance ratio after which any two UTs are uncorrelated in distance. This model starts with a set of independent random variables

$$h(\vec{r_1}, \vec{r_2}) = \max\{1 - \phi/\phi_0, 0\} \cdot \max\{1 - R/R_0, 0\}. \tag{A.1}$$

where,

$$\phi = |\angle \vec{r_1} - \angle \vec{r_2}| \in [0\,^\circ, 180\,^\circ], \tag{A.2}$$

$$R[dB] = |10 \log_{10}(\|\vec{r_1}\|/\|\vec{r_2}\|)|, \tag{A.3}$$

and R_0 and ϕ_0 are the tuning parameters of the model.

This specific shadowing model was chosen partly because it has two tunable parameters and it is separable in its two dimensions [91]. A separable model is necessary to reduce the simulation complexity of calculating the spectral efficiency for too many points over the coverage area. Separability means that the filtering of the spatial field can be done in one dimension first and then in the other dimension to obtain the correlated shadowing field according to (A.1) [91], as seen in Fig. A.4.

The qualitative description of this model is that if two UTs are located at the same point, then their shadowing values are 100% correlated (the same). This correlation ratio decreases as the distance ratio and/or the angle between the UTs increases [91]. After certain distances, the two UTs are considered to be totally uncorrelated. These values are defined as ϕ_0: the maximum angle after which any two UTs are uncorrelated in angle, and R_0: the maximum distance ratio after which any two UTs are uncorrelated in distance.

Generating a 2D shadowing field according to this model starts with a set of independent random variables to obtain an independent shadowing field (such as Fig. A.3). After that, the independent Gaussian field (Fig. A.3) is passed through a linear filter in both the radial and the angular direction in order to obtain the correlated shadowing field (Fig. A.4) as described in [91]. Applying this model guarantees that each shadowing value will be correlated with all the neighbouring points. After obtaining this correlated shadowing field, the shadowing value at any point can be obtained directly by mapping the location of that point onto the field and reading the corresponding shadowing value from the field.

A.3 Simulation Results

The performance study is done by finding the average cell spectral efficiency before and after applying the UIL concept, and the methodology is as described in [83]. First, it is informative to visualize the effect of correlated shadowing on the SINR map. Fig. A.6(a) shows the LOS SINR distribution in the simplified case (without

shadowing). In this case, the SINR values depend on the distances and antenna patterns only. The 2D SINR map changes when the correlated shadowing is included, as shown in Fig. A.6(b). The importance of correlated shadowing on the distribution of the SINR is observed in Fig. A.6.

The spectral efficiency values obtained by running our simulation are very similar to those obtained in the original UIL work in [83]. Although the SINR distribution is different in the two cases, the average spectral efficiency is almost the same.

Moderate values are chosen for the p_M and the γ_Θ as 0.5 and 2.5 bps/Hz respectively. $p_M = 0.5$ means half of the users are willing to walk to better locations. The user moving distance depends on the chosen p_M and γ_Θ, as well as the parameters of the evaluation scenarios.

In order to understand the effect of spatially-correlated shadowing on the moving distance, the results with spatially-independent shadowing are shown in row 3 of Table A.1. This result shows a shorter distance to move compared with the original UIL approach without the shadowing effect (row 2). This distance can be as small as the grid resolution used for the simulation model. In fact, shorter moving distances are expected with independent shadowing as users will likely find at least one adjacent location with $\gamma \geq \gamma_\Theta$. Therefore, spatially-independent shadowing is not a good model for studying UIL. To analyze the model in a more realistic scenario, the correlated shadowing model in [91] is applied. In this case, the moving distance depends on the correlation parameters ϕ_0 and R_0. Different ϕ_0 and R_0 values were selected to evaluate their impact on the spectral efficiency and the user movement distance. Some results are tabulated in Table A.1 and can be summarized as: the smaller the correlation parameters, the smaller the distance to move.

Figs. A.7, A.8, and A.9 illustrate the relations between the correlation parameters and the corresponding moving distance. As extracted from these figures, the average moving distance is as low as 3.34 m for small correlation parameters ($R_0 = 1$ dB and $\phi_0 = 3\,^\circ$), that is approximately 30% shorter than the average moving distance in the original UIL. On the other hand, large correlation parameters result in a longer average moving distance (6.06 m compared with 4.7 m). However, calculated cell-average spectral efficiencies is very similar for the different shadowing models.

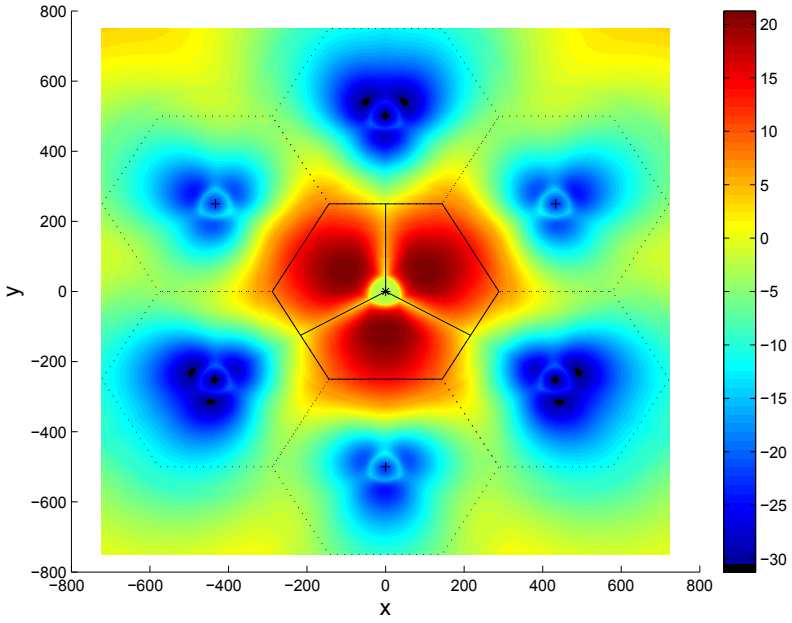

(a) LOS SINR without correlated shadowing.

Fig. 4. Examples of the effect of shadowing on the strength of the SINR.

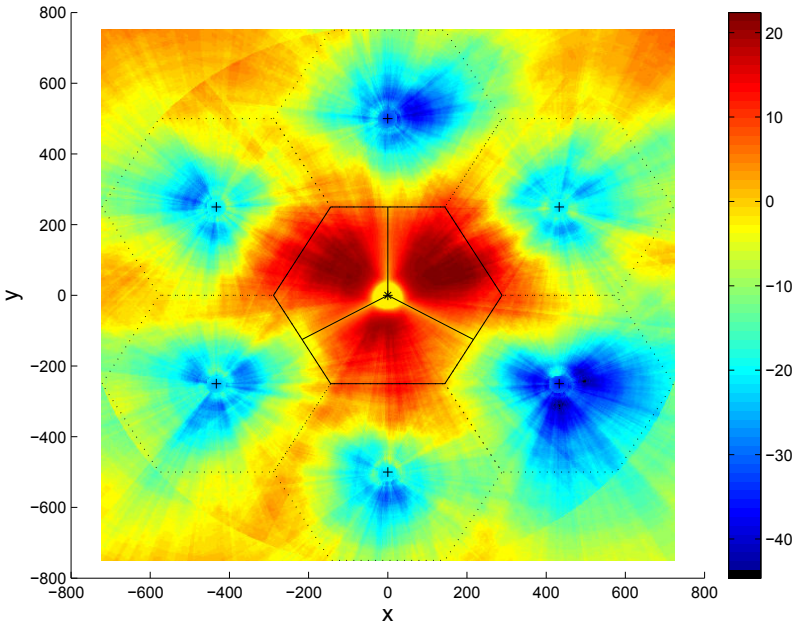

(b) LOS SINR with correlated shadowing.

Fig. 7. A 3-D presentation of the relation between the maximum correlation (angle ϕ_0 and distance ratio R_0) and the average moving distance d.

REFERENCES

[1] J. Gozalvez, "Mobile traffic expected to grow more than 30-fold," *IEEE Vehicular Technology Magazine*, vol. 6, no. 3, pp. 9–15, 2011.

[2] A. Ghosh, R. Ratasuk, B. Mondal, N. Mangalvedhe, and T. Thomas, "LTE-Advanced: next-generation wireless broadband technology [invited paper]," *IEEE Wireless Communications Magazine*, vol. 17, no. 3, pp. 10–22, 2010.

[3] G. Hardin, "The tragedy of the commons," *Science*, vol. 162, pp. 1243–1248, 1968.

V. CONCLUSION

The massive growth of data traffic in cellular network requires a paradigm shift to be more user-centric. The UIL approach is a user-centric approach based on convincing users to be part of the system by providing them some incentive.

Table A.1: Cell-average spectral efficiencies [bps/Hz/sector] with and without UIL and the resulting moving distance for different shadowing models, with $p_M = \frac{1}{2}$ and $\gamma_\Theta = 2.5$ bps/Hz.

Scenario	γ without UIL	γ with UIL	Average moving distance [m]
No shadowing effect	1.254	1.974	4.7
Uncorrelated shadowing model	1.225	2.028	2.69
Correlated shadowing $R_0 = 1$ dB, $\phi_0 = 3\,^\circ$	1.227	2.041	3.34
Correlated shadowing $R_0 = 3$ dB, $\phi_0 = 30\,^\circ$	1.234	2.016	4.69
Correlated shadowing $R_0 = 6$ dB, $\phi_0 = 60\,^\circ$	1.220	2.005	6.06

A.4 Conclusion

The massive growth of data traffic in cellular networks requires a paradigm shift to be more user-centric. UIL is a user-centric approach based on encouraging users through incentives to be active participants of the system. Users can cooperate by moving to better SINR locations. This user cooperation can lead to a significant increase in the cell-average spectral efficiency without any changes on the supply side of the cellular networks. A further investigation was done in this chapter by including the shadowing effect to analyze the performance of the UIL approach in a more realistic environment and to obtain more accurate results. The results obtained confirm the previous promising results for the cell-average spectral efficiency increase. However, the average moving distance was affected: Results show the relation between the spatial correlation parameters and the average moving distance.

In summary, the average moving distance increases with the correlation parameters. The shortest moving distance is achieved when modeling the shadowing as uncorrelated in space.

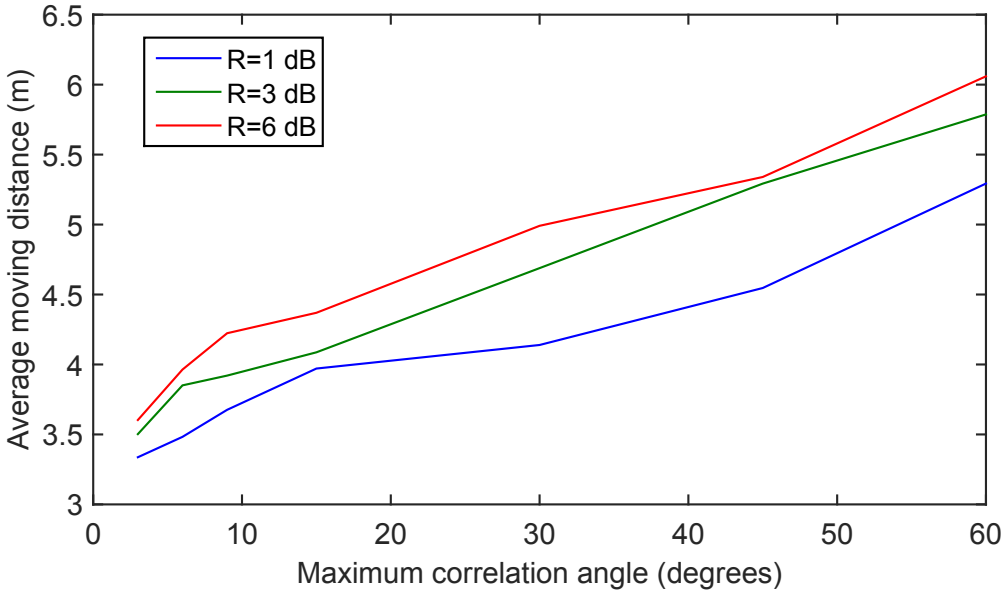

Figure A.7: Moving distance vs. different correlation angles ϕ_0.

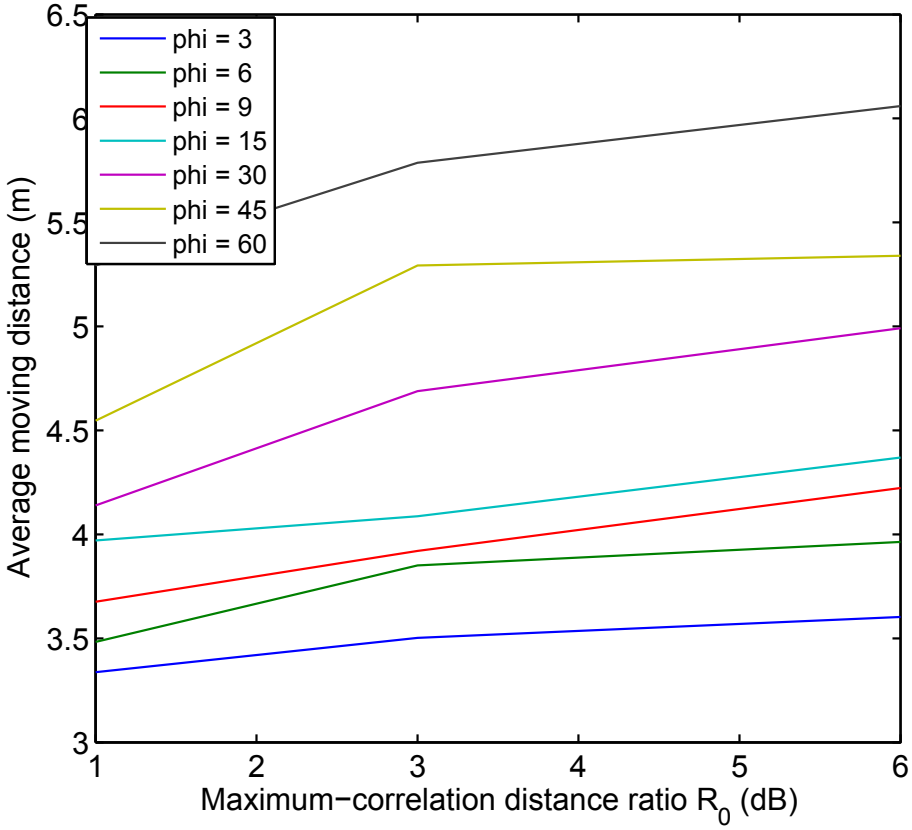

Figure A.8: Moving distance vs. different correlation distance ratios R_0.

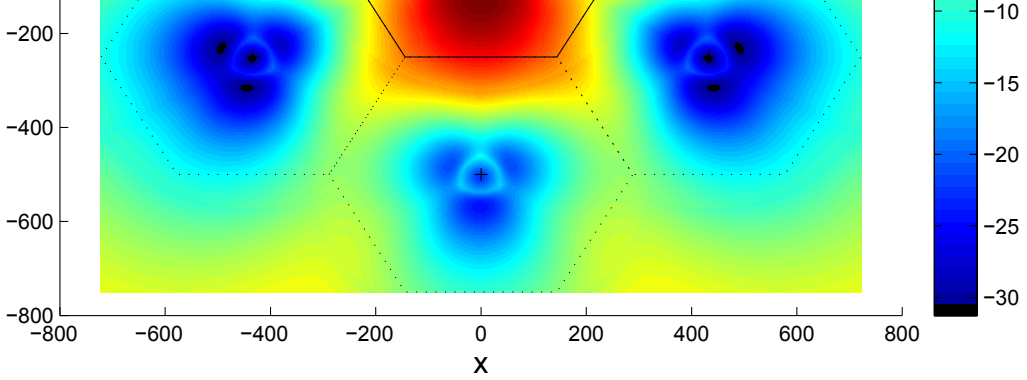

(a) LOS SINR without correlated shadowing.

Fig. 4. Examples of the effect of shadowing on the strength of the SINR.

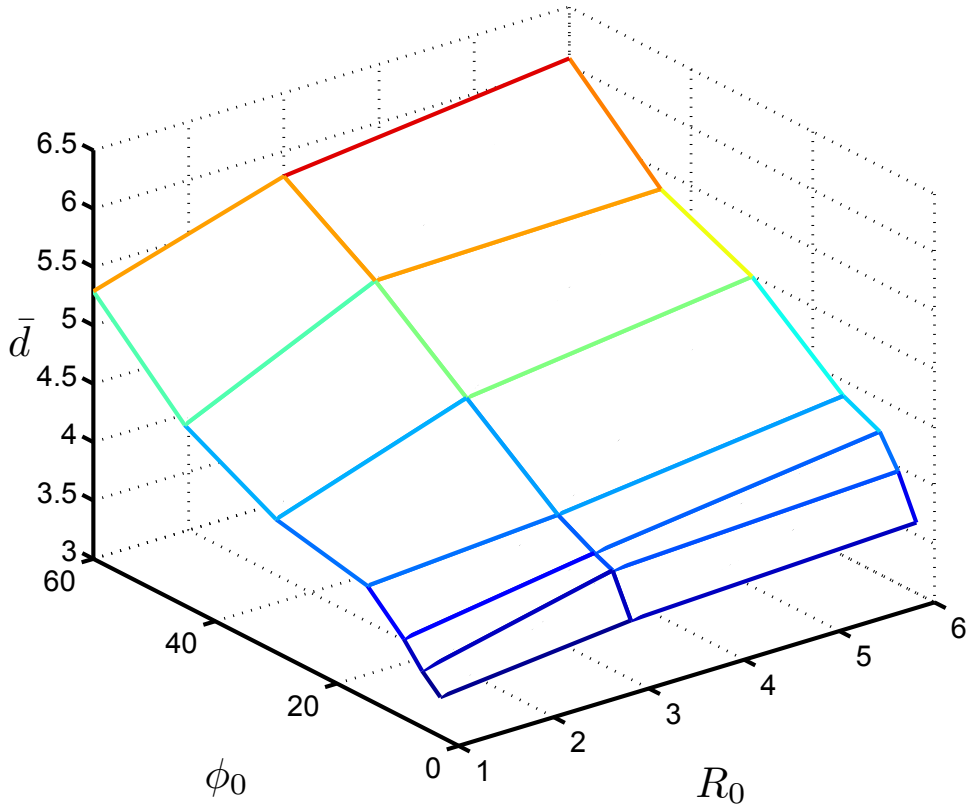

Figure 5. A 3-D presentation of the relation between the maximum correlations (angle ϕ_0 and distance ratio R_0) and the average moving distance $\bar{d}$.

V. Conclusion

The massive growth of data traffic in cellular network requires a paradigm shift to be more user-centric. The UIL approach is a user-centric approach based on convincing users to be part of the system by providing them some incentive. Users can cooperate by moving to higher SINR locations. This user cooperation can lead to a significant increase in the cell spectral efficiency with no change to the current cellular

List of References

[1] J. Gozalvez, "Mobile traffic expected to grow more than 30-fold," *IEEE Veh. Technol. Mag.*, vol. 6, pp. 9–15, Sept. 2011.

[2] J. G. Andrews, S. Buzzi, W. Choi, S. V. Hanly, A. Lozano, A. C. Soong, and J. C. Zhang, "What will 5G be?," *IEEE J. Sel. Areas Commun.*, vol. 32, pp. 1065–1082, June 2014.

[3] Z. Hasan, H. Boostanimehr, and V. K. Bhargava, "Green cellular networks: A survey, some research issues and challenges," *IEEE Commun. Surveys Tuts.*, vol. 13, pp. 524–540, 4th Quarter 2011.

[4] I. Humar, X. Ge, L. Xiang, M. Jo, M. Chen, and J. Zhang, "Rethinking energy efficiency models of cellular networks with embodied energy," *IEEE Network*, vol. 25, pp. 40–49, Mar. 2011.

[5] T. Beitelmal and H. Yanikomeroglu, "A set cover based algorithm for cell switch-off with different cell sorting criteria," in *IEEE International Conference on Communications Workshops (ICC Workshops)*, pp. 641–646, June 2014.

[6] D. González G, H. Yanikomeroglu, M. Garcia-Lozano, and S. Ruiz Boque, "A novel multiobjective framework for cell switch-off in dense cellular networks," in *IEEE International Conference on Communications (ICC)*, pp. 2641–2647, June 2014.

[7] Z. Niu, Y. Wu, J. Gong, and Z. Yang, "Cell zooming for cost-efficient green cellular networks," *IEEE Commun. Mag.*, vol. 48, pp. 74–79, Nov. 2010.

[8] Ł. Budzisz *et al.*, "Dynamic resource provisioning for energy efficiency in wireless access networks: A survey and an outlook," *IEEE Commun. Surveys Tuts.*, vol. 16, pp. 2259–2285, 4th Quarter 2014.

[9] K. C. Tun and K. Kunavut, "An overview of cell zooming algorithms and power saving capabilities in wireless networks," *KMUTNB: International Journal of Applied Science and Technology*, vol. 7, pp. 1–13, July 2014.

[10] S. Kokkinogenis and G. Koutitas, "Dynamic and static base station management schemes for cellular networks," in *IEEE Global Communications Conference (GLOBECOM)*, pp. 1–6, Dec. 2012.

[11] F. Han, Z. Safar, W. Lin, Y. Chen, and K. Liu, "Energy-efficient cellular network operation via base station cooperation," in *IEEE International Conference on Communications (ICC)*, pp. 4374–4378, June 2012.

[12] L. Chiaraviglio, D. Ciullo, M. Meo, and M. A. Marsan, "Energy-efficient management of UMTS access networks," in *IEEE International Teletraffic Congress (ITC)*, pp. 1–8, Sept. 2009.

[13] L. B. Le, "QoS-aware BS switching and cell zooming design for OFDMA green cellular networks," in *IEEE Global Communications Conference (GLOBECOM)*, pp. 1544–1549, Dec. 2012.

[14] X. Weng, D. Cao, and Z. Niu, "Energy-efficient cellular network planning under insufficient cell zooming," in *IEEE Vehicular Technology Conference (VTC-Spring)*, pp. 1–5, May 2011.

[15] M. Marsan, L. Chiaraviglio, D. Ciullo, and M. Meo, "Optimal energy savings in cellular access networks," in *IEEE International Conference on Communications Workshops (ICC Workshops)*, pp. 1–5, June 2009.

[16] A. Kumar and C. Rosenberg, "Energy and throughput trade-offs in cellular networks using base station switching," *IEEE Trans. Mobile Comput.*, vol. 15, pp. 364–376, Feb. 2016.

[17] "Telecommunication management; study on energy savings management (ESM)," TR 32.826, 3rd Generation Partnership Project (3GPP), Apr. 2010.

[18] F. Alaca, A. Bin Sediq, and H. Yanikomeroglu, "A genetic algorithm based cell switch-off scheme for energy saving in dense cell deployments," in *IEEE Global Communications Conference Workshops (GLOBECOM Workshops)*, pp. 63–68, Dec. 2012.

[19] S. Zhou, J. Gong, Z. Yang, Z. Niu, and P. Yang, "Green mobile access network with dynamic base station energy saving," in *ACM MobiCom*, vol. 9, pp. 10–12, Sept. 2009.

[20] A. Yildiz, T. Girici, and H. Yanikomeroglu, "A pricing based algorithm for cell switching off in green cellular networks," in *IEEE Vehicular Technology Conference VTC-Spring*, pp. 1–6, June 2013.

[21] A. Alam, L. Dooley, and A. Poulton, "Traffic-and-interference aware base station switching for green cellular networks," in *IEEE International Workshop on Computer Aided Modeling and Design of Communication Links and Networks (CAMAD)*, pp. 63–67, Sept. 2013.

[22] M. Marsan, L. Chiaraviglio, D. Ciullo, and M. Meo, "Switch-off transients in cellular access networks with sleep modes," in *IEEE International Conference on Communications Workshops (ICC Workshops)*, pp. 1–6, June 2011.

[23] D. González G, J. Hämäläinen, H. Yanikomeroglu, M. García-Lozano, and G. Senarath, "A novel multiobjective cell switch-off framework for cellular networks," *IEEE Access*, vol. PP, no. 99, date of publication: 07 Nov. 2016. DOI: 10.1109/ACCESS.2016.2625743.

[24] L. Suárez, L. Nuaymi, and J.-M. Bonnin, "Energy-efficient BS switching-off and cell topology management for macro/femto environments," *Computer Networks*, vol. 78, pp. 182–201, Nov. 2014.

[25] I. Aydin, H. Yanikomeroglu, and U. Aygolu, "User-aware cell switch-off algorithms," in *IEEE International Wireless Communications & Mobile Computing Conference (IWCMC)*, pp. 1236–1241, Aug. 2015.

[26] ITU-R, "Report ITU-R M.2135-1; guidelines for evaluation of radio interface technologies for IMT-Advanced," 2009.

[27] Z. Drezner and H. W. Hamacher, *Facility Location: Applications and Theory*. Springer, 2004.

[28] "Calibration for IMT-Advanced Evaluations," tech. rep., CELTIC/CP5-026 Project WINNER+, Munich, Germany, May 2010.

[29] D. Bultmann, T. Andre, and R. Schoenen, "Analysis of 3GPP LTE-Advanced cell spectral efficiency," in *IEEE International Symposium on Personal Indoor and Mobile Radio Communications (PIMRC)*, pp. 1876–1881, Sept. 2010.

[30] V. V. Vazirani, *Approximation Algorithms*. Springer, 2001.

[31] X. Xu, S. Tang, X. Mao, and M. Li, "Distributed gateway placement for cost minimization in wireless mesh networks," in *IEEE International Conference on Distributed Computing Systems (ICDCS)*, pp. 507–515, June 2010.

[32] B. Aoun, R. Boutaba, Y. Iraqi, and G. Kenward, "Gateway placement optimization in wireless mesh networks with qos constraints," *IEEE J. Sel. Areas Commun.*, vol. 24, pp. 2127–2136, Nov. 2006.

[33] S. Agathos and E. Papapetrou, "On the set cover problem for broadcasting in wireless ad hoc networks," *IEEE Commun. Lett.*, vol. 17, pp. 2192–2195, Nov. 2013.

[34] M. Cardei and J. Wu, "Energy-efficient coverage problems in wireless ad-hoc sensor networks," *Computer Communications*, vol. 29, pp. 413–420, Feb. 2006.

[35] H. Aslanyan and J. Rolim, "Interference minimization in wireless networks," in *IEEE/IFIP International Conference on Embedded and Ubiquitous Computing (EUC)*, pp. 444–449, Dec. 2010.

[36] F. Kuhn, P. von Rickenbach, R. Wattenhofer, E. Welzl, and A. Zollinger, "Interference in cellular networks: The minimum membership set cover problem," in *Computing and Combinatorics Conference (COCOON)*, vol. 3595, pp. 188–198, Springer, Sept. 2005.

[37] S. Jenjaturong and C. Intanagonwiwat, "A set cover-based density control algorithm for sensing coverage problems in wireless sensor networks," in *IEEE International Conference on Cognitive Radio Oriented Wireless Networks and Communications (CrownCom)*, pp. 1–6, May 2008.

[38] R. Ghaderi, M. Esnaashari, and M. R. Meybodi, "An adaptive scheduling algorithm for set cover problem in wireless sensor networks: A cellular learning automata approach," *International Journal of Machine Learning and Computing*, vol. 2, pp. 626–632, Oct. 2012.

[39] Y.-l. Li, X.-m. Hu, and J. Zhang, "A new genetic algorithm for the set k-cover problem in wireless sensor networks," in *IEEE International Conference on Systems, Man and Cybernetics (SMC)*, pp. 1405–1410, 2009.

[40] D. Li and H. Liu, "Sensor coverage in wireless sensor networks," *International Journal of Sensor Networks*, vol. 2, pp. 3–31, 2009.

[41] X. Han, X. Cao, E. L. Lloyd, and C.-C. Shen, "Deploying directional sensor networks with guaranteed connectivity and coverage," in *IEEE Communications Society Conference on Sensor, Mesh and Ad Hoc Communications and Networks*, pp. 153–160, June 2008.

[42] N. Pervin, D. Layek, and N. Das, "Localized algorithm for connected set cover partitioning in wireless sensor networks," in *International Conference on Parallel Distributed and Grid Computing (PDGC)*, pp. 229–234, Oct. 2010.

[43] M. Ashouri, Z. Zali, S. Mousavi, and M. R. Hashemi, "New optimal solution to disjoint set k-coverage for lifetime extension in wireless sensor networks," *IET Wireless Sensor Systems*, vol. 2, no. 1, pp. 31–39, 2012.

[44] S. Bosio, "On a new class of nonlinear set covering problems arising in wireless network design," *A Quarterly Journal of Operations Research (4OR)*, vol. 6, pp. 183–186, July 2008.

[45] Z. Abrams, A. Goel, and S. Plotkin, "Set k-cover algorithms for energy efficient monitoring in wireless sensor networks," in *ACM International Symposium on Information Processing in Sensor Networks*, pp. 424–432, Apr. 2004.

[46] P. Tague, J. Lee, and R. Poovendran, "A set-covering approach for modeling attacks on key predistribution in wireless sensor networks," tech. rep., DTIC Document, 2005.

[47] R. Mulligan and H. M. Ammari, "Coverage in wireless sensor networks: a survey," *Network Protocols and Algorithms*, vol. 2, pp. 27–53, June 2010.

[48] N. Bansal, R. Krishnaswamy, and B. Saha, "On capacitated set cover problems," in *Approximation, Randomization, and Combinatorial Optimization. Algorithms and Techniques*, pp. 38–49, Springer, Aug. 2011.

[49] A. Guo and M. Haenggi, "Spatial stochastic models and metrics for the structure of base stations in cellular networks," *IEEE Trans. Wireless Commun.*, vol. 12, pp. 5800–5812, Nov. 2013.

[50] A. K. M. F. Haque, A. F. M. S. Shah, A. Hannan, N. Jahan, U. Ahmed, and A. Saleh, "High performance analysis of frequency reuse schemes in cellular mobile environment," *International Journal of Latest Trends in Computing*, vol. 2, pp. 29–34, Mar. 2011.

[51] T. Beitelmal, D. González G, S. S. Szyszkowicz, and H. Yanikomeroglu, "Sector and site switch-off regular patterns for energy saving in cellular networks," *IEEE Trans. Wireless Commun.*, submitted Oct. 2016.

[52] S. M. Ross, *Introduction to Probability Models*. 2010.

[53] H. Holtkamp, G. Auer, V. Giannini, and H. Haas, "A parameterized base station power model," *IEEE Commun. Lett.*, vol. 17, pp. 2033–2035, Nov. 2013.

[54] T. Beitelmal, S. S. Szyszkowicz, and H. Yanikomeroglu, "Regular and static sector-based cell switch-off patterns," in *IEEE Vehicular Technology Conference (VTC-Fall)*, pp. 1–5, Sept. 2016.

[55] F. Lagum, Q.-N. Le-The, T. Beitelmal, S. S. Szyszkowicz, and H. Yanikomeroglu, "Cell switch-off for networks deployed with variable spatial regularity," *IEEE Wireless Commun. Lett.*, submitted Oct. 2016.

[56] Q.-N. Le-The, T. Beitelmal, F. Lagum, S. S. Szyszkowicz, and H. Yanikomeroglu, "Cell switch-off algorithms for spatially irregular base station deployments," *IEEE Wireless Commun. Lett.*, submitted Oct. 2016.

[57] J. G. Andrews, F. Baccelli, and R. K. Ganti, "A tractable approach to coverage and rate in cellular networks," *IEEE Trans. Commun.*, vol. 59, pp. 3122–3134, Oct. 2011.

[58] B. Rengarajan, G. Rizzo, and M. A. Marsan, "Energy-optimal base station density in cellular access networks with sleep modes," *Computer Networks*, vol. 78, pp. 152–163, Feb. 2015.

[59] E. Altman, C. Hasan, M. K. Hanawal, S. S. Shitz, J.-M. Gorce, R. El-Azouzi, and L. Roullet, "Stochastic geometric models for green networking," *IEEE Access*, vol. 3, pp. 2465–2474, Nov. 2015.

[60] J. Peng, P. Hong, and K. Xue, "Stochastic analysis of optimal base station energy saving in cellular networks with sleep mode," *IEEE Commun. Lett.*, vol. 18, pp. 612–615, Apr. 2014.

[61] F. Lagum, S. S. Szyszkowicz, and H. Yanikomeroglu, "CoV-based metrics to quantify the regularity of hard-core point processes for modeling the locations of base stations.," *IEEE Wireless Commun. Lett.*, vol. 5, pp. 276–279, June 2016.

[62] J. G. Andrews, "Seven ways that HetNets are a cellular paradigm shift," *IEEE Commun. Mag.*, vol. 51, pp. 136–144, Mar. 2013.

[63] D. B. Taylor, H. S. Dhillon, T. D. Novlan, and J. G. Andrews, "Pairwise interaction processes for modeling cellular network topology," in *IEEE Global Communications Conference (GLOBECOM)*, pp. 4524–4529, Dec. 2012.

[64] Y. Li, F. Baccelli, H. S. Dhillon, and J. G. Andrews, "Fitting determinantal point processes to macro base station deployments," in *IEEE Global Communications Conference (GLOBECOM)*, pp. 3641–3646, Dec. 2014.

[65] T. V. Nguyen and F. Baccelli, "On the spatial modeling of wireless networks by random packing models," in *IEEE International Conference on Computer Communications (INFOCOM)*, pp. 28–36, Mar. 2012.

[66] M. Haenggi, "Mean interference in hard-core wireless networks," *IEEE Commun. Lett.*, vol. 15, pp. 792–794, Aug. 2011.

[67] F. Lagum, S. S. Szyszkowicz, and H. Yanikomeroglu, "Quantifying the regularity of perturbed triangular lattices using CoV-based metrics for modeling the locations of base stations in HetNets," in *IEEE Vehicular Technology Conference (VTC-Fall)*, pp. 1–5, Sept. 2016.

[68] M. Mirahsan, R. Schoenen, and H. Yanikomeroglu, "HetHetNets: Heterogeneous traffic distribution in heterogeneous wireless cellular networks," *IEEE J. Sel. Areas Commun.*, vol. 33, pp. 2252–2265, Oct. 2015.

[69] D. Pisinger, "Upper bounds and exact algorithms for p-dispersion problems," *Computers & Operations Research*, vol. 33, pp. 1380–1398, May 2006.

[70] E. Erkut, Y. Ülküsal, and O. Yenicerioğlu, "A comparison of p-dispersion heuristics," *Computers & Operations Research*, vol. 21, pp. 1103–1113, Dec. 1994.

[71] M. Drosou and E. Pitoura, "Comparing diversity heuristics," tech. rep., Technical Report 2009-05. Computer Science Department, University of Ioannina, May 2009.

[72] F. J. Rodriguez, C. Garcia-Martinez, and M. Lozano, "Hybrid metaheuristics based on evolutionary algorithms and simulated annealing: taxonomy, comparison, and synergy test," *IEEE Trans. Evol. Comput*, vol. 16, pp. 787–800, Dec. 2012.

[73] M. Haenggi, "The mean interference-to-signal ratio and its key role in cellular and amorphous networks," *IEEE Wireless Commun. Lett.*, vol. 3, pp. 597–600, Sept. 2014.

[74] "Loxcel geomatics." `https://www.loxcel.com/celltower`. Accessed 28 July, 2016.

[75] C. Liang, F. R. Yu, and S. Member, "Wireless network virtualization : A survey, some research issues and challenges," *IEEE Commun. Surveys Tuts.*, vol. 17, pp. 358–380, 1st Quarter 2015.

[76] 3GPP, "Service aspects and requirements for network sharing," TR 22.951, 3rd Generation Partnership Project (3GPP), Oct. 2014. V12.0.0.

[77] M. Marsan and M. Meo, "Energy efficient wireless Internet access with cooperative cellular networks," *Elsevier Computer Networks*, vol. 55, pp. 386–398, Feb. 2011.

[78] H. Ghazzai, E. Yaacoub, and M.-S. Alouin, "A game theoretical approach for cooperative environmentally friendly cellular networks powered by the smart grid," in *IEEE Online Conference on Green Communications (OnlineGreencomm)*, pp. 1–6, Nov 2014.

[79] A. Bousia, E. Kartsakli, A. Antonopoulos, L. Alonso, and C. Verikoukis, "Game theoretic approach for switching off base stations in multi-operator environments," in *IEEE International Conference on Communications (ICC)*, pp. 4420–4424, June 2013.

[80] H. Ghazzai, E. Yaacoub, and M.-S. Alouini, "Multi-operator collaboration for green cellular networks under roaming price consideration," in *IEEE Vehicular Technology Conference (VTC-Fall)*, pp. 1–5, Sept. 2014.

[81] A. Khan, W. Kellerer, K. Kozu, and M. Yabusaki, "Network sharing in the next mobile network: TCO reduction, management flexibility, and operational independence," *IEEE Commun Mag.*, vol. 49, pp. 134–142, Oct. 2011.

[82] G. Hardin, "The tragedy of the commons," *New York*, Dec. 1968.

[83] R. Schoenen, "On increasing the spectral efficiency more than 100% by user-in-the-control-loop," in *Asia-Pacific Conference on Communications (APCC)*, (Auckland), pp. 159 – 164, Oct. 2010.

[84] R. Schoenen, H. Yanikomeroglu, and B. Walke, "User-in-the-loop: Mobility aware users substantially boost spectral efficiency of cellular OFDMA systems," *IEEE Commun. Lett.*, vol. 15, pp. 488–490, May 2011.

[85] R. Schoenen, G. Bulu, A. Mirtaheri, and H. Yanikomeroglu, "Green communications by demand shaping and User-in-the-Loop tariff-based control," in *IEEE Online Green Communications Conference (GreenCom)*, (Online), pp. 64–69, Sept. 2011.

[86] R. Schoenen and H. Yanikomeroglu, "User-in-the-loop: Spatial and temporal demand shaping for sustainable wireless networks," *IEEE Commun. Mag.*, vol. 52, pp. 196–203, Feb. 2014.

[87] T. Beitelmal, R. Schoenen, and H. Yanikomeroglu, "On the impact of correlated shadowing on the performance of user-in-the-loop for mobility," in *IEEE International Conference on Communications Workshop (ICC Workshops)*, pp. 7040–7044, June 2012.

[88] R. Schoenen, G. Bulu, A. Mirtaheri, T. Beitelmal, and H. Yanikomeroglu, "Quantified user behavior in user-in-the-loop spatially and demand controlled cellular systems," in *European Wireless Conference (EW)*, pp. 1–8, Apr. 2012.

[89] R. Schoenen, G. Bulu, A. Mirtaheri, T. Beitelmal, and H. Yanikomeroglu, "First survey results of quantified user behavior in user-in-the-loop scenarios for sustainable wireless networks," in *IEEE Vehicular Technology Conference (VTC-Fall)*, pp. 1–5, Sept. 2012.

[90] D. Bültmann, T. Andre, and R. Schoenen, "Analysis of 3GPP LTE-Advanced cell spectral efficiency," in *IEEE International Symposium Personal Indoor and Mobile Radio Communications (PIMRC)*, pp. 1876–1881, Sept. 2010.

[91] S. S. Szyszkowicz, F. Alaca, H. Yanikomeroglu, and J. S. Thompson, "Aggregate interference distribution from large wireless networks with correlated shadowing: An analytical–numerical–simulation approach," *IEEE Trans. Veh. Technol.*, vol. 60, pp. 2752–2764, July 2011.

[92] S. S. Szyszkowicz, H. Yanikomeroglu, and J. S. Thompson, "On the feasibility of wireless shadowing correlation models," *IEEE Trans. Veh. Technol.*, vol. 59, pp. 4222–4236, Nov. 2010.

[93] F. Graziosi and F. Santucci, "A general correlation model for shadow fading in mobile radio systems," *IEEE Commun. Lett.*, vol. 6, pp. 102–104, Aug. 2002.

[94] M. Gudmundson, "Correlation model for shadow fading in mobile radio systems," *IET Electronics Letters*, vol. 27, pp. 2145–2146, Nov. 1991.

[95] K. Kumaran, S. Golowich, and S. Borst, "Correlated shadow-fading in wireless networks and its effect on call dropping," *Wireless Networks*, vol. 8, pp. 61–71, Jan. 2002.

[96] I. Forkel, M. Schinnenburg, and M. Ang, "Generation of two-dimensional correlated shadowing for mobile radio network simulation," in *International Symposium on Wireless Personal Multimedia Communication (WPMC)*, pp. 10–22, May 2004.